Efficient Ranking of Metal Organic Framework Adsorbents and Membranes Using Molecular Simulations

by

Zeynep Sümer

A Thesis Submitted to the
Graduate School of Sciences and Engineering
in Partial Fulfillment of the Requirements for
the Degree of

Master of Science
in
Chemical and Biological Engineering

Koc University

July 2017

Koc University

Graduate School of Sciences and Engineering

This is to certify that I have examined this copy of a master's thesis by

Zeynep Sümer

and have found that it is complete and satisfactory in all respects,
and that any and all revisions required by the final
examining committee have been made.

Committee Members:

_____

Seda Keskin Avcı, Ph. D. (Advisor)

_____

Alper Uzun, Ph. D.

_____

İlknur Eruçar Fındıkçı, Ph. D.

Date: _____

ABSTRACT

In this thesis, efficient ranking methods for promising metal organic framework (MOF) adsorbents and membranes were defined using molecular simulations. First, MOF adsorbents that can efficiently separate CO_2 from natural gas (CO_2/CH_4), power plant flue gas (CO_2/N_2) and petroleum refineries (CO_2/H_2) were investigated. Several adsorbent evaluation metrics including selectivity, working capacity, adsorption figure of merit, sorbent selection parameter, per cent regenerability were computed for 100 different MOFs and for each gas separation. Results showed that regenerability is a very important metric to screen the materials at the first step of the adsorbent search and MOFs can be then ranked based on their selectivities. In the second part of thesis, gas permeability and selectivity of 700 new mixed matrix membranes (MMMs) composed of 70 different MOFs and 10 different polymers were calculated for CO_2/N_2 separations. This was the largest number of MOF-based MMMs for which computational screening was done to date. Selecting the appropriate MOFs as filler particles in polymers resulted in MMMs that have higher CO_2/N_2 selectivities and higher CO_2 permeabilities compared to pure polymer membranes. It was found that for polymers that have low CO_2 permeabilities but high CO_2 selectivities, the identity of the MOF used as filler is not important. The outcome of adsorbent evaluation and membrane evaluation results were then applied for nitrogen separation from methane (CH_4/N_2). Combined adsorption and diffusion data obtained from molecular simulations were used to predict both membrane selectivities and gas permeabilities of 102 MOFs for separation of CH_4/N_2 mixtures. The relations between easily computable structural properties such as pore sizes, surface areas and porosities of MOFs and performance evaluation metrics were also examined to provide structure-property relationships that can serve as a guide for experimental studies.

ÖZET

Bu tezde, moleküler simülasyonlar kullanılarak adsorbent ve membran olarak kullanılan metal organik yapıların (MOF) performanslarına göre verimli bir şekilde sıralanması için yöntemler tanımlanmaktadır. İlk olarak doğal gaz (CO_2/CH_4), güç santrali baca gazı (CO_2/N_2) ve petrol rafinerilerinde (CO_2/H_2) rastlanan gaz karışımlarından etkili bir şekilde CO_2 gazını ayırabilen MOF adsorbentler incelenmiştir. Seçicilik, iş kapasitesi, adsorpsiyon performans katsayısı, sorbent seçim parametresi, ve yenilenme yüzdesi gibi bazı adsorbent değerlendirme kriterleri 100 MOF'ta tüm gaz karışımları için incelenmiştir. Sonuçlar yenilenme yüzdesinin çok önemli bir malzeme tarama kriteri olduğunu ve seçicilikten önce değerlendirilmesi gerektiğini göstermektedir. Tezin ikinci kısmında membran temelli ayırma işlemleri için 70 farklı MOF ve 10 farklı polimerin kombinasyonundan oluşan 700 farklı karışık yataklı membran (MMM) incelenmiştir. Bu sayı şu ana kadar hesaplamalı tarama kullanılarak taranan en yüksek malzeme sayısıdır. Polimerlere dolgu malzemesi olarak uygun MOF'u seçmek, karışık yataklı membranların polimerlere göre daha yüksek CO_2/N_2 seçiciliğine ve CO_2 geçirgenliğine sahip olmasını sağlamıştır. Halihazırda yüksek CO_2/N_2 seçiciliğine ve düşük CO_2 geçirgenliğine sahip polimerler için MOF'un yapısal özelliklerinin bir önemi olmadığı da keşfedilmiştir. Adsorbent ve membran değerlendirme kriterlerinden edinilen bu sonuçlar daha sonra metandan azot ayrımında (CH_4/N_2) uygulanmıştır. CH_4/N_2 ayrımında kullanılan 102 MOFun membran seçiciliği ve gaz geçirgenliğini ölçmek için adsorpsiyon ve difüzyon verileri kullanılmıştır. Ek olarak, deneysel çalışmalara rehberlik edebilmesi amacıyla, kolayca hesaplanabilen gözenek boyu, yüzey alanı ve porozite gibi bazı yapısal özelliklerle, performans değerlendirme kriterleri arasındaki ilişki incelenmiş ve bir yapı-nitelik bağlantısı sunulmuştur.

ACKNOWLEDGEMENTS

I want to thank NEMO group members for giving me unforgettable memoirs in such a warm, friendly research group. Firstly, without my lovely mentors, Çiğdem Altıntaş, Elda Adatoz and İlknur Eruçar I would not be in this point. I also want to thank Pelin Kınık, Burak Koyutürk, Vahid Nozari, Özge Kadıoğlu, Derya Dokur, Ayda Nemati and Mohammad Zeeshan because their friendship always kept me motivated for research and studying. I cannot forget to thank our one and only honorary NEMO member, Benay Uzer.

I want to thank my friends in Ankara. Half of them are not in Ankara anymore, but it is where everything started. Berna Sezgin, Deniz Kaya, Elif Kocaman, Gülçin Çağlayan and Merve Tufan showed me that friends are the family we choose for ourselves. Without their limitless gossip capability, serious talks, fun talks, suggestions, or comments, this thesis would hardly been written. I cannot even begin to express my gratitude to my brother from another mother, Onur Dereli. He has been my closest friend in this tough period of our lives. I am also indebted to Mert Bayer for his endless support, understanding, and care. I will always be grateful to my parents for being the best and for everything they taught me throughout life.

I want to thank my advisor Assoc. Prof. Seda Keskin Avcı for her guidance. I would like to express my gratitude to my committee members, Asst. Prof. Alper Uzun and Asst. Prof. İknur Eruçar Fındıkçı for their valuable time and advices. Finally, I would like to thank Fabrizio Pinto for being such a reputable yet humble academician who does not hesitate to give gold-worth advices to a student he randomly met in a flight. Financial support provided by The Scientific and Technological Research Council of Turkey (TUBITAK) Grant MAG-213M401 is gratefully acknowledged.

Zeynep Sümer

25/07/2017

TABLE OF CONTENTS

LIST OF TABLES

LIST OF FIGURES

NOMENCLATURE

CO_2 : Carbon dioxide
CH_4 : Methane
N_2 : Nitrogen
H_2 : Hydrogen
MMM : Mixed matrix membrane
MOF : Metal organic framework
ZIF : Zeolite Imidazolate Framework
PCN : Porous Coordination Network
GCMC : Grand Canonical Monte Carlo
EMD : Equilibrium Molecular Dynamics
IRMOF : Isoreticular MOF
PDMS : Polydimethylsiloxane
XLPEO : Cross-linked polyethylene oxide
PI : Polyimide
PVAc : Polyvinyl acetate
PIM : Polymers of intrinsic microporosity
PTMGP : Polytrimethylgermylpropyne
PTMSP : Polytrimethylsilylpropyne
ϕ : Volume fraction of filler in polymer matrix
ε : Potential well depth
σ : Potential diameter
S_{ads} : Adsorption selectivity
S_{diff} : Diffusion selectivity
S_{mem} : Membrane selectivity
ΔN : Working capacity
R% : Regenerability
S_{sp} : Sorbent selection parameter
EQeq : Extended charge equilibriation method
NVT : Constant number of molecules, volume and temperature

ε_0 : Dielectric constant
r : Position of atom
D_0 : Corrected diffusivity
D_t : Transport diffusivity
c : Adsorbed gas amount
f : Bulk phase fugacity
∇c : Concentration gradient
J : Gas flux
P_f : Filler's permeability
ΔP : Pressure drop
L : Membrane thickness
V_{pore} : Pore volume
PLD : Pore limiting diameter
LCD : Largest cavity diameter
UFF : Universal force field
P : MMM's gas permeability
P_p :Polymer's permeability

Chapter 1

INTRODUCTION

The main component of natural gas, methane (CH_4), has been considered as a strong alternative to the petroleum.[1] Natural gas extracted from unconventional hydrocarbon sources such as landfill gas and shale gas contains major impurities, mainly CO_2 and N_2. Cost-effective technologies for capturing CO_2 from conventional uses of fossil fuels are very important since fossil fuels are expected to contribute to the world's energy supply in the following years. Gas separations that are relevant to mitigating CO_2 emissions include removal of CO_2 from natural gas (CO_2/CH_4), power plant flue gas (CO_2/N_2) and petroleum refineries (CO_2/H_2). The key challenge of CO_2 capture is the identification of materials that can separate CO_2 from other gases with high selectivity. Additionally, separation of CH_4 from N_2, which is another major impurity in natural gas, is particularly difficult because similar molecule sizes of these gases lead to a low selectivity.[2] These impurities are generally separated by cryogenic distillation, however this process is energy-intensive with high operating costs. These gas mixtures can be separated using either adsorption-based or kinetic-based separation processes. Adsorption-based and membrane-based gas separations offer very large reductions in the energy consumption and costs of the separation processes. The greatest limitation in applications of these separation technologies is the low selectivity of the materials used as adsorbents and/or membranes.

Adsorption-based gas separations rely on the fact that gases can reversibly adsorb into the porous materials at densities that exceed the densities of gases in equilibrium with the

porous solids. The choice of the porous material, called as adsorbent, is perhaps the most important decision in the design and development of adsorption-based gas separations. Structural features, chemical and physical properties of the adsorbents directly affect the separation efficiency of the process. Membrane-based gas separation is one of the cost-effective methods to apply in industry. Polymer membranes have been widely used for gas separation. Unfortunately, the main disadvantage of polymer membranes is the trade-off between gas permeability and selectivity.[3] Polymer membranes' selectivities tend to decrease as their permeabilities increase. For an efficient and economic gas separation process, both high gas selectivity and high gas permeability are required. High gas selectivity provides high purity and high gas permeability decreases the required surface area of the membrane, hence the capital cost. In order to overcome the trade-off of the polymer membranes, mixed matrix membranes (MMMs) are fabricated. In this way, the advantages of nanoporous filler particles such as high gas permeability and high gas selectivity can be combined with the advantages of polymers such as easy processability and low cost.[4] MMMs can be fabricated on large scales with relatively minor adaptation of existing commercial technology developed for polymer membranes. If the appropriate fillers are chosen, both the selectivity and permeability of the polymer membrane can be improved.

Metal organic frameworks (MOFs) have emerged as a new class of nanoporous materials with exceptional physical and chemical properties that can be used both as adsorbents and as membranes for various gas separations. Thousands of MOFs have been synthesized to date and theoretically unlimited number of structures can be synthesized by combining different metals and organic linkers. MOFs have been considered as promising adsorbents and membranes due to their wide range of pore sizes and shapes, low densities (0.2-1 g/cm^3), large surface areas (500-6000 m^2/g), high porosities, reasonable thermal and mechanical stabilities.[5] The large versatility in geometry and chemical property of MOFs suggest that it is possible to find an ideal MOF adsorbent and/or membrane for a target gas

separation. A good comparison of CO_2 separation performances of different nanoporous adsorbents including MOFs, zeolites and activated carbons can be found in a recent review.[6] Results show that MOFs can outperform zeolites and carbon-based adsorbents due to their high CO_2 selectivities and working capacities. MOFs can also improve the gas separation performances of polymers when they are used as filler particles. MOF-based MMMs can exhibit higher CO_2/N_2 selectivity and/or higher CO_2 permeability than the pure polymer membranes.

Although a very small number of MOFs has been experimentally tested for CH_4/N_2 separation, some MOFs have the potential to outperform traditional adsorbents by achieving high selectivity as the experimental studies suggested. Considering the very large number of available of MOFs, it is not possible to test the adsorption-based CH_4/N_2 separation performance of every single MOF using purely experimental techniques. Molecular simulations play a very important role in assessing the gas separation performance of large number of materials in a reasonable time. Most molecular simulation studies predicted properties of MOFs from the single-component gas adsorption/diffusion data. It is necessary to perform molecular simulations for gas mixtures rather than for single gases to correctly assess the real potential of MOFs. The effects of competitive adsorption between different gas species cannot be reflected in single-component gas simulations, especially for mixtures such as CO_2/CH_4, CO_2/N_2, where two gas components compete strongly for the same adsorption sites of the adsorbent. Assessing membrane-based separation performance of materials using the single-component gas diffusion data can also be misleading. It is also important to rank the materials considering a set of different metrics. If only a single criterion such as selectivity is used, materials' properties can be misjudged. For example, an adsorbent material that exhibit high selectivity for CO_2 may have low regenerability which leads to economically inefficient separation process, or a MOF membrane can possess very high selectivity, but if its permeability is low using that material will negatively affect the size of

membrane. Therefore, screening materials based on several performance evaluation metrics would be much more useful to assess the real potential of MOFs. Furthermore, most of the simulation studies in the literature reported selectivities computed at infinite dilution. However, in real applications, operating pressures are generally around atmospheric pressures. Selectivities computed at infinite dilution are generally significantly higher than the ones computed at atmospheric pressures and overestimate the separation performance of adsorbents/membranes.[7] Therefore, adsorption (feed) and desorption (permeate) pressures of the simulation studies must be set to represent real operating conditions. Molecular simulation studies in the literature generally focused on either CO_2/N_2 or CO_2/CH_4 separations. It is highly desirable to identify adsorbents that will be useful in all three industrially and economically important CO_2 separation processes.

In this thesis, molecular simulations were used to identify both the adsorption-based and membrane-based separation performances of a large number of MOFs. Chapter 2 reviews the literature, provides experimental and computational studies which are investigating MOF adsorbents, fillers or membranes for various gas separation applications. Computational methods and adsorbent/membrane evaluation strategy are provided in Chapter 3. Chapter 4 demonstrates MOF adsorbents for separation of CO_2/CH_4, CO_2/N_2 and CO_2/H_2 mixtures. In Chapter 5, MOF-based MMMs for CO_2/N_2 separation are discussed. CO_2/N_2 selectivity and CO_2 permeability of MOFs were computed to provide the first information about the separation potential of these materials. Molecular simulations were performed to identify both the adsorption-based and membrane-based CH_4/N_2 separation performances of a large number of MOFs and results were provided in Chapter 6. Finally in Chapter 7, results obtained throughout the thesis are summarized.

Chapter 2

LITERATURE REVIEW

2.1. Adsorption-based Separation by MOFs

The main challenge in choosing a MOF adsorbent is the high number of available materials. Thousands of MOF materials have been synthesized to date however, only a small fraction of these materials has been tested in adsorption-based CO_2 separation applications. It is not possible to test separation performances of all synthesized MOFs using purely experimental efforts. Computational studies that can accurately predict the gas separation potential of MOF adsorbents based on a variety of performance metrics are highly important to identify the most promising materials and to direct the experimental efforts, time and resources to those materials. Although design for adsorption-based gas separation processes is influenced by multiple factors, one key criteria is the adsorption selectivity of the material for the desired gas relative to the undesired one.[8] Adsorbents that have high selectivity for CO_2 are desired for an efficient and economic CO_2 capture. The absolute CO_2 uptake capacity of MOFs is used to evaluate the potential of MOF adsorbents for CO_2 capture.[9] Working capacity which defines the CO_2 loading difference between the adsorption and desorption pressures is another widely used metric to assess the performance of MOF adsorbents.[10] Molecular simulations have been used to screen MOF adsorbents generally based on two metrics, selectivity and working capacity. For example, Wilmer et al.[11] used molecular simulations to calculate adsorption of pure CO_2, N_2 and CH_4 in over 130,000 hypothetical MOFs. Adsorbent performances of MOFs such as selectivity and working capacity were

computed using single-component gas adsorption data. MOFs have been experimentally[12] and computationally[1, 13, 14] studied for many different gas separations. Most of these studies have focused on the CO_2 separation and examined either separation of CO_2/CH_4 or CO_2/N_2 mixtures using MOFs.[8, 15, 16] Watanabe and Sholl[17] used molecular simulations to predict single-component adsorption of CO_2 and N_2 in 359 MOFs. They reported the CO_2/N_2 selectivity of these MOFs as a function of pore sizes of the materials. Wu et al.[18] computed adsorption of CO_2/N_2 mixtures in 105 MOFs. They concluded that increasing the difference of isosteric heats of adsorption between CO_2 and N_2 at infinite dilution and simultaneously decreasing the porosity is an appropriate route to enhance the CO_2/N_2 selectivity of MOFs. Qiao et al.[13] recently reported a molecular simulation study that screens 4764 MOFs for CO_2 separation from flue gas and natural gas. They established quantitative relationships between the metal type of materials and their adsorption selectivity, working capacity and regenerability.

On the other hand, research on the CH_4/N_2 separation using MOFs has recently started and the number of experimental and computational studies on the separation of CH_4/N_2 mixture is very limited in the literature. Möllmer et al.[19] experimentally reported binary gas adsorption isotherms of CH_4/N_2 mixture using two commercially available MOFs, Basolite® A100 and $^3_\infty$[Cu(Me-4py-trz-ia)] up to 20 bar. They calculated CH_4/N_2 selectivities of these MOFs as 3.4-4.4 at 298 K. Ren et al.[20] investigated 4 types of MOFs and 2 types of zeolites performing breakthrough experiments for separation of equimolar CH_4/N_2 mixture. Their breakthrough experiments showed that MOFs, Ni-formate and Co-formate, have high CH_4/N_2 selectivities (6.0-6.5 and 5.1-5.8, respectively) whereas Al-BDC, Cu-BTC, zeolite 5A and SAPO-34 show moderate selectivities between 2.0-4.8 at 1-10 bar, 298 K. Sun et al.[21] measured CH_4/N_2 selectivity of Al-BDC using breakthrough experiments for equimolar CH_4/N_2 mixture at 303 K up to 10 bar. They reported that as-prepared Al-BDC has a CH_4/N_2 selectivity of 2.9, whereas calcinated Al-BDC has a selectivity of 4.3. Hu et

al.[22] reported CH_4/N_2 selectivities of 4 different MOFs, namely Ni-MOF-74, Al-BDC, $[Ni_3(HCOO)_6]$ and $[Cu(INA)_2]$ as 2.0, 3.4, 6.2 and 7.2, respectively for separation of equimolar CH_4/N_2 mixtures at 298 K up to 10 bar. To the best of knowledge, two molecular simulation studies which examined adsorption-based separation of CH_4/N_2 mixture using MOFs were performed by Liu and Smit.[23, 24] They used Grand Canonical Monte Carlo (GCMC) simulations to calculate selectivity of three zeolites (MFI, LTA and DDR) and seven MOFs (Cu-BTC, MIL-47(V), and isoreticular MOFs, IRMOF-1, IRMOF-11, IRMOF-12, IRMOF-13, IRMOF-14) for separation of CH_4/N_2:50/50 mixtures up to 20 bar at 298 K. They also calculated CH_4/N_2 selectivity of two zeolitic imidazolate frameworks, ZIF-68 and ZIF-69, as ~3.5 and ~3.2, respectively using GCMC simulations up to 30 bar at 298 K.[24] Qiao et al.[25] studied a very large number of hypothetical MOFs (>17,000) using GCMC simulations and predicted their adsorption-based selectivities for separation of ternary $CO_2/N_2/CH_4$:0.1/0.7/0.2 mixture. Among the 24 promising MOFs they identified, N_2/CH_4 adsorption selectivities were predicted to be 0.22-6.57 at 298 K, 10 bar.

2.2. Membrane-based Separation by MOFs

Incorporation of MOFs into polymers to improve the gas selectivity and permeability of the membrane has been recently investigated by several experimental and computational studies in the literature. Several of these studies focused on CO_2/N_2 separations: Car et al.[26] studied the CO_2/N_2 selectivities of four different MMMs composed of CuBTC and Mn-$(HCOO)_2$ as filler particles incorporated into polydimethylsiloxane (PDMS) and polysulfone (PSf) polymers. They obtained slight improvements in CO_2 selectivity over N_2. Perez and co-workers[27] incorporated MOF-5 into Matrimid and showed that the permeabilities increased 124% for CO_2 and 108% for N_2 while selectivity remains almost same with the pure polymer. Basu et al.[28] synthesized CuBTC/Matrimid and CuBTC/Matrimid/PSf MMMs and investigated mixed-gas permeation properties for CO_2/N_2. They observed increases both in the CO_2 permeability and CO_2/N_2 selectivity. The same group[29] also

incorporated CuBTC, ZIF-8 and MIL-53(Al) into Matrimid and these MMMs showed higher CO_2/N_2 selectivity and higher CO_2 permeability than unfilled Matrimid. Bae and Long[30] incorporated Mg_2(dobdc) into PDMS, cross-linked polyethylene oxide (XLPEO) and polyimide (6FDA-TMPDA). While the CO_2 permeabilities of Mg_2(dobdc)/PDMS and Mg_2(dobdc)/XLPEO membranes decreased, the CO_2/N_2 selectivities were reported to slightly increase. Duan et al.[31] synthesized CuBTC/Ultem MMM with CuBTC and showed that the CO_2 permeability is increased up to 2.6 times while the CO_2/N_2 selectivity is almost unchanged. Kim et al.[32] investigated Cu-MOF as filler particle in polymer membranes, amorphous poly(2-ethyl-2-oxazoline) and semicrystalline poly(amide-6-b-ethylene oxide) and reported that ideal CO_2/N_2 selectivity of polymer membranes significantly increases with the addition of MOF particles.

As can be seen from the results of these experimental studies, MOF-based MMMs can exhibit higher CO_2/N_2 selectivity and/or higher CO_2 permeability than the pure polymer membranes. There are thousands of available MOFs that can be used as filler particles in polymer membranes. This high number of materials represents both an opportunity and challenge to select the correct MOF/polymer combinations for MMM fabrications. It is not possible to synthesize all the possible MOF/polymer MMMs and report their gas separation performances using purely experimental manners. Computational studies that can accurately predict the selectivity and permeability of MOF-based MMMs are highly useful to efficiently screen large numbers of MOFs prior to experiments. In this way, experimental efforts, time and resources can be directed to the most promising MOF fillers among many possible candidates. Our research group recently developed a computational approach that combines atomically-detailed simulations with continuum modeling to assess gas separation performances of MOF-based MMMs.[33] The accuracy of this approach was validated by comparing the predictions of our method with the available experimental gas permeability measurements of fabricated MOF-based MMMs such as IRMOF-1/Matrimid, CuBTC/PSf,

CuBTC/PDMS.[34] This method was then used to estimate the potential of new MOF-based MMMs in CO_2/CH_4 and CH_4/H_2 separations.[35],[34] MMMs in which ZIFs[36] and porous coordination networks, PCNs[37] were used as fillers in polymers for CO_2/N_2 separations were recently studied. 80 ZIF-based MMMs and 200 PCN-based MMMs were examined using molecular simulations and our results showed that a large number of ZIF and PCN-filled MMMs has higher CO_2 permeability and higher CO_2/N_2 selectivity than the pure polymers. Polymeric membranes selectively separate N_2 from CH_4. N_2 selectivities of polymeric membranes are less than 5 whereas inorganic membranes, such as zeolites exhibit higher selectivities.[38] For example, zeolite DD3R was reported to have a N_2 selectivity of 30 for separation of equimolar N_2/CH_4 mixture under 300 K and 1 bar. [39] Wu et al.[40] reported N_2 selectivity of SAPO-34 as 7 at 298 K under a feed pressure of 3.5 bar and N_2 selectivity of SSZ-13 as 13 at 293 K under 2.7 bar. However, these highly selective zeolite membranes suffer from low N_2 permeabilities. A limited number of MOF membranes was computationally investigated for CH_4/N_2 separation. Keskin and Sholl[41] computed CH_4 selectivity of IRMOF-1 as 3.2 at 298 K, 40 bar and Battisti et al.[42] reported CH_4 selectivities of ZIF-2, ZIF-4 and ZIF-8 as 2.70, 2.71 and 1.74, respectively at 298 K under 10 bar.

As it is seen in the literature review, there is a very limited number of studies in which adsorption based separation is investigated by considering all performance evaluation criteria including selectivity, working capacity, regenerability and so on. In order to fill the gap in the research area, Chapter 4 of this thesis covered 100 different MOFs and their adsorption based CO_2/CH_4, CO_2/N_2 and CO_2/H_2 separation performances. Identification of top performing MOFs has been done by using different metrics, and it is seen that in each criterion another MOF is found to be the best adsorbent. The same method is also applied in Chapter 6, in which adsorption and membrane based CH_4/N_2 separation is covered by using

102 MOFs. It is shown throughout the thesis that adsorption selectivity as the only criterion is not sufficient in determining the industrially practical and promising adsorbents.

In the literature review it is also seen that there is a lack of investigation of MMMs. Both experimental and computational studies so far studied only a small fraction of MOFs and polymers. In Chapter 5, 70 MOFs and 10 different polymers were investigated and combinations of MOF and polymer pairs created 700 different MMMs. This is the largest number of MMMs studied to date. Outcome of the results has shown that polymers with high selectivity and low permeability are not affected by the identity of MOF. This results will help to accelerate the experimental studies due to reduction in cost and effort spend on MOF-polymer combinations. Details of MMMs are provided in Chapter 5.

For each Chapter, simulation results for gas adsorption of MOFs were first compared with the experimentally available data in the literature to show the accuracy of molecular simulations. Adsorption data obtained from GCMC simulations were used to calculate adsorbent selection metrics of MOFs. The relations between easily computable structural properties such as pore size, surface area and porosity of MOFs and their adsorption selectivities are investigated to provide the structure-performance relationships that can serve as a map for experimental synthesis of new MOFs with better gas separation performances. Combining adsorption data with the diffusion data obtained from equilibrium molecular dynamics (EMD) simulations, membrane selectivities and gas permeabilities of MOFs were predicted.

Chapter 3

COMPUTATIONAL METHODS

3.1. MOF Selection

This thesis has been prepared in three different working packages. In the first working package that is provided in Chapter 4, 100 MOFs are used for adsorption based CO_2/CH_4, CO_2/N_2, CO_2/H_2 separations. In Chapter 5, second working package is given, in which membrane based CO_2/N_2 separation performance of 70 MOFs were considered. Lastly, Chapter 6 consists of third working package with 102 MOFs. In Chapter 6, adsorption and membrane based separation of CH_4/N_2 mixture is investigated by 102 MOFs. In total 182 different MOFs were examined. 115 MOFs were taken from the solvent-free MOF database constructed by Chung et al.[43] These MOFs were not considered in the recent large scale computational MOF screening study of Qiao et al.[13] 67 MOFs were taken from the library of our previous simulation study[44] to cover well-known materials (such as MOF-5, CuBTC) and widely studied subfamilies of MOFs (such as porous coordination networks, PCNs and zeolite imidazolate frameworks, ZIFs). In this way, a representative structural database was obtained to span a wide range of chemical functionalities. Crystal structures of all MOFs were taken from the Cambridge Crystallographic Data Centre (CCDC).[45] The complete list of the materials with CCDC names and structural properties such as pore limiting diameter (PLD), largest cavity diameter (LCD), pore volume, porosity, surface area of the MOFs are given in Appendix A. These structural properties were computed using Zeo++ software.[46] For surface area (pore volume) calculations, number of trials was set to

2000 (50000) and probe size was set to 1.86 (zero) Å. Sarkisov and Harrison's algorithm, Poreblazer,[47] was used for some MOFs for which the Zeo++ software was not able to calculate the surface area and/or pore volume. Universal force field (UFF)[48] was used for the Poreblazer algorithm. Parameters such as He atom's sigma, He atom's epsilon, N atom's sigma, temperature, cut-off distance and number of trials were set to 2.58 Å, 10.22 K, 3.314 Å, 298 K, 12.8 Å and 500, respectively. The largest anticipated pore diameter was set to 20 Å and the size of the bin was set to 0.25 Å.

The force fields used to represent MOF atoms were selected based on the results of previous simulation studies[44, 49, 50] which show a good agreement with the available experimental gas uptake data of MOFs. UFF[48] and Dreiding[51] force fields were combined for all MOFs in this thesis. In cases where the potential parameters were not available in the Dreiding force field, these parameters were taken from the UFF. Three-site rigid molecule with LJ 12-6 potential was used to model CO_2 and locations of partial point charges were set as center of each side.[52] N_2 was also modeled as three-site molecule, two sites were located at the N atoms and the third site was located at the center of the mass with partial point charges.[53] H_2[54] and CH_4[55] were modeled by using single-site spherical Lennard-Jones (LJ) 12-6 potential. For CO_2 and N_2 molecules electrostatic interactions were taken into consideration using the Coulomb potential. In order to compute the electrostatic interactions between gas molecules and MOFs, partial point charges were assigned to MOF atoms using extended charge equilibration method (EQeq).[56] The cut-off distance for truncation of electrostatic interactions was set to 25 Å.

3.2. Grand Canonical Monte Carlo (GCMC)

Grand Canonical Monte Carlo (GCMC)[57] simulations have been widely used to compute adsorption isotherms of various gas molecules through porous materials. In a typical experiment, chemical potential and temperature inside the adsorbent is considered the same as that of outside of adsorbent. In order GCMC simulations to give consistent results with

experiments, chemical potential, volume and temperature are kept constant inside the system. Number of gas molecules in an equilibrium condition is determined by GCMC simulations.

In a GCMC simulation, adsorbed amounts of each gas component were calculated by specifying the bulk pressure, temperature and composition of the bulk gas mixture. Five different types of moves were considered for GCMC simulations of gas mixtures including translation, rotation, insertion, deletion and exchange of molecules. The Lorentz-Berthelot mixing rules were employed. The cut-off distance for truncation of the intermolecular interactions was set to 13 Å. Periodic boundary conditions were applied in all simulations. A simulation box of 2×2×2 crystallographic unit cells was used. During the simulations, 1.5×10^7 steps were performed to guarantee the equilibration and 1.5×10^7 steps were performed to sample the desired properties. Rigid framework assumption was used in all simulations. Almost all of the molecular simulations for MOFs in the literature used this assumption because it saves a significant amount of computational time. Recent studies showed that including lattice flexibility does not make any significant change in the gas adsorption results of MOFs that have pore sizes larger than the guest molecules.[58-60]

In this thesis, GCMC simulations were performed to compute adsorption isotherms of binary gas mixtures, CO_2/CH_4, CO_2/N_2, CO_2/H_2, CH_4/N_2 in MOFs in Chapter 4 and Chapter 6. Single-component adsorption isotherms of CO_2 and N_2 in MOFs were also measured in Chapter 5. The adsorbed amount of each gas was calculated by specifying the pressure and temperature. In Chapter 4, two different operating cases are used to represent industrial operating conditions. In Case 1, adsorption pressure was set to 1 bar and desorption pressure was set to 0.1 bar. In Case 2, adsorption pressure was set to 10 (5) bar for CO_2/H_2 and CO_2/N_2 mixtures (CO_2/CH_4) and desorption pressure was set to 1 bar. The composition of the gas mixtures were set as follows in the simulations: CO_2/H_2:15/85, CO_2/N_2: 15/85, CO_2/CH_4: 50/50. In Chapter 5, the adsorbed amount of CO_2 and N_2 were calculated by specifying the pressure of 2 bar and 10^{-6} bar and at 298 K since most MMMs are experimentally tested for

a feed pressure of 2 bar and permeate pressure of vacuum at room temperature. Finally in Chapter 6, two different cases for operating pressure with equimolar CH_4/N_2 mixture were considered. In Case 1, adsorption pressure was set to 1 bar and desorption pressure was set to 0.1 bar to represent vacuum swing adsorption (VSA) operating conditions. In Case 2, adsorption pressure was set to 10 bar and desorption pressure was set to 1 bar to represent pressure swing adsorption (PSA) conditions. All simulations were done at room temperature, 298 K.

3.3. Equilibrium Molecular Dynamics (EMD)

Diffusion defines the movement of a particle. The term self-diffusivity gives us the movement of a tagged single particle, while corrected-diffusivity is used for the movement of a bulk solution. For binary-gas systems self-diffusivity is preferred but for systems with a single chemical species, the corrected diffusivity is used. Self-diffusivities or corrected-diffusivities of each gas component in MOFs were calculated using Equilibrium Molecular Dynamics (EMD) simulations at NVT ensemble (constant number of molecules, constant volume and constant temperature) with the Nose-Hoover thermostat algorithm.[57] At least 10 independent trajectories were collected for self-diffusivities, and at least 20 independent trajectories were collected for corrected-diffusivities for 16 ns length during the EMD simulations. Simulation boxes were increased up to 6×5×5 crystallographic unit cells in order to have enough number of the weakly adsorbed components to increase the statistical accuracy of the simulations. Self-diffusion coefficients were reported by taking the average of diffusivities at each direction. Diffusion coefficient found to be less than 10^{-8} cm^2/s were not considered since this value means diffusion is not accessible on the nanosecond time scales using MD.

3.4. Mixed Matrix Membranes (MMMs)

For MMM calculations that are described in Chapter 5, EMD simulations were performed to calculate the corrected diffusivity (D_0) of each gas. These simulations were

done at average of feed and permeate pressure loadings that were obtained from the GCMC simulations. In each EMD simulation, 20 independent trajectories with 16 ns length were collected. Corrected diffusivities of gases were calculated in three directions and average diffusivity was reported. If diffusion was in one (two) direction(s), only that diffusivity (average diffusivity of these directions) was used. The simulation volume was increased up to 6×6×6 crystallographic unit cells to ensure that it contains enough gas molecules at the lowest loadings to increase the statistical accuracy of the simulations. In Chapter 6, binary gas uptakes obtained from the GCMC simulations at the desired pressure were the input of the EMD simulations. At least 10 independent trajectories were collected for 16 ns length during the EMD simulations. Simulation boxes were increased up to 3×3×3 crystallographic unit cells at 10 bar and 15×15×15 crystallographic unit cells at 0.01 bar in order to have enough number of the weakly adsorbed components to increase the statistical accuracy of the simulations. Self-diffusion coefficients were reported by taking the average of diffusivities at each direction.

3.4. Calculating Adsorbent Properties of MOFs

Several quantitative criteria have been used so far by experimental and simulation studies to evaluate adsorption-based gas separation performances of materials. In this thesis, six widely used criteria were used, adsorption selectivity (S_{ads}), working capacity (ΔN), regenerability (R%), pressure swing adsorption (PSA) sorbent parameter (S), sorbent selection parameter (S_{sp}) and adsorption figure of merit (AFM). How these terms were calculated are explained below.

Adsorption selectivity, S_{ads} is the most widely used criteria to evaluate adsorbents and it is simply defined as the ratio of compositions of the adsorbed gases (x) in the adsorbent material normalized by the ratio of bulk phase compositions (y) of component 1 to component 2:

$$S_{ads(1/2)} = \frac{x_1 / x_2}{y_1 / y_2} \quad (1)$$

Here, subscript 1 represents strongly adsorbed gas and subscript 2 represents weakly adsorbed gas. In Chapters 4 and 5, component 1 is always CO_2 and component 2 changes with respect to the mixture (CH_4, H_2, N_2). In Chapter 6, component 1 is always CH_4 and component 2 is N_2.

Bae and Snurr[61] stated that adsorption selectivity cannot represent cyclic PSA and vacuum swing adsorption (VSA) processes by itself. Therefore, working capacity (ΔN) which can be considered as the second most widely used criteria to rank the adsorbents was defined. Working capacity is generally defined for the strongly adsorbed component of the gas mixture, therefore working capacities were reported for CO_2 in Chapter 4 and Chapter 5, and for CH_4 in Chapter 6. It can be calculated as the difference between the gas uptakes at the adsorption (N_{ads}) and desorption (N_{des}) pressures in the unit of mol gas/kg adsorbent:

$$\Delta N = N_{ads} - N_{des} \quad (2)$$

Regenerability (R%) is an important criterion in cyclic PSA and VSA processes[7] and used to determine the per cent regeneration of the adsorption sites while desorption step is ongoing.[61] It is the ratio of working capacity to the amount of the strongly adsorbed gas component at the adsorption pressure:

$$R\% = \frac{\Delta N}{N_{ads}} \times 100\% \quad (3)$$

Notaro and coworkers[62] proposed a criterion that is applicable for non-Langmuir systems. It was called adsorption figure of merit (AFM) and empirically derived to obtain a sorbent parameter for N_2 selectivity in air separation processes. AFM was used to calculate N_2/O_2 separation performance of various zeolites. In this thesis, AFM for CO_2 is calculated by using selectivity from N_2, CH_4 and H_2. AFM is defined as follows:

$$AFM = \Delta N \times \frac{S_{ads}^2}{S_{des}} \quad (4)$$

Rege and Yang[63] proposed a dimensionless sorbent parameter (S) that is suitable for PSA processes. They investigated binary O_2/N_2 separation in zeolites using this term. S is particularly suitable for binary gas separation based on the differences in equilibrium adsorption capacity. This parameter considers the ratio of working capacities of gases in the mixture and the adsorption selectivity of the adsorbent:

$$S = S_{ads,1} \times \frac{\Delta N_1}{\Delta N_2} \quad (5)$$

Bae and Snurr[61] stated that PSA sorbent parameter (S) is suitable for Langmuir adsorption because S_{ads} is equivalent to the ratio of Henry's law constants of two components, and S_{ads} term should be replaced with (S_{ads}^2/S_{des}) for non-Langmuir systems as it was proposed by Notaro et al. for AFM.[62] They used sorbent selection parameter (S_{sp}) shown in Eq. (6) to investigate 40 MOFs for their CO_2 separation performances from natural gas, landfill gas and flue gas.

$$S_{sp} = \frac{S_{ads}^2}{S_{des}} \times \frac{\Delta N_1}{\Delta N_2} \quad (6)$$

3.5. Calculating Membrane Properties of MOFs

MOFs that were identified to exhibit high performance in adsorption-based separations were also examined for kinetic-based separation. Membrane selectivity and permeability are generally used to assess kinetic-based separation performance of materials. Calculations of membrane selectivity and permeability require the self-diffusion coefficients ($D_{i,self}$) of gas components in their binary mixtures. Self-diffusivities of gas components (1, 2) computed from EMD simulations were used to calculate diffusion selectivity (S_{diff}) of MOFs:

$$S_{diff\,(1/2)} = \frac{D_{1,self}}{D_{2,self}} \quad (7)$$

Membrane selectivity (S_{mem}) of MOFs were then estimated by multiplying the adsorption and diffusion selectivities as suggested by Keskin and Sholl:[64]

$$S_{mem} = S_{ads(1/2)} \times S_{diff\,(1/2)} \tag{8}$$

High gas permeability is also required for an efficient membrane based gas separation. Permeabilities of components were calculated by using the following equation,[65]

$$P_1 = \frac{\phi \times D_{1,self} \times c_1}{f_1} \tag{9}$$

where P, ϕ, D_{self}, c and f represent the permeability of gas (mol/m/s/Pa), porosity of the MOF, self-diffusion coefficient of the component in the binary mixture (m^2/s), concentration of the component at the upstream face of the membrane (mol/m^3) and bulk phase fugacity (bar), respectively. Permeability is then converted to Barrer (10^{-8} cm^3(STP)×cm/s×cm^2×bar) since this unit is widely used to report membranes' gas permeabilities.[3] Both selectivity and permeability of membranes were calculated at a membrane feed pressure of 1 bar and permeate pressure of vacuum. The accuracy of this approach was validated for a large number of MOF membranes by comparing with the experimentally measured selectivity and permeability in previous studies of our research group.[66, 67]

3.6. Calculating Gas Permeability of MMMs

These calculations were performed only for CO_2/N_2 separation discussed in Chapter 5. Transport diffusivity (D_t) was calculated by multiplying the corrected diffusivity (D_0) obtained from EMD simulations with the thermodynamic correction factor,[68] the partial derivative relating adsorbate concentration, *c* and the bulk phase fugacity, *f*. If the single-component adsorption isotherm of the gas is known, the thermodynamic correction factor can be fully defined as follows:

$$D_t(c) = D_0(c) \cdot \frac{\delta \ln f}{\delta \ln c} \tag{10}$$

Steady-state gas fluxes (*J*) through a MOF were then calculated based on Fick's law,[68]

$$J = -D_t(c) \cdot \nabla c \tag{11}$$

where ∇c is the concentration gradient of the adsorbed species based on the difference between feed and permeate pressures of the membrane. Gas flux in a MOF was then converted to gas permeability (P_{MOF}), using the pressure drop (ΔP) and membrane thickness (L), as shown below:

$$P_{MOF} = \frac{J}{\Delta P / L} \tag{12}$$

Permeation selectivity (also referred as membrane selectivity) of a MOF (S) was calculated from the ratio of gas permeability of two components:

$$S_{i/j} = \frac{P_i}{P_j} \tag{13}$$

Gas permeabilities of MMMs were calculated using the well-known Maxwell model.[69] Erucar and Keskin[35] previously compared several theoretical permeation models, including the Maxwell, modified Maxwell, Bruggeman, Lewis-Nielson, Pal, Felske and modified Felske and showed that the Maxwell model is the best predicting model among the ones considering ideal morphology. In addition to these, a recent study used the Maxwell model to predict CO_2 and N_2 permeabilities of MOF-based MMMs with a MOF volume fraction of 0.3 and showed the good agreement between simulation results and experiments for gas permeabilities of MOF-based MMMs.[37] These results suggested that it is reasonable to use the Maxwell model for estimating separation performance of new MOF-based MMMs for which experimental gas permeability data are not available. The Maxwell model predicts a MMM's gas permeability (P) based on the polymer's gas permeability (P_p), filler particle's permeability (P_f) and the volume fraction of the filler particle within the polymer matrix (ϕ) as follows:

$$P = P_p\left[\frac{2(1-\phi)+(1+2\phi)\lambda_{fp}}{(2+\phi)+(1-\phi)\lambda_{fp}}\right] \quad (14)$$

$$\lambda_{fp} = \frac{P_f}{P_p} \quad (15)$$

MOF's permeability, P_{MOF}, calculated from Eq.(12) was used as the filler particle's permeability (P_f) in Eq.(15). Gas selectivities of MMMs were computed as the ratio of gas permeabilities obtained from the Maxwell model similar to Eq.(13).

Chapter 4

RANKING OF MOF ADSORBENTS FOR CO_2 SEPARATIONS*

In this chapter molecular simulations were used to examine adsorption-based separation performances of MOFs in separation of CO_2/CH_4, CO_2/N_2 and CO_2/H_2 mixtures under different operating conditions. In Case 1, adsorption pressure was set to 1 bar and desorption pressure was set to 0.1 bar. In Case 2, adsorption pressure was set to 10 (5) bar for CO_2/H_2 and CO_2/N_2 mixtures (CO_2/CH_4) and desorption pressure was set to 1 bar. The composition of the gas mixtures were set as follows in the simulations: CO_2/H_2:15/85, CO_2/N_2: 15/85, CO_2/CH_4: 50/50. First, the results of our molecular simulations with the experimentally available data for CO_2 adsorption and separation performances of various MOFs were compared. Motivated from the good agreement between simulations and experiments, our simulations were extended to 100 different MOF materials. Several adsorbent evaluation metrics including selectivity, working capacity, adsorption figure of merit, sorbent selection parameter, per cent regenerability were computed for each MOF and for each gas separation. Ranking of the MOFs based on these metrics was examined in detail to understand which parameters play key roles in assessing gas separation potential of MOF adsorbents. Results showed that regenerability is a very important metric to screen the materials at the first step of the adsorbent search and MOFs can be then ranked based on selectivity. The relations between easily computable structural properties such as pore sizes, surface areas and porosities of MOFs and adsorbent evaluation metrics were also examined to provide structure-property relationships that can serve as a guide for experimental studies. Materials

*The results given in this chapter were published in Industrial & Engineering Chemistry Research with following reference: Z. Sumer and S. Keskin, "Ranking of MOF Adsorbents for CO_2 Separations: A Molecular Simulation Study", Industrial & Engineering Chemistry Research 55(39), 10404-10419 (2016). The original manuscript has been rearranged to conform to the format requirements of the dissertation.

with pore sizes of 4-7 Å, surface areas of 200-800 m^2/g and porosities of 0.18-0.50 were found to be the best adsorbent candidates for CO_2/CH_4, CO_2/N_2 and CO_2/H_2 separations. Finally, kinetic-based separation potential of MOFs which were identified as the top performing materials for adsorption-based separations was analyzed. Both membrane selectivities and permeabilities of MOFs were computed for three gas separation processes. Several MOFs were identified to outperform polymers and zeolites in membrane-based CO_2 separations.

4.1. Adsorbent Performances of MOFs

In order to validate the accuracy of our molecular simulations, first the results of GCMC simulations with the available experimental data were compared. 22 experimental data points for CO_2 uptake and 15 experimental data points for CO_2/CH_4 and CO_2/N_2 selectivities of various MOFs including widely-studied subfamilies such IRMOFs, ZIFs, MILs, MOF-74 series were collected. Our molecular simulations were performed under the same pressure and temperature conditions with the experiments. The name of the MOFs, operating conditions (pressure and temperature), and related experimental references for Figure 4.1(a) were reported in Table B1. Figure 4.1(a) shows that there is a good agreement between simulations and experiments for single-component CO_2 uptake of several different types of MOFs. Some experimental studies performed mixture adsorption isotherm measurements to report selectivities whereas some others only performed single-component adsorption isotherm measurements and used Ideal Adsorbed Solution Theory (IAST)[70] to predict mixture selectivities of MOFs. The method of experiments used to report selectivities and corresponding references of these experimental studies were given in Table B2 together with the pressure and temperature conditions. All selectivities were calculated using molecular simulations for gas mixtures having the same composition with the corresponding experimental study. Figure 4.1(b) also shows the good agreement between simulations and experiments for CO_2/CH_4 and CO_2/N_2 selectivities of MOFs. These results suggested that the

atomic models used in our simulations are accurate to predict adsorption-based CO_2 separation performances of MOFs for which there is no available experimental data.

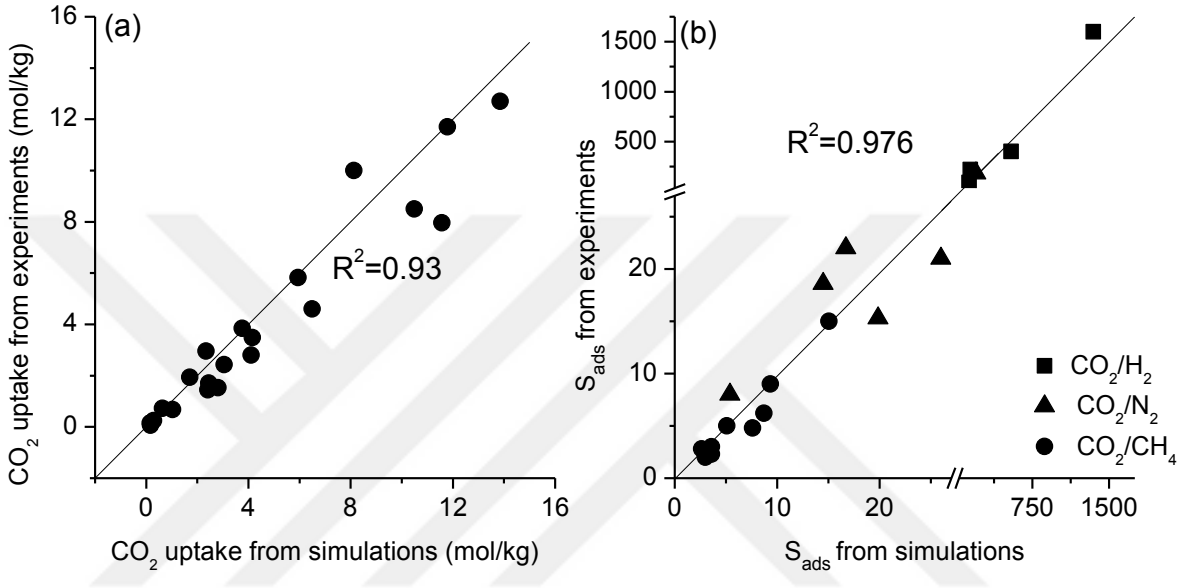

Figure 4.1. Comparison of simulation results with the experiments (a)CO_2 uptake (b)CO_2/N_2 and CO_2/CH_4 adsorption selectivities of various MOFs. Tables B1 and B2 show the complete data set.

In order to assess adsorption-based gas separation performances of MOFs, adsorption selectivity (S_{ads}), working capacity (ΔN), PSA sorbent parameter (S), sorbent selection parameter (S_{sp}), regenerability (R%), adsorption figure of merit (AFM) for CO_2/H_2, CO_2/N_2, CO_2/CH_4 separations were calculated. The results of Case 1 was shown throughout the thesis and gave the results of Case 2 in Appendix B. Molecular simulations showed that CO_2 is more strongly adsorbed compared to H_2, N_2 and CH_4 as expected. The preferential adsorption of CO_2 over other gases can be explained by the van der Waals interactions and electrostatic interactions. CO_2 was represented as a three-site molecule which has more interactions sites

with the MOF atoms compared to other gases. In addition to van der Waals interactions, CO_2 has additional electrostatic interactions with the MOF atoms due to its quadrupole moment. In fact, N_2 also has electrostatic interactions with MOFs but its quadrupole moment (4.7 C m^2) is lower compared to the that of CO_2 (13.4 C m^2).[71] Since adsorption favors CO_2 over other gases in the mixtures, CO_2 selectivities of MOFs were reported.

First adsorption selectivity and working capacity of MOFs for three different gas separation processes were examined in Figure 4.2. The CO_2 selectivities of MOFs are in the range of 10-2260, 3-192 and 1-57 for CO_2/H_2, CO_2/N_2 and CO_2/CH_4 mixtures, respectively. Calculated CO_2 working capacities are in the range of 0.1-2.2, 0.1-2.1, 0.2-3.8 mol/kg for CO_2/H_2, CO_2/N_2, CO_2/CH_4 mixtures, respectively. Figure 4.2(a) shows that EMIVAY and EYOQAL exhibit both high selectivity (2259.8 and 2080.6, respectively) and high working capacity (1.49 and 1.64 mol/kg, respectively) for separation of CO_2/H_2 mixtures. Figures 4.2(b) and (c) show that the two MOFs that have the highest CO_2 selectivities exhibit low working capacities. KEYFIF and KEYFIF01 have high CO_2/N_2 selectivity, around 192, but their working capacities are lower (~0.56 mol/kg) compared to the other MOFs. Similarly, these two MOFs have significantly higher CO_2/CH_4 selectivities (~60) than the other MOFs (1-20) but again these MOFs suffer from low working capacities (~0.8 mol/kg). The high CO_2/N_2 and CO_2/CH_4 selectivities of KEYFIF and KEYFIF01 can be explained with very small N_2 and CH_4 uptake of these materials. These MOFs have relatively lower pore volumes (0.25 cm^3/g) and narrow pore sizes (4.8-5.4 Å) compared to other MOFs which hinder adsorption of larger gas molecules such as N_2 and CH_4.

Materials exhibiting both high selectivity and high working capacity are considered as highly promising adsorbents. Kim and coworkers[72] previously studied zeolites for C_2H_6/C_2H_4 separation and defined a reference performance curve of selectivity×working capacity=3 to separate high and low performance regions within zeolite search space. The choice of 3 was arbitrary to provide a reference that qualitatively defines a number of

promising materials for C_2H_6/C_2H_4 separation. Following their idea, reference curves for CO_2 separations in order to identify highly promising materials among 100 MOFs considered were arbitrarily defined. Reference performance curves of selectivity×working capacity=1000, 100 and 20 were chosen for CO_2/H_2, CO_2/N_2 and CO_2/CH_4 separations, respectively and these curves were shown with red dotted lines in Figure 4.2. Figure 4.2(a) shows that 11 MOFs exceed the reference curve for CO_2/H_2 separation. For example, EYOQAL, EMIVAY and BERGAI01 were able to exceed the reference curve due to their high CO_2/H_2 selectivities (2080.6, 2259.7 and 1723.9, respectively). They also have moderate working capacities (1.6 mol/kg, 1.5 mol/kg and 0.9 mol/kg, respectively) which make them promising adsorbents for CO_2/H_2 separation. EMIHAK, HAJKOU, RAYLIO and EYOPOY exceed the curve due to their moderate CO_2/H_2 selectivities (696.7, 772.2, 751 and 616.1, respectively) and high working capacities (2.2, 1.9, 1.8 and 1.8 mol/kg, respectively). Remaining of the 11 MOFs was very close to curve with moderate selectivities and working capacities. In Figure 4.2(b), only 8 of the MOFs could exceed the reference curve. There is an observable trade-off between adsorption selectivity and working capacity of the materials above the curve. Two MOFs, KEYFIF and KEYFIF01, were able to exceed the curve due to their high CO_2/N_2 selectivities (192.2 and 191.2), but they have the lowest working capacities among the 8 MOFs (both ~0.56 mol/kg). EMIHAK, on the other hand, has low CO_2/N_2 selectivity (53.4) but the highest working capacity (2.1 mol/kg) among 100 MOFs studied for CO_2/N_2 separation. The highest number of MOFs that could exceed the curve was for CO_2/CH_4 separation as shown in Figure 4.2(c). 14 MOFs were identified to be promising for this separation. The highest CO_2/CH_4 selectivities belong to KEYFIF (56.6) and KEYFIF01 (55.7), but as discussed for CO_2/N_2 separation, these two MOFs have very low working capacities (both ~0.8 mol/kg). The other MOFs were able to exceed the curve due to their high working capacities although their CO_2/CH_4 selectivities are either low or moderate.

Results of Figure 4.2 illustrate that MOFs generally classified as promising due to their high working capacities rather than their selectivities. In order to better evaluate the potential of MOF adsorbents, the CO_2 selectivities and working capacities of MOFs with zeolites were compared. Available experimental gas adsorption isotherms of several zeolites taken from the literature were used to calculate adsorption selectivity and working capacity of these materials at 298 K, at an adsorption (desorption) pressure of 1 bar (0.1 bar).

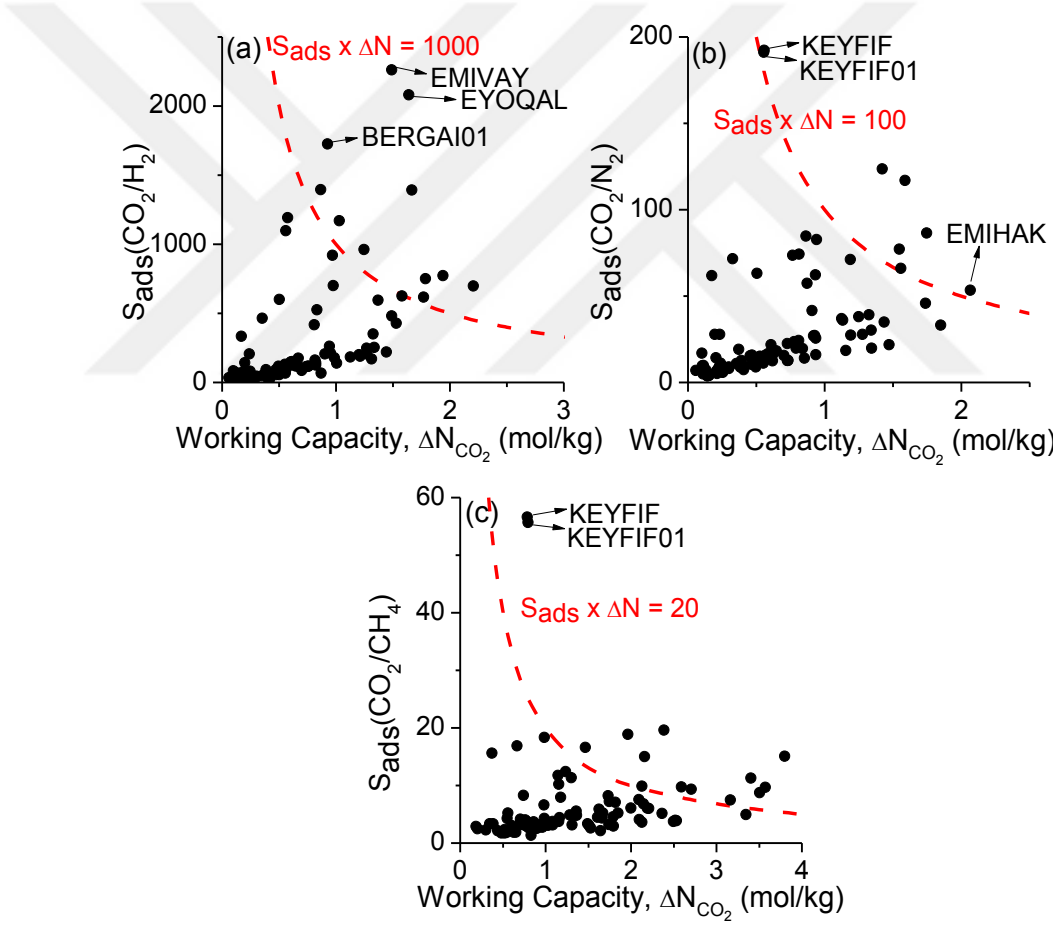

Figure 4.2. Adsorption selectivity (S_{ads}) vs. working capacity (ΔN_{CO_2}) of MOFs for separation of (a)CO_2/H_2 (b)CO_2/N_2 and (c)CO_2/CH_4 mixtures.

Cavenati et al.[73] measured single-component gas adsorption isotherms for CO_2, N_2 and CH_4 in zeolite 13X. Using these adsorption isotherm data, CO_2 working capacity was calculated as 2.12 mol/kg and ideal adsorption selectivities as 90.6 for CO_2/N_2 and 8.02 for CO_2/CH_4. Merel et al.[74] measured single-component gas adsorption in zeolite 5A. Ideal CO_2/N_2 selectivity was calculated as 41.3 and CO_2 working capacity as 0.75 mol/kg. Xu et al.[75] studied zeolites Hβ and Naβ at 303 K. Ideal CO_2/N_2 (CO_2/CH_4) selectivity was calculated as 66.1 (5) in Hβ and as 38.3 (4.9) in Naβ using their reported adsorption isotherms. Working capacities of Hβ and Naβ were calculated to be around 1.3 mol/kg. This comparison shows that several MOFs can outperform traditional zeolites in adsorption-based CO_2 separations under the same operating conditions.

Krishna et al.[76] performed molecular simulations for CO_2/H_2, CO_2/N_2 and CO_2/CH_4 adsorptions in commonly used zeolites including NaX, NaY, AFX and CHA as well as several MOFs at 300 K at an adsorption (desorption) pressure of 10 bar (1 bar). These operating conditions are similar to the ones considered in Case 2 for which the results were presented in Figure B1. According to their results, NaX (~2000) and NaY (~550) have high CO_2 selectivity in CO_2/H_2 separation because of their non-framework cations that lead to strong electrostatic interaction between CO_2 and Na^+. However, these zeolites have low working capacities (~1 and ~2.5 mol/kg, respectively) which prevent their practical usage. The highest CO_2/H_2 selectivities obtained in this thesis for Case 2 were ~1000 (EYOQAL) and 892 (EMIHAK) which are lower than those of zeolites as shown in Figure B1(a). The highest working capacity was obtained for NUTQEZ (PCN-16') for CO_2/H_2 separation as 7.71 mol/kg which is higher than any zeolite that was investigated by Krishna et al.[76] According to their results, NaX and NaY were also reported to show the highest CO_2/N_2 selectivity (~3000 and 500, respectively) whereas Mg-MOF-74 and Zn-MOF-74 were reported to have the highest working capacities ~6 mol/kg and ~4 mol/kg, respectively. Calculated CO_2 working capacity of Zn-MOF-74 in this thesis is 4.1 mol/kg, which agreed

with the previously reported one.[48] PCN-16' exhibited higher working capacity than Zn-MOF-74, 6.33 mol/kg for CO_2/N_2 separation as shown in Figure B1(b). Most MOFs that considered in this thesis have similar CO_2/CH_4 separation performance with zeolites.[76] For example, KEYFIF and KEYFIF01 have similar selectivity with NaX (~40) and they outperform NaY (~30). The highest reported working capacity for CO_2/CH_4 separation belongs to CHA (~4 mol/kg) among the zeolites, which is exceeded by many MOFs. MOCKAR (6.7 mol/kg), PCN-16' (6.6 mol/kg) and OWIVEW (6.4 mol/kg) are the MOFs with highest CO_2 working capacities, and almost quarter of MOFs shown in Figure B1(c) have working capacity greater than 4 mol/kg. These results show that MOFs have generally similar CO_2 selectivities (or lower) with zeolites but their working capacities are significantly higher than traditional zeolites, especially under the operating conditions of Case 2.

Figure 4.3 shows S_{sp} of MOFs as a function of their adsorption selectivities for three gas separations. Similar data is also shown for Case 2 in Figure B2. A significant portion of MOFs is located in a region where selectivity is less than 500 and S_{sp} is less than 10,000 for CO_2/H_2 separation as shown in Figure 4.3(a). The most promising adsorbent candidates are positioned at the top right corner of this figure. There are two MOFs, EYOQAL and EMIVAY, which exhibit high S_{sp} (390,000 and 340,000, respectively) and high CO_2/H_2 selectivity (2080.6 and 2259.8, respectively). In Figure 4.3(b) (Figure 4.3(c)) most MOFs are located in a region where selectivity is in the range of 1-100 (1-15) and S_{sp} is in the range of 1-600 (1-200). KEYFIF and KEYFIF01 have the highest S_{sp} and selectivity both for CO_2/N_2 and CO_2/CH_4 separations. It is important to note that MOFs which are widely studied in the literature as adsorbents or membranes for CO_2 separation such as IRMOF-1, ZIF-8, ZIF-79, MIL-47, BioMOF-11 are generally located in a region where S_{sp} and selectivity are not very high as shown in Figure 4.3. This observation highlights the fact that the most promising materials for CO_2 separation have not been experimentally studied as adsorbents yet. Even by studying only 100 different MOFs, it can be shown that there are many more

candidate materials with better separation properties than the materials which have been widely studied in the literature.

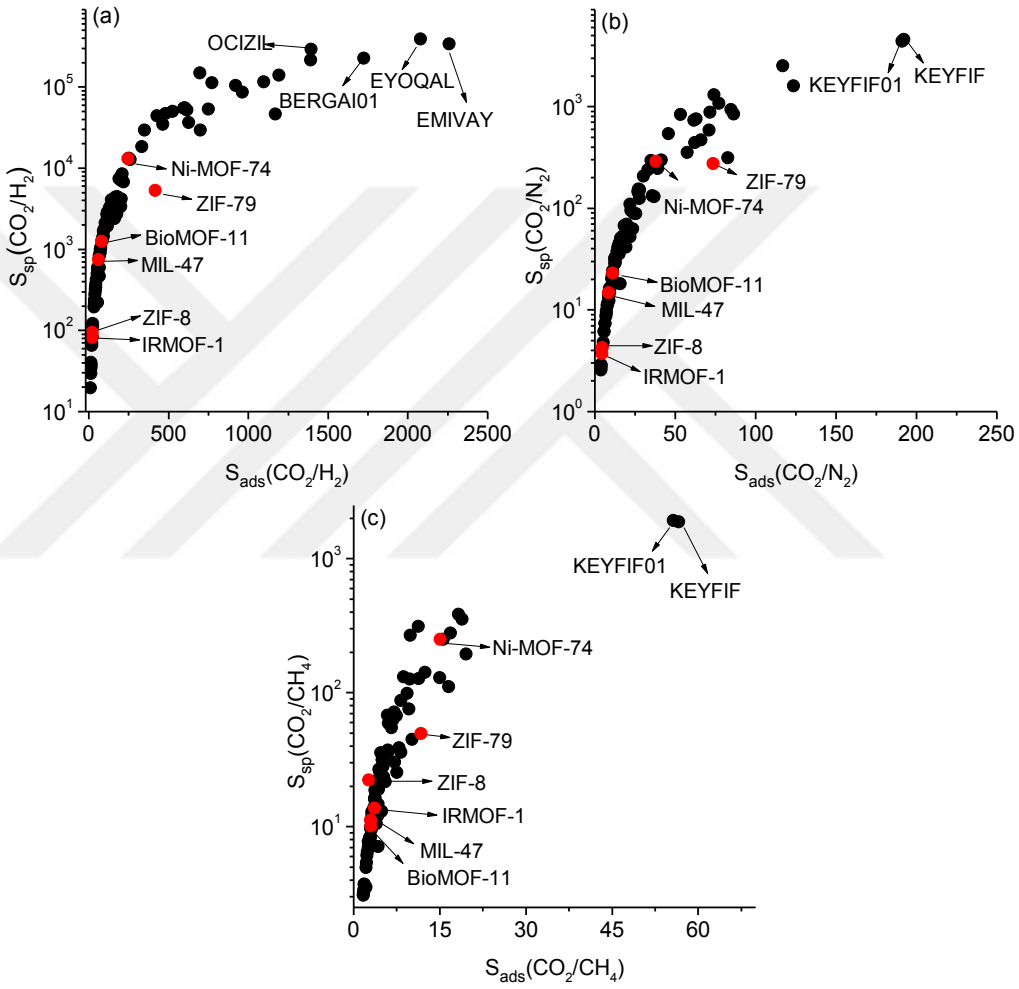

Figure 4.3. Sorbent selection parameter (S_{sp}) vs. adsorption selectivity (S_{ads}) of MOFs for separation of (a)CO_2/H_2 (b)CO_2/N_2 and (c)CO_2/CH_4 mixtures.

High per cent regenerability (R%) is desired in addition to high selectivity and high working capacity for practical applications of adsorbents. The relation between R% and

adsorption selectivity of MOFs is shown in Figure 4.4. As the selectivity increases, R% tends to decrease for all three gas separations. Figure 4.4(a) shows that several MOFs exhibit very high CO_2/H_2 selectivities (>1000) but their R% values are less than 75% suggesting that these materials may not find place in practical applications. 82 out of 100 MOFs for CO_2/H_2 separation have R% between 80-100%.

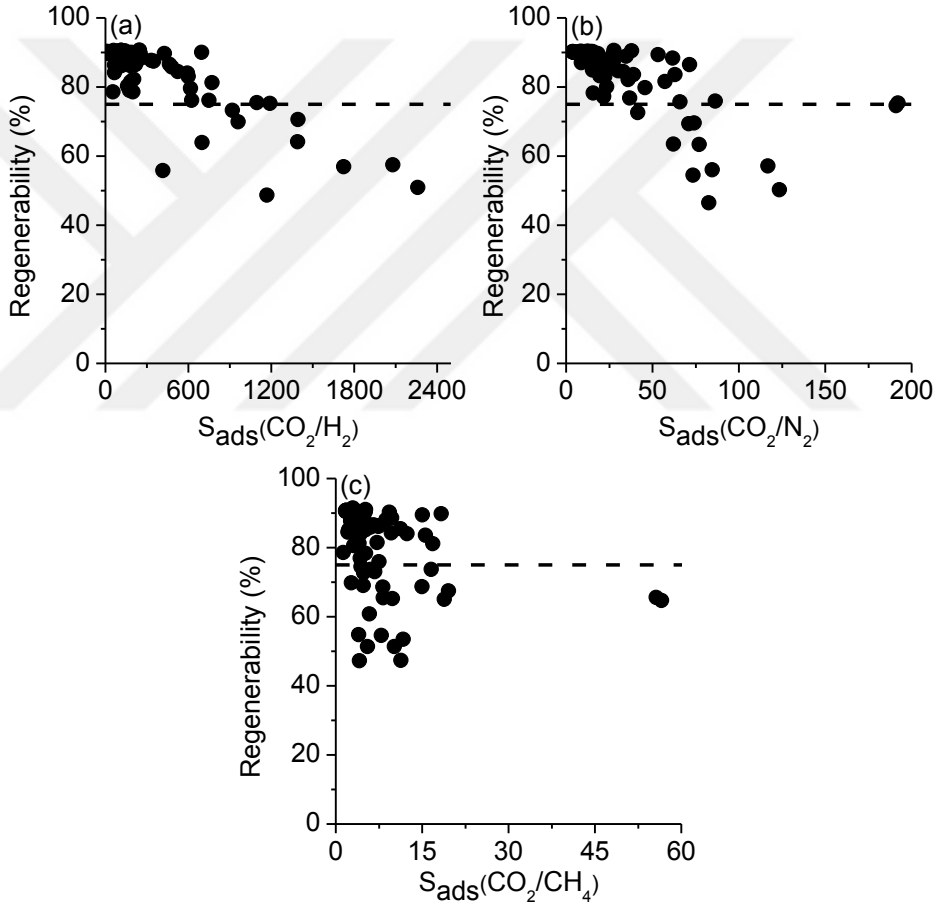

Figure 4.4. Regenerability (R%) vs. adsorption selectivity (S_{ads}) of MOFs for separation of (a)CO_2/H_2 (b)CO_2/N_2 and (c)CO_2/CH_4 mixtures. Dashed line indicates 75% regenerability.

Same discussion is valid for Case 2 as shown in Figure B3. Tong et al.[77] calculated R% of 46 COFs for CO_2/N_2 separation and reported that 42 COFs have R% between 80-90%. R% of 100 MOFs for CO_2/N_2 separation were shown in Figure 4.4(b). 80 MOFs have R% between 80-100%. 73 out of 100 MOFs for CO_2/CH_4 separation have R% between 80-100% (Figure 4.4(c)). The R% of MOFs that were identified to show high S_{sp} and selectivity in Figure 4.3 are also checked. For example, one of the promising MOFs for CO_2/H_2 separation shown in Figure 3(a), OCIZIL, has a reasonable regenerability, 71%. However, most of the MOFs that were identified as highly promising materials (EMIVAY, EYOQAL, BERGAI01) have R% values lower than 65%. It was shown in Figure 4.3(b) that KEYFIF and KEYFIF01 have high CO_2/N_2 selectivities and high S_{sp} values. These materials also have reasonable R% values (75% and 74%, respectively). EMIVAY and EYOQAL were also considered as promising with selectivities above 115, but their R% values were not promising (50% and 57%, respectively) for CO_2/N_2 separation. KEYFIF and KEYFIF01 were identified as promising adsorbents for CO_2/CH_4 separation in Figure 4.3(c) with very high S_{sp} values (1880 and 1929, respectively), but they have low R% values (both 65%), again limiting their practical usage. These results are very important because they illustrate that assessing the MOF adsorbents based on only their selectivities is not an accurate approach. Regenerability should be also used in ranking of MOF adsorbents as an important metric.

4.2. Ranking of MOF Adsorbents

After calculating several metrics to assess adsorption-based CO_2 separation performances of MOFs, ranking the MOF adsorbents based on these metrics to identify the most promising materials was aimed. The top ten MOFs with the highest CO_2 separation performance based on six different criteria are given in Table 4.1. Data on this table was calculated for Case 1 and similar list for Case 2 can be found in Table B3. The first

observation from this table is that although ranking of the adsorbents change depending on the performance metric used, the materials that appear in the lists are generally common.

For example, EMIVAY, EYOQAL and QIFLOI are the three MOFs that appear in the top ten lists prepared based on S_{sp}, S_{ads}, ΔN, AFM and S values both for CO_2/H_2 and CO_2/N_2 separations. In other words, regardless of which criterion is used, these MOFs can be identified as promising adsorbents. As shown in section 3.4, some metrics are closely related and same MOFs appear in the rankings based on these related metrics. The number of common MOFs in ranking of materials based on two different criteria is listed in Table B5. The closest relation can be seen between S_{ads} and S: For CO_2/H_2 and CO_2/CH_4 separations, MOFs in the top ten list are totally same, for CO_2/N_2 separation 8 MOFs are same but with different rankings. This is an expected outcome because S is calculated as the multiplication of S_{ads} with the ratio of working capacities of gases. There is also a strong correlation between S_{sp} and S_{ads}. 8 MOFs in the top ten list are the same in the rankings based on S_{sp} and S_{ads} for all three gas separations. Although S_{sp} considers more parameters than S_{ads} such as working capacities of both gases and desorption selectivity, results of Table 4.1 indicate that using S_{ads} as the sole criterion can lead to the same promising materials list with using S_{sp}. Another close relation is observed between ΔN and AFM. 8 (6) MOFs in the top ten list are the same for CO_2/H_2 and CO_2/N_2 (CO_2/CH_4) separation with different rankings. Either of them can be used to rank MOFs based on their gas uptake capacities.

The most important outcome of this table is perhaps the ranking of materials based on R%. The top ten adsorbents identified based on R% values are completely different than the rankings based on other criteria. This result highlights the challenge of finding an adsorbent that can achieve CO_2 separation with high efficiency in addition to being reusable. No single MOF was found to exist at the top ten materials lists of both selectivity and regenerability. This observation suggests that R% can be one important criterion to eliminate the materials at the first step of MOF adsorbent search. In other words, large scale material screening can

be done to eliminate adsorbents with low R% (preferentially lower than 75%) and then adsorbents can be ranked based on either their S_{ads} or S_{sp} values. In fact, S_{ads} and R% can be considered as the two important criteria that will be useful to rank the materials at low pressure operating conditions (Case 1). At high pressure operating conditions as considered in Case 2, relation between evaluation metrics generally weakens. The number of common MOFs in rankings based on two different criteria decreases as shown in Table B5. This weakened relationship can be explained by the decrease in the working capacity of CO_2 at the conditions of Case 2. For example, EMIVAY has the highest CO_2/H_2 selectivity (2259.8) and the second highest S_{sp} (~340,000) for Case 1. Although its' selectivity sharply decreases to 860.3 at high pressures (Case 2), it is still the third best adsorbent in terms of selectivity. However, with increasing adsorption (desorption) pressure, CO_2 working capacity decreases from 1.49 mol/kg to 0.87 mol/kg whereas H_2 working capacity increases from 5.4×10^{-3} mol/kg to 1.8×10^{-2} mol/kg. As a result the S_{sp} decreases to ~16,000 and EMIVAY cannot remain in the top ten list of S_{sp} values for CO_2/H_2 separation in Case 2. Similar discussion is valid for CO_2/N_2 separation performance of the EMIVAY. Although adsorption selectivity does not change very much when the pressure is increased from 1 bar to 10 bar (from 123.5 to 105.4), due to the decrease in the CO_2 working capacity (from 1.42 to 0.79 mol/kg), material shows low S_{sp} value (1094.5) for Case 2. S_{ads} and S are still the two parameters that have the highest relation. Same 9 (7) MOFs appear in the ranking based on S_{ads} and S for CO_2/H_2 and CO_2/N_2 (CO_2/CH_4) separations.

Table 4.1. Ranking of the top ten MOFs based on different metrics (Case 1).

CO_2/H_2

S_{sp}		S_{ads}		ΔN (mol/kg)		AFM (mol/kg)		S		R (%)	
EYOQAL	389619.17	EMIVAY	2259.75	EMIHAK	2.21	EMIHAK	2494.88	EMIVAY	624950.45	LECQEQ	90.65
EMIVAY	338143.88	EYOQAL	2080.55	HAJKOU	1.94	EYOQAL	2199.12	EYOQAL	604536.22	IDIWOH	90.56
OCIZIL	291695.31	BERGAI01	1723.94	RAYLIO	1.79	EMIVAY	1821.08	BERGAI01	396190.82	DIDBID	90.51
BERGAI01	226673.81	OCIZIL	1393.89	EYOPOY	1.77	QIFLOI	1685.39	OCIZIL	327788.80	DIDBOJ	90.51
QIFLOI	215443.38	QIFLOI	1391.42	QIFLOI	1.67	HAJKOU	1583.29	QIFLOI	296399.02	GALBUS	90.50
EMIHAK	149418.85	KEYFIF01	1192.14	EYOQAL	1.64	OCIZIL	1076.39	KEYFIF01	223376.53	LARVIL	90.48
KEYFIF01	140128.62	EYOPUE	1170.18	RAYLOU	1.58	BERGAI01	915.30	KEYFIF	188458.38	WOBHIF	90.33
KEYFIF	115840.15	KEYFIF	1096.41	AJIHOQ	1.53	EYOPOY	887.26	EYOPUE	141403.03	KUGZIW	90.27
HAJKOU	112693.37	BOWSIQ	962.09	HAJKIO	1.49	AJIHOQ	863.40	BOWSIQ	139976.69	LUMDIG	90.23
PEQHOK	103895.84	PEQHOK	920.67	EMIVAY	1.49	RAYLIO	812.16	PEQHOK	137332.90	HECQUB	90.21

CO_2/N_2

S_{sp}		S_{ads}		ΔN (mol/kg)		AFM (mol/kg)		S		R (%)	
KEYFIF	4582.65	KEYFIF	192.19	EMIHAK	2.07	EYOQAL	190.08	KEYFIF	6040.08	LARVIL	90.55
KEYFIF01	4376.84	KEYFIF01	191.15	ACODED	1.85	EMIHAK	171.67	KEYFIF01	5920.57	LECQEQ	90.49
EYOQAL	2509.62	EMIVAY	123.50	RAYLIO	1.75	EMIVAY	130.78	EYOQAL	2455.90	IDIWOH	90.39
EMIVAY	1601.08	EYOQAL	117.00	HAJKOU	1.74	QIFLOI	120.78	EMIVAY	2148.20	DIDBOJ	90.32
OCIZIL	1304.64	RAYLIO	86.48	EYOQAL	1.59	HAJKOU	105.96	RAYLIO	1204.86	DIDBID	90.27
QIFLOI	1070.28	BERGAI01	84.76	RAYLOU	1.56	RAYLIO	105.86	BERGAI01	1122.10	GALBUS	90.27
BERGAI01	937.06	EYOPUE	82.71	QIFLOI	1.55	KEYFIF	81.33	OCIZIL	1073.09	MOCKAR	90.26
NUJCIE	874.75	QIFLOI	77.09	EYOPOY	1.47	KEYFIF01	78.31	QIFLOI	1056.71	KUGZIW	90.23
RAYLIO	843.76	OCIZIL	74.22	AJIHOQ	1.44	OCIZIL	73.37	NUJCIE	901.63	WOBHIF	90.21
EMIHAK	838.44	YOZBOF	73.55	EMIVAY	1.42	ACODED	72.61	BOWSIQ	799.18	OWIVEW	90.20

CO_2/CH_4

S_{sp}		S_{ads}		ΔN (mol/kg)		AFM (mol/kg)		S		R (%)	
KEYFIF01	1929.03	KEYFIF	56.61	LECQEQ	3.80	AJIHOQ	77.57	KEYFIF	2736.30	IDIWOH	91.45
KEYFIF	1880.12	KEYFIF01	55.68	NUTQEZ	3.57	LECQEQ	62.28	KEYFIF01	2696.62	OWIVEW	90.95
LARVIL	384.79	RAYLIO	19.63	FIQCEN	3.51	FIQCEN	48.42	EMIHAK	354.76	HECQUB	90.80
EMIHAK	352.44	EMIHAK	18.87	AJIHOQ	3.40	EMIHAK	36.86	LARVIL	340.23	OWITAQ	90.77
AJIHOQ	311.70	LARVIL	18.31	HASSUR	3.35	HAJKOU	35.86	RAYLIO	323.21	OWIVAS	90.75
NUJCIE	278.69	NUJCIE	16.86	NEFTOJ	3.16	EMIHIS	32.25	NUJCIE	283.09	OFERUN	90.69
HAJKOU	267.18	FEVFUJ	16.60	WOBHIF	2.71	KEYFIF01	31.74	GIWNUV	244.90	OWITUK	90.67
LECQEQ	249.21	GIWNUV	15.62	EMIHIS	2.59	KEYFIF	30.65	FEVFUJ	232.12	LUKLIN	90.65
GIWNUV	249.06	LECQEQ	15.05	GALBUS	2.53	NUTQEZ	28.80	LECQEQ	228.94	KUGZIW	90.62
RAYLIO	194.57	RAYLOU	14.98	DIDBOJ	2.52	WOBHIF	28.26	RAYLOU	194.31	OWITOE	90.61

The number of different MOFs that appears in Table 4.1 (Case 1) and Table B4 (Case 2) is 57. This means 57 out of 100 MOFs that were considered in this thesis exhibit high gas separation performance based on at least one of the adsorbent selection criteria for any of the three CO_2 separation processes. Table 4.2 demonstrates the 5 different MOFs that are identified as ideal adsorbents for all three gas separations, there are 3 MOFs for case 1 and 3 MOFs for case 2. The common feature of these MOFs is that they are promising based on at least three different selection criteria for each gas separation. In Case 1, EMIHAK shows high S_{sp} and AFM for all gas separations, it has a high ΔN for CO_2/H_2 and CO_2/N_2 separations as well as high S_{ads} and S for CO_2/CH_4 separation. In Case 2, it shows high S_{sp}, S_{ads} and S for all three separations, particularly high AFM for CO_2/H_2 and CO_2/N_2 separations. The reason of the different performances of EMIHAK for different cases is the change in the uptake amounts of components due to the pressure. KEYFIF and KEYFIF01 are the other materials in Case 1 that can be used as promising adsorbents for all three gas separations due to their high S_{sp}, S_{ads}, S and particularly high AFM values for CO_2/N_2 and CO_2/CH_4 separations. The other promising materials for Case 2 are AJIHOQ and EMIHIS. AJIHOQ has high S_{sp}, S_{ads}, AFM and S for all three separations. EMIHIS exhibits high S_{sp} and AFM for all gas separations and it also has high ΔN for CO_2/H_2 and CO_2/N_2 separations, high S_{ads} and S for CO_2/CH_4 separation. Complete values for each criterion can be found in Table 4.1 (Case 1) and Table B4 (Case 2).

R% values of the 5 MOFs that were identified to be promising both in Case 1 and Case 2 were further investigated. The R% values of 3 MOFs in Case 1 for CO_2/H_2, CO_2/N_2, CO_2/CH_4 separations are as follows: KEYFIF, 75.4%, 75.3%, 64.7%; KEYFIF01, 75.2%, 74.5%, 65.6%; and EMIHAK, 90%, 89.3%, 65%. The R% values of 3 MOFs in Case 2 for CO_2/H_2, CO_2/N_2, CO_2/CH_4 separations are as follows: AJIHOQ, 71.4%, 70.8%, 34.5%; EMIHAK, 57.7%, 58.1%, 30%; and EMIHIS, 82.8%, 81.5%, 56.7%. Although they are not in the top ten MOF list based on R%, regenerabilities of these MOFs in Case 1 are not low

indicating that they may be used in practical applications. At that point it is important to note that once a material is found to be highly promising by computational studies, it must be further investigated experimentally for its chemical stability. The stability information of MOFs that were identified to be promising for all three gas separations in Table 4.2. KEYFIF and KEYFIF01 were reported to be stable after being exposed to the open air for three months.[78] EMIHAK (SCIF-7) and EMIHIS (SCIF-9) were synthesized in the same experimental study.[79] One of the materials belonging to the same family, SCIF-3, was reported to be thermally stable up to 200˚C but no specific information about stability of EMIHAK or EMIHIS was given. AJIHOQ was reported to be thermally stable up to 300˚C.[80]

Table 4.2. MOFs that exhibit high separation performance for all three CO_2 separations.

Case 1

MOFs	CO_2/H_2						CO_2/N_2						CO_2/CH_4					
	S_{sp}	S_{ads}	ΔN	AFM	S	R%	S_{sp}	S_{ads}	ΔN	AFM	S	R%	S_{sp}	S_{ads}	ΔN	AFM	S	R%
KEYFIF	✓	✓			✓		✓	✓		✓	✓		✓	✓		✓	✓	
KEYFIF01	✓	✓			✓		✓	✓		✓	✓		✓	✓		✓	✓	
EMIHAK	✓		✓	✓			✓		✓	✓			✓	✓		✓	✓	

Case 2

MOFs	CO_2/H_2						CO_2/N_2						CO_2/CH_4					
	S_{sp}	S_{ads}	ΔN	AFM	S	R%	S_{sp}	S_{ads}	ΔN	AFM	S	R%	S_{sp}	S_{ads}	ΔN	AFM	S	R%
AJIHOQ	✓	✓		✓	✓		✓	✓		✓	✓		✓	✓		✓	✓	
EMIHAK	✓	✓		✓	✓		✓	✓		✓	✓		✓	✓			✓	
EMIHIS	✓		✓	✓			✓		✓	✓			✓	✓		✓	✓	

4.3. Structure-Performance Relations of MOF Adsorbents

Finding relations between structure and performance of MOF adsorbents will be highly useful to guide the future experimental studies on the desired structural characteristics that can result in materials with high CO_2 separation properties. Clear identification of this type

of relations is challenging because separation performance of a material is determined by the interplay of various factors such as chemical topology, porosity, pore size and shape and it cannot be simply correlated to only a single or two structural properties. Several studies in the literature examined the relation between adsorption selectivity and the difference between isosteric heat of adsorption of gases at infinite dilution, ΔQ_{st}^0.[7, 11, 13, 18] As the ΔQ_{st}^0 increases, adsorption selectivity generally increases. However, it was recently shown that if ΔQ_{st}^0 values are large at low adsorbate loadings, then adsorbents' selectivity can be overpredicted.[7] Furthermore, obtaining ΔQ_{st}^0 values require either experimental measurements or GCMC simulations. Therefore, in this thesis to understand the simple relations between adsorption selectivity and easily measurable/computable structural properties were aimed.

Figure 4.5 shows adsorption selectivities of MOFs as a function of their largest cavity diameters (LCDs). The LCD of MOFs that considered in this thesis ranges from 3.96 to 22.93 Å. As the LCD increases, selectivity generally decreases. MOFs with LCDs around 5 Å exhibit higher selectivity than MOFs with larger pore sizes. MOFs that have larger LCDs (>10 Å) have lower selectivities since both gas molecules of the mixture are able to enter into the pores. Wilmer et al.[11] examined hypothetical MOFs and concluded that optimal LCD value is around 5 to 6 Å to achieve high selectivity for separation of CO_2/N_2 under the same adsorption pressure and temperature studied. Their calculations were based on single-component adsorption data.

Results in this thesis based on mixture adsorption data and a small number of real MOFs support the same finding. The agreement between two studies suggests that some common selectivity-pore size relations exist for MOFs regardless of their topology, either real or hypothetical. Figure 4.5 shows that MOFs with LCD values around 4.4 to 6 Å exhibit high selectivity for CO_2/N_2 and CO_2/H_2 separation. For CO_2/CH_4 separation, higher LCD values, 5.3-7.6 Å, are required to obtain high selectivity, supporting the previous findings in

the literature.[11] Not only the pore diameter but also porosity strongly influences CO_2 separation ability of MOFs. Calculated porosities of materials are shown using color labeling in Figure 4.5 for Case 1 (for Case 2 in Figure B4). As the porosity increases, adsorption selectivity tends to decrease. This finding was also validated in Figure B5 (Case 1) and Figure B6 (Case 2), where selectivity was shown as a function porosity. As the available pore volume increases it becomes easier for both gas components to be adsorbed into the pores and as a result selectivity decreases.

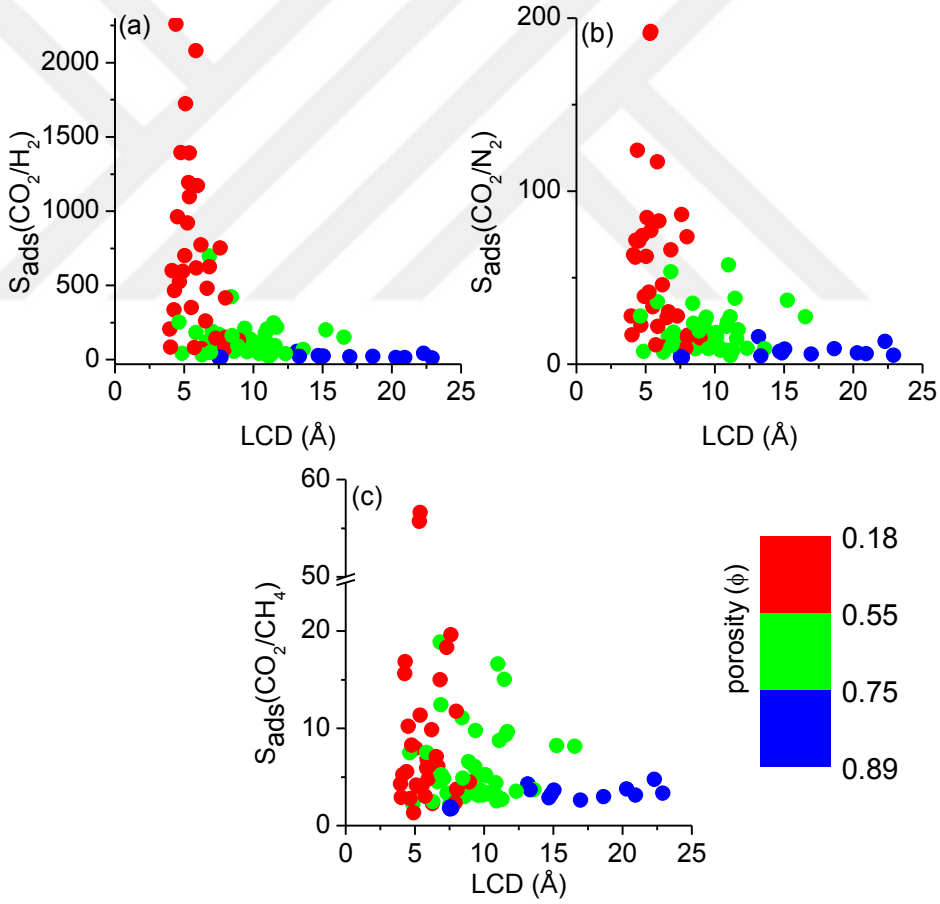

Figure 4.5. Adsorption selectivity (S_{ads}) of MOFs as a function of LCD and porosity for (a)CO_2/H_2 (b)CO_2/N_2 and (c)CO_2/CH_4 separations.

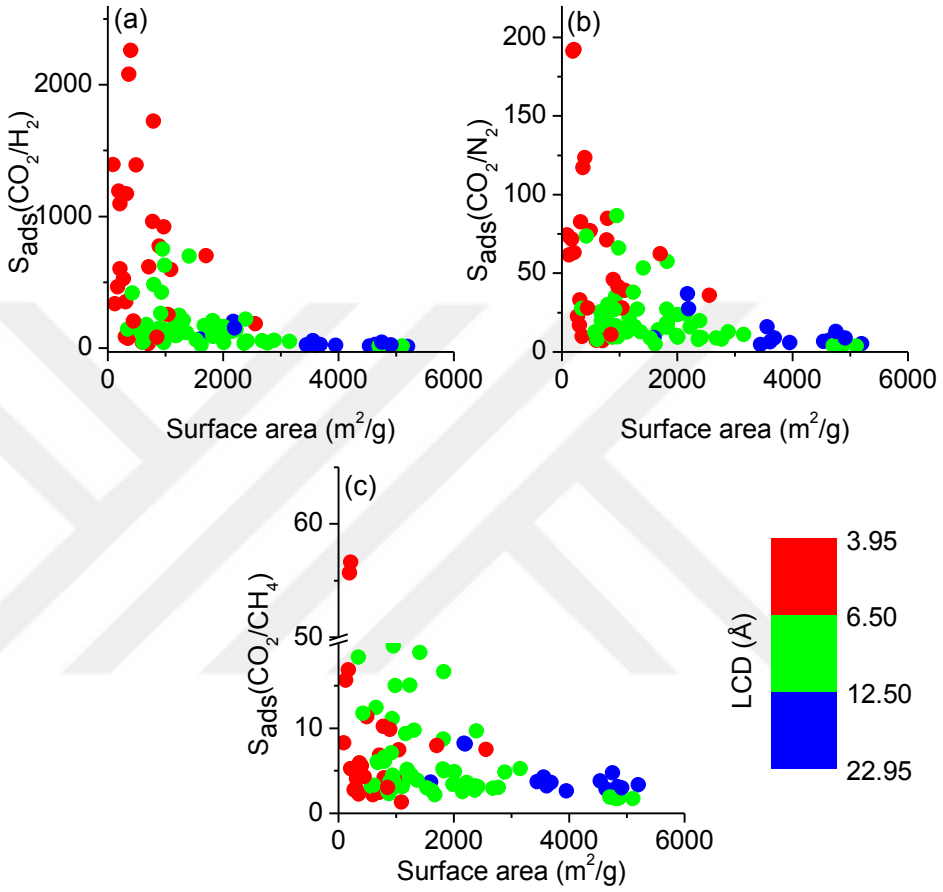

Figure 4.6. Adsorption selectivity (S_{ads}) of MOFs as a function of surface area and LCD for (a)CO_2/H_2 (b)CO_2/N_2 and (c)CO_2/CH_4 separations.

For the materials that have the same LCD, lower porosity generally results in higher adsorption selectivity. For example, PODKUQ (NU-140) has the second highest LCD (22.2 Å) but it has a higher CO_2 selectivity (65.6 for CO_2/H_2, 7.2 for CO_2/CH_4, 19.6 for CO_2/N_2) than any MOF that has almost the same LCD due to its smaller porosity relative to the materials with similar LCDs. Figure 4.6 shows adsorption selectivity of MOFs as a function of their surface areas and LCDs. The surface areas of MOFs that considered in this thesis

ranges from 90.8 to 5202.8 m^2/g. The optimal surface area was observed around 200 to 800 m^2/g to achieve high CO_2 selectivity. Figure 4.6 (Figure B7) shows that for high CO_2 selectivity in Case 1 (2), both low LCD and low surface area are preferable. For example, two of the materials that were identified to be promising, KEYFIF and KEYFIF01, have both low LCD (5.4 Å and 5.3 Å) and low surface areas (214.1 m^2/g and 192 m^2/g).

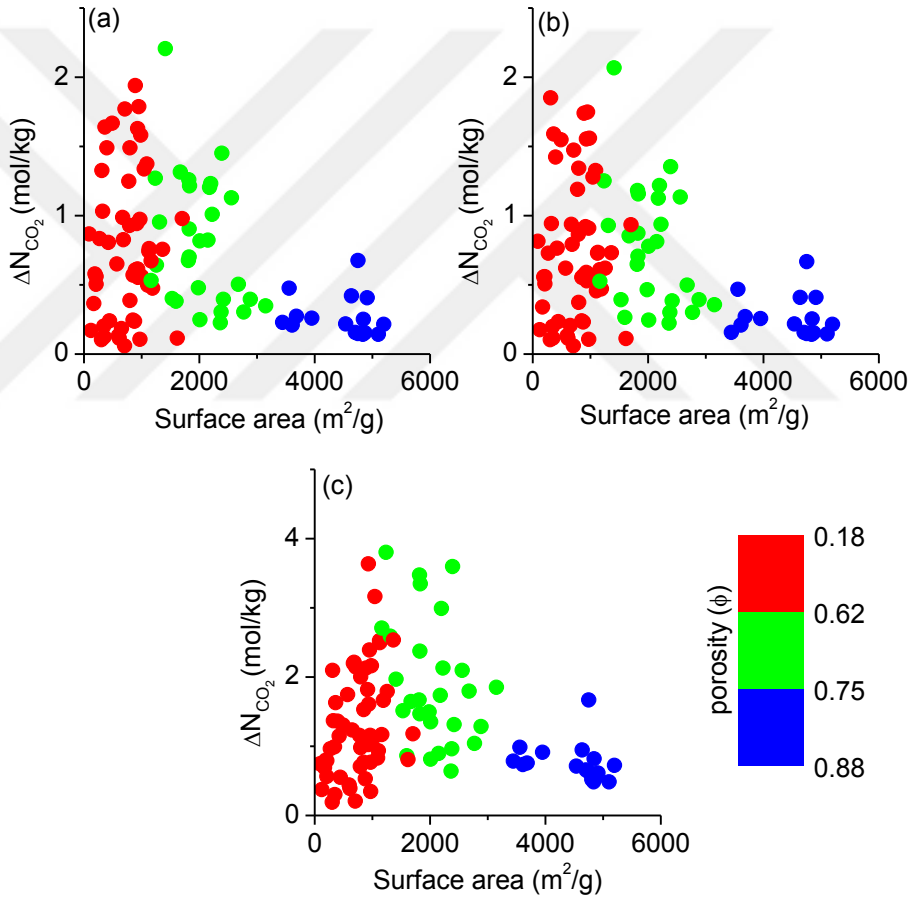

Figure 4.7. Working capacity (ΔN) of MOFs as a function of surface area and porosity for (a)CO_2/H_2 (b)CO_2/N_2 and (c)CO_2/CH_4 separations.

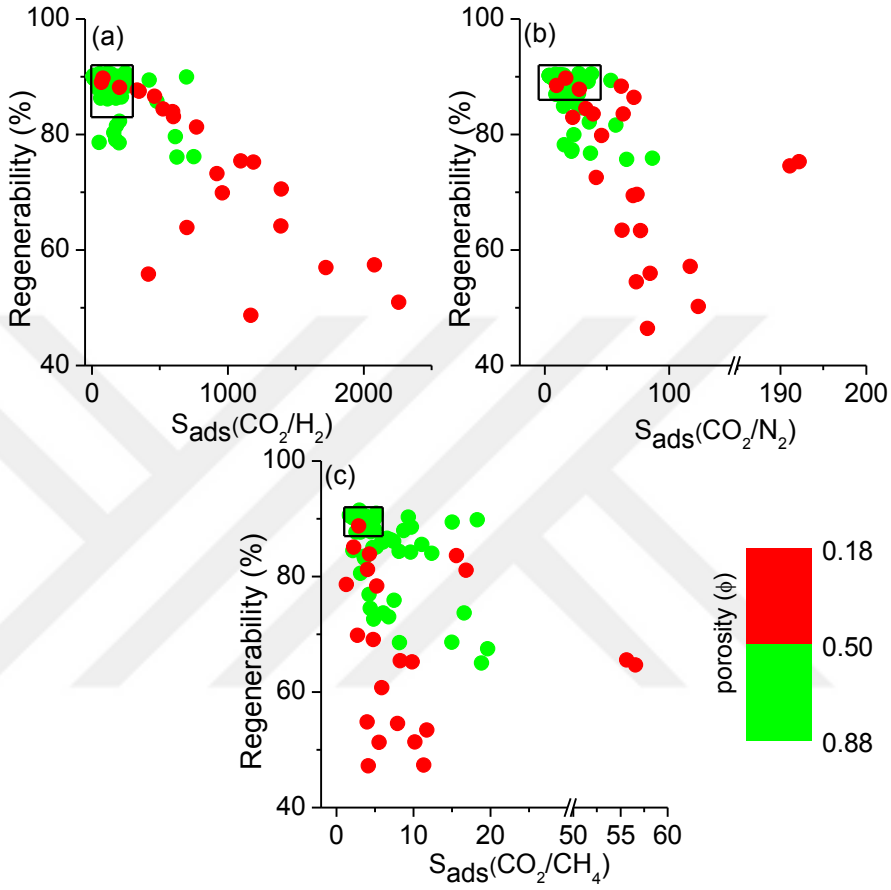

Figure 4.8. Regenerability (R%) vs. adsorption selectivity (S_{ads}) for (a)CO_2/H_2 (b)CO_2/N_2 and (c)CO_2/CH_4 separations as a function of porosity of MOFs. Black boxes represent MOFs having high regenerability but low selectivity.

The group of materials that start with OWIT- in their names, have relatively low LCD values (~7.5 Å) but higher surfaces areas (~4800 m^2/g) than materials with similar LCD. As a result, they have lower selectivities (~14 for CO_2/H_2, ~1.7 for CO_2/CH_4, ~5 for CO_2/N_2). NIMPEG01 (PCN-39), also has low LCD (5.9 Å) but relatively high surface area (2557.8 m^2/g). PCN-39 has the highest selectivity for CO_2/N_2 and CO_2/CH_4 separations among the

materials with similar surface area due to its low LCD. CO_2 working capacities of MOFs as a function of their surface areas and porosities were also examined in Figure 4.7. Since surface area and porosity of MOFs are highly correlated as shown in Figure B8, the color labeling based on porosity is distinct. Similar to the selectivity results, the highest working capacities were observed for materials with surface areas around 890-1500 m^2/g with low to medium porosities around 0.2-0.7.

Similar figure representing the relation between working capacity, surface area and porosity for Case 2 is given in Figure B9. Finally, the structural properties of the MOFs discussed in section 3.1 which have high adsorption selectivity but low R% (<75%) for CO_2 separations were studied. Figure 4.8 shows that porosities of these MOFs are generally small, less than 0.5, for all separations. Due to these small porosities, uptake amounts of CO_2 under adsorption (1 bar) and desorption (0.1 bar) pressures are close to each other, resulting with low R%. Black boxes in Figure 4.8 illustrates that a large number of MOFs is available with high regenerability but they suffer from low adsorption selectivity.

4.4. Membrane Performances of Selected MOFs

So far, adsorption-based CO_2 separation performances were examined. Diffusion of gases in the pores of a MOF should not be very slow to limit the potential use of the adsorbent material. In order to understand diffusion of gas mixtures in MOFs, EMD simulations were performed. Considering the high computational demand of EMD simulations for gas mixtures, these simulations were performed only for the promising MOF adsorbents. Self-diffusivities of gases were computed in their mixtures in the pores of 5 MOFs, KEYFIF, KEYFIF01, EMIHAK, IDIWOH and KUGZIW. The first three MOF was selected due to their high selectivities and the last two were chosen because of their high R% for three gas separations. Table 4.3 shows adsorption selectivity, diffusion selectivity, membrane selectivity, self-diffusion coefficients and gas permeabilities of the 5 MOFs for each separation. Self-diffusivities show that H_2 is the fastest (8×10^{-4}-6×10^{-3} cm^2/s) since H_2 is

lighter and smaller than the other gases considered. CO_2 is the slowest (10^{-5}-10^{-4} cm^2/s) gas component since it adsorbs more strongly into the pores of MOFs than other gases. As a result, diffusion selectivities of MOFs for CO_2 are less than 1. The 5 MOFs studied in Table 4.3 favor CO_2 for adsorption but other gases for diffusion. In other words, high adsorption selectivities for CO_2 are compensated by the low diffusion selectivities towards CO_2. Since membrane selectivity is predicted as the multiplication of adsorption and diffusion selectivities, predicted membrane selectivities for CO_2 are lower than the adsorption selectivities. This outcome suggests that MOFs would be much more efficient in adsorption-based separations than in membrane-based separations.

Results shown in Table 4.3 highlights the importance of the diffusion rates of gases in determining the kinetic-based separation potential of MOFs. Identifying a MOF with high adsorption selectivity does not guarantee the high membrane selectivity of the material for separation of the same gas mixture. For example, KEYFIF01 has significantly higher CO_2/H_2 adsorption selectivity (1192) than EMIHAK (697). When the diffusion is considered, membrane selectivity of EMIHAK (47) becomes larger than that of KEYFIF01 (17). Gas permeability is as important as gas selectivity of the membrane because membranes with high gas permeabilities require less surface area hence lower capital costs. Calculated CO_2 permeabilities of MOF membranes are large compared to traditional polymer membranes. Robeson[3] established an upper bound to show the highest performances that polymeric membranes could achieve for several membrane-based CO_2 separations. Membrane materials above that bound are known to exhibit both high selectivity and permeability. Polymeric membranes generally have selectivities of 50-10 (100-1) and permeabilities of 350-40,000 (30-550,000) Barrers for CO_2/N_2 (CO_2/CH_4) separation. For CO_2/N_2 separation, 5 MOFs that were studied in Table 4.3 exceed the upper bound. While KUGZIW and IDIWOH exceed the bound due to their high CO_2 permeabilities, KEYFIF and KEYFIF01 exceed the bound due to their high CO_2/N_2 selectivities. EMIHAK is located above the upper

bound due to both high permeability and selectivity. For CO_2/CH_4 separation, only KEYFIF is on the bound, other four MOFs are above the bound due to their high permeabilities. No comparison was done for CO_2/H_2 separation because polymeric membranes are generally selective for H_2 over CO_2 and the upper bound was defined based on the H_2 selectivities and permeabilities whereas MOF membranes are CO_2 selective. The membrane selectivities and permeabilities of MOFs were compared with zeolites. For CO_2/H_2 separation, EMIHAK shows better performance than well-known zeolites such as NaX, NaY, DDR and CHA.[81] This MOF's membrane selectivity is slightly lower than NaX and NaY but its permeability is much higher than the zeolites. For CO_2/N_2 and CO_2/CH_4 separations, zeolites show higher selectivities (40-650 and 20-260, respectively) than the 5 MOF membranes studied but their CO_2 permeabilities are lower than EMIHAK, IDIWOH and KUGZIW. It can be concluded that MOFs exhibiting high adsorption selectivity can be efficiently used for membrane-based separation of CO_2 mixtures.

Table 4.3. Adsorption selectivity, diffusion selectivity, membrane selectivity and gas permeability of 5 promising MOFs. MOFs are ranked based on their membrane selectivities.

CO_2/H_2

MOF	S_{ads}	D_{self}, CO_2 (cm^2/s)	D_{self}, H_2 (cm^2/s)	S_{diff}	S_{mem}	P_{CO2} (Barrer)	P_{H2} (Barrer)
EMIHAK	696.73	5.46×10^{-5}	8.04×10^{-4}	0.07	47.29	3313258.88	70069.86
KEYFIF01	1192.14	1.17×10^{-5}	7.94×10^{-4}	0.01	17.51	116875.49	6675.76
KEYFIF	1096.41	1.23×10^{-5}	8.04×10^{-4}	0.02	16.81	119696.07	7120.05
IDIWOH	61.55	7.69×10^{-4}	6.16×10^{-3}	0.12	7.68	4286052.18	558309.39
KUGZIW	92.49	9.52×10^{-5}	1.93×10^{-3}	0.05	4.57	554398.88	121303.66

CO_2/N_2

MOF	S_{ads}	D_{self}, CO_2 (cm^2/s)	D_{self}, N_2 (cm^2/s)	S_{diff}	S_{mem}	P_{CO2} (Barrer)	P_{N2} (Barrer)
EMIHAK	53.35	7.45×10^{-5}	1.70×10^{-4}	0.44	23.41	4264722.97	182174.59
KEYFIF	192.19	1.48×10^{-5}	1.56×10^{-4}	0.10	18.32	143873.27	7852.07
KEYFIF01	191.15	1.41×10^{-5}	1.77×10^{-4}	0.08	15.26	136677.09	8955.83
IDIWOH	8.71	7.68×10^{-4}	1.19×10^{-3}	0.65	5.62	4204748.51	747534.33
KUGZIW	14.71	8.90×10^{-5}	2.94×10^{-4}	0.30	4.45	513248.85	115358.84

CO_2/CH_4

MOF	S_{ads}	D_{self}, CO_2 (cm^2/s)	D_{self}, CH_4 (cm^2/s)	S_{diff}	S_{mem}	P_{CO2} (Barrer)	P_{CH4} (Barrer)
KEYFIF01	55.68	1.18×10^{-5}	8.08×10^{-05}	0.15	8.15	56275.22	6902.81
EMIHAK	18.87	7.53×10^{-5}	2.30×10^{-4}	0.33	6.17	1692006.97	274109.09
KEYFIF	56.61	1.17×10^{-5}	1.17×10^{-4}	0.10	5.63	55758.49	9909.52
KUGZIW	5.16	1.06×10^{-4}	1.86×10^{-4}	0.57	2.95	648090.90	219933.01
IDIWOH	2.98	7.37×10^{-4}	1.49×10^{-3}	0.50	1.48	4605119.68	3117671.56

Chapter 5

MOF-BASED MIXED MATRIX MEMBRANES FOR CO_2/N_2 SEPARATIONS*

In this chapter, atomically-detailed simulations were used to examine CO_2/N_2 separation potential of metal organic framework (MOF)-based mixed matrix membranes (MMMs) in this study. Gas permeability and selectivity of 700 new MMMs composed of 70 different MOFs and 10 different polymers were calculated for CO_2/N_2 separation. This is the largest number of MOF-based MMMs for which computational screening is done to date. Selecting the appropriate MOFs as filler particles in polymers results in MMMs that have higher CO_2/N_2 selectivities and higher CO_2 permeabilities compared to pure polymer membranes. Several MOF-based MMMs were identified to exceed the upper bound established for polymers. For polymers that have low CO_2 permeabilities but high CO_2 selectivities, the identity of the MOF used as filler is not important. All MOFs enhanced the CO_2 permeabilities of this type of polymers without changing their selectivities. The methods introduced in this thesis will create many opportunities to select the MOF/polymer combinations with useful properties for CO_2 separation applications.

5.1. Permeability and Selectivity of MOFs

Before analyzing the results for MOF-based MMMs, the CO_2/N_2 separation performances of MOFs were firstly examined. Predicted CO_2 permeabilities, N_2 permeabilities and CO_2/N_2 selectivities of MOFs are given in Table C1 of Appendix C. Figure 5.1 shows the CO_2/N_2 selectivities and CO_2 permeabilities of 70 different MOFs calculated from atomically-detailed simulations. The selectivity and permeability data for 10

*The results given in this chapter were published in Journal of Nanomaterials with following reference: Z. Sumer and S. Keskin, "Computational Screening of MOF-based Mixed Matrix Membranes for CO_2/N_2 Separations", Journal of Nanomaterials, 2016, 6482628, 1-12 (2016). The original manuscript has been rearranged to conform to the format requirements of the dissertation.

calculated from atomically-detailed simulations. The selectivity and permeability data for 10 different polymers that considered in this thesis together with the Robeson's upper bound established for CO_2/N_2 separation were also shown. Membrane materials that can exceed this upper bound are considered to be highly promising.

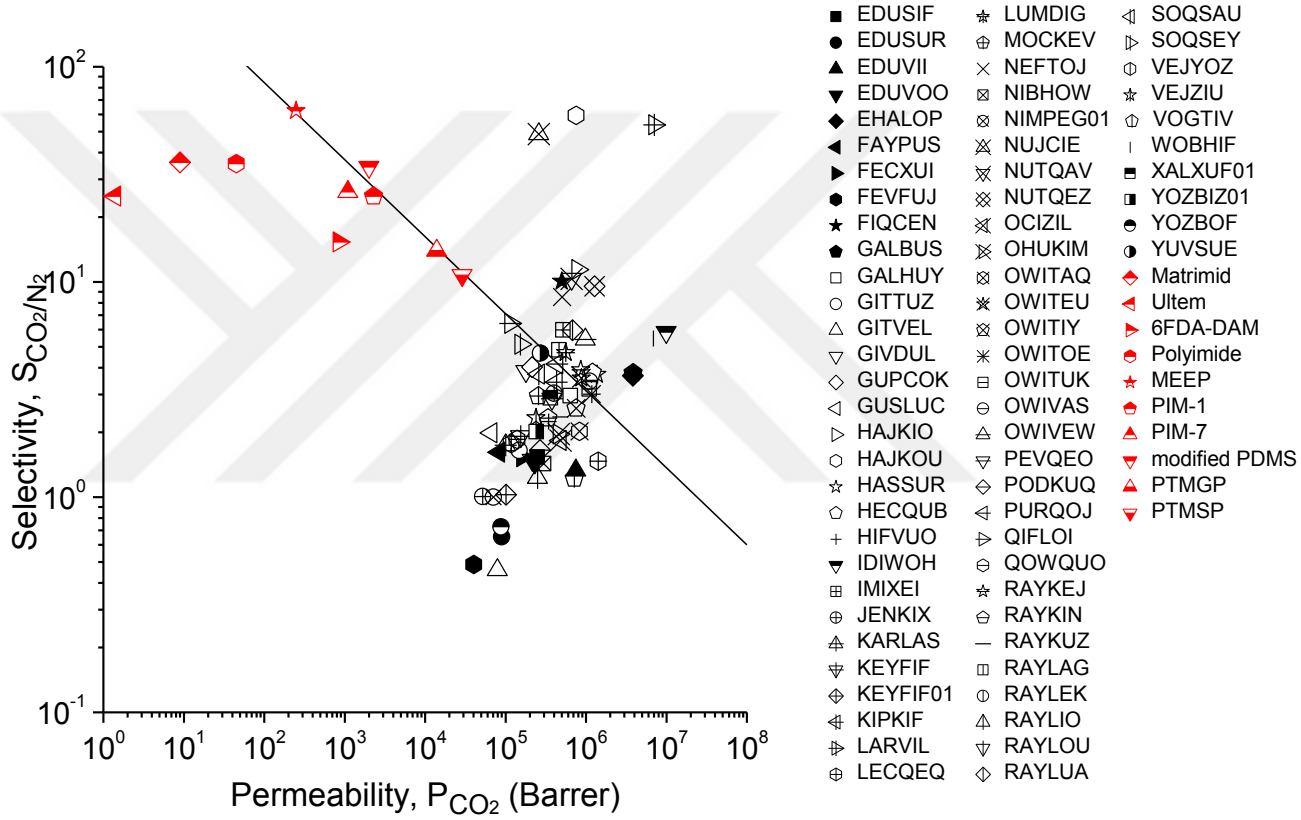

Figure 5.1. Predicted CO_2/N_2 selectivities and CO_2 permeabilities of 70 MOFs considered in this thesis. Experimental data of polymer membranes is taken from the literature.[3] The line represents the Robeson's upper bound for the CO_2/N_2 separation.

The first observation from Figure 5.1 is that there are several MOFs that can exceed the Robeson's upper bound. 27 of the 70 MOFs are located above the upper bound. Most of

these MOFs have generally similar or lower CO_2/N_2 selectivities than the polymers but significantly higher CO_2 permeabilities. MOFs, HAJKOU, LARVIL and NUJCIE exhibit high CO_2/N_2 selectivities, 59, 54, 49, respectively and their CO_2 permeabilities are 7.5×10^5, 7×10^6, 2.6×10^5 Barrer. These values are higher than the selectivities and permeabilities of the polymers. Therefore, it is expected that if these three MOFs are used as filler particles in the polymers, they can significantly enhance both the selectivity and permeability of the polymer membranes. IDIWOH has the highest CO_2 permeability among all MOFs considered, $\sim10^7$ Barrer. However, the CO_2/N_2 selectivity of this MOF is lower than that of polymers, 6. If IDIWOH is incorporated into polymers, an increase is expected in the CO_2 permeabilities of the polymers but decrease or no change in their selectivities.

One important observation from Figure 5.1 is that almost all MOFs considered in this thesis have higher CO_2 permeabilities than the polymers. The CO_2 permeabilities of polymers are in the range of $1\text{-}10^4$ Barrers whereas MOFs exhibit CO_2 permeabilities of $10^4\text{-}10^7$ Barrers. These high permeabilities can be attributed to the large pore volumes of MOFs. The calculated surface areas and pore volumes of all 70 MOFs were shown in Figure C1. Surface areas of MOFs vary between 90-5210 m^2/g and pore volumes are in the range of 0.1-3.1 cm^3/g, which explains the high gas permeabilities of MOFs compared to polymers. As can be seen from Figure C1, the computed surface area in general closely correlates with the pore volume. As the pore volumes increase, surface areas also increase. The MOFs that were identified to be highly promising for CO_2/N_2 separations in Figure 5.1, NUJCIE, LARVIL and HAJKOU have low surface areas (175 m^2/g, 350 m^2/g, 890 m^2/g, respectively) and low pore volumes (0.28 cm^3/g, 0.24 cm^3/g, 0.39 cm^3/g, respectively). As previously discussed by Watanabe and Sholl,[17] high surface areas and pore volumes are generally preferred for materials used for adsorbent applications but are not critical for membrane materials. Overall, Figure 5.1 suggests that there are several promising MOFs with high CO_2/N_2

selectivities and high CO_2 permeabilities and these MOFs can be promising fillers for MMMs to enhance polymers' separation performances.

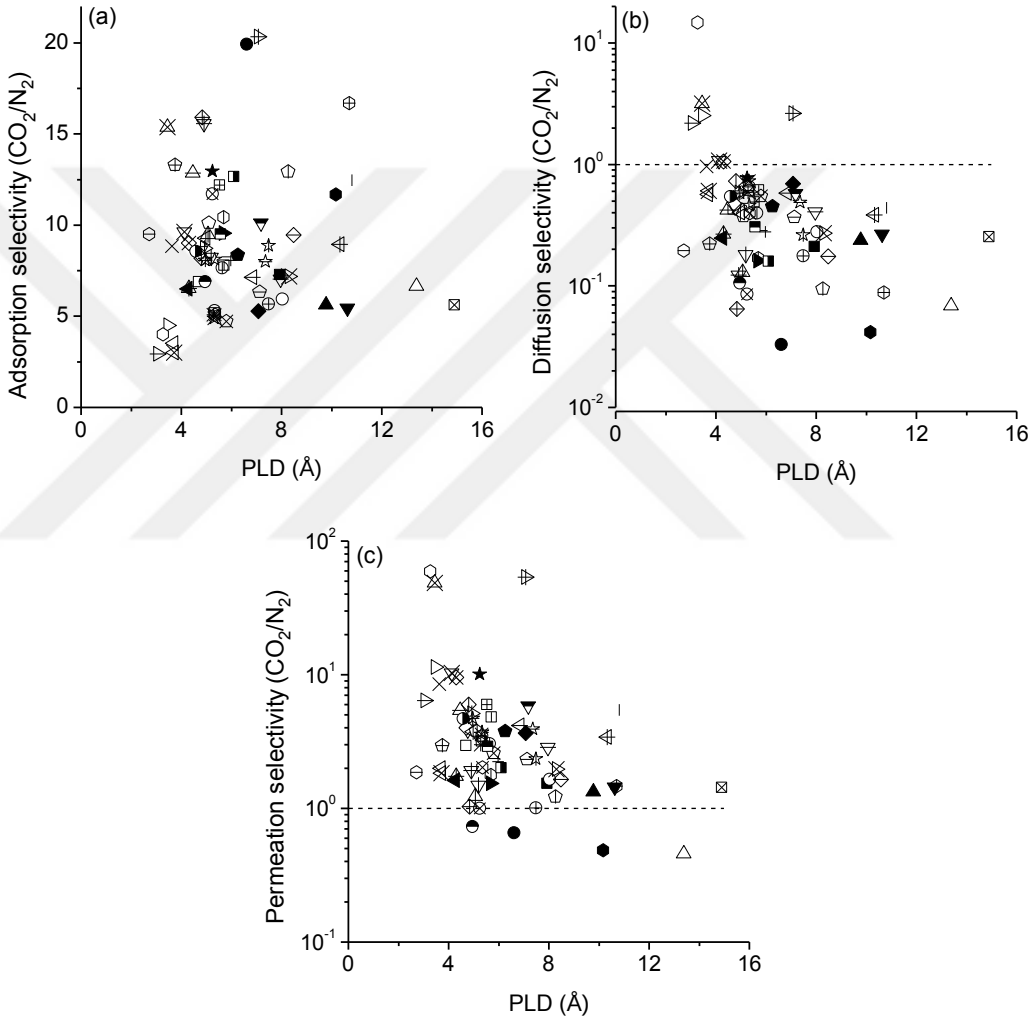

Figure 5.2. (a) Adsorption selectivity, (b) diffusion selectivity, (c) permeation selectivity of MOFs as a function of their PLDs (pore limiting diameters). The dotted lines in (b), (c) represent the selectivity of 1.

In order to better assess gas separation performances of MOFs, adsorption and diffusion selectivities of MOFs were separately examined. Figure 5.2 shows adsorption, diffusion and permeation (membrane) selectivity of MOFs as a function of their PLDs. Adsorption selectivities were computed as the ratio of adsorbed amount of CO_2 to N_2 at the average loadings of feed and permeate pressures. All MOFs are CO_2 selective in adsorption regardless of their pore sizes as shown in Figure 5.2(a). This is expected since CO_2 molecules have stronger energetic interactions with the MOF atoms compared to N_2 molecules as a result of higher quadrupole moment of CO_2. Strong adsorption of CO_2 molecules over weak adsorption of N_2 molecules gives rise to the CO_2 selective trend in adsorption. Adsorption selectivities of MOFs are moderate, close to each other in the range of 3-20. The best performing MOFs in adsorption are LECQEQ, EDUSUR and LARVIL with adsorption selectivities of 17, 20 and 20.3, respectively. The MOFs that identified to be highly promising for CO_2/N_2 separation based on permeation selectivity results, HAJKOU, NUJCIE and LARVIL have adsorption selectivities of 4, 15, 20.3, respectively. This result suggests that the most promising membrane candidates for selective CO_2 separation are not necessarily the ones with the highest CO_2 adsorption selectivities.

Figure 5.2(b) shows diffusion selectivities of MOFs calculated as the ratio of corrected diffusivity of CO_2 over N_2 obtained from the EMD simulations. It is important to note that both CO_2 and N_2 diffusivities were greater than 10^{-8} cm^2/s in all studied MOFs since gas diffusion can be readily characterized with EMD simulations above this limit. One important observation from Figure 5.2(b) is that there is no correlation between diffusion selectivity of MOFs and their PLDs. There are many MOFs having similar PLDs but different diffusion selectivities. A significant amount of MOFs, 63 out of 70, has diffusion selectivity less than 1 for CO_2 over N_2. In other words, these MOFs are N_2 selective in diffusion. This is an expected result since N_2 molecules are lighter than the CO_2 molecules leading to faster diffusion of N_2 compared to CO_2. Furthermore, CO_2 molecules are strongly adsorbed in

MOFs as shown in Figure 5.2(a) and slow diffusion of the strongly adsorbed components is a common observation. Interestingly, there are five MOFs that favor CO_2 in diffusion. These MOFs are QIFLOI, HAJKIO, LARVIL, NUJCIE and HAJKOU which have diffusion selectivities of 2.2, 2.5, 2.6, 3.2, 14.8, respectively for CO_2 over N_2. Three of these MOFs, LARVIL, NUJCIE and HAJKOU were identified to be highly promising materials for CO_2/N_2 separations due to their high permeation selectivities in Figure 5.1. The reason for their high permeation selectivities is that both adsorption and diffusion favor the same component, CO_2 in these MOFs. Therefore, these three MOFs are highly CO_2 selective materials. Although QIFLOI and HAJKIO are CO_2 selective in diffusion, their adsorption selectivities for CO_2 are low (3 and 4.5) compared to other MOFs therefore, they are not as selective for CO_2 as the other three MOF materials in permeation. Finally, there are several MOFs with diffusion selectivities close to 1, suggesting that diffusion rates of CO_2 and N_2 are similar in the pores of these materials. As a result, permeation selectivities of these materials are determined by their adsorption selectivities.

Permeation (membrane) selectivities of MOFs are shown in Figure 5.2(c). Except four, all MOFs are CO_2 selective membranes. The CO_2/N_2 selectivities are in the range of 0.45-59.5. The CO_2/N_2 selectivities of FEVFUJ, GITVEL, EDUSUR and YOZBOF are 0.5, 0.5, 0.7, 0.7 respectively, which show that they are N_2 selective. Adsorption favors CO_2 in these MOFs with selectivities of ~12, 7, 20, 7, but diffusion very strongly favors N_2 over CO_2 with selectivities of 24, 15, 30, 9, respectively. Diffusion selectivities for N_2 dominate the adsorption selectivities for CO_2 and as a result these MOFs become N_2 selective membranes. FEVFUJ, GITVEL, EDUSUR and YOZBOF can be promising adsorbent candidates for selective separation of CO_2 from N_2 and at the same time they are promising membrane materials for selective separation of N_2 from CO_2. For example, EDUSUR exhibits one of the highest adsorption selectivity for CO_2, 20, as shown in Figure 5.2(a) but when the kinetic properties of gases are considered, EDUSUR becomes weakly N_2 selective membrane as

shown in Figure 5.2(c). This example signifies the importance of diffusion selectivity in governing a material's membrane selectivity. Overall, analysis of adsorption, diffusion and permeation selectivities of MOFs obtained from atomically-detailed simulations can be summarized as follows: (i) Adsorption selectivity favors CO_2 in all MOFs. (ii) If the diffusion selectivity also favors CO_2, then these MOFs become highly CO_2 selective in permeation. (iii) If the diffusion selectivity weakly favors N_2, then these MOFs become weakly CO_2 selective in permeation. (iv) If the diffusion selectivity strongly favors N_2, then these MOFs become N_2 selective in permeation.

5.2. Permeability and Selectivity of MOF-based MMMs

In a recent work of our research group, CO_2 and N_2 permeability predictions of atomically-detailed simulations with the experimentally measured ones for various MOF and ZIF-based MMMs were compared.[37] Collected 98 experimental data points from the literature for CO_2 and N_2 permeability of 15 different types of MOF and ZIF-based MMMs showed that predictions of the Maxwell model are in good agreement with the experimental measurements of CO_2 and N_2 permeability. This good agreement validated the accuracy of our computational methodology to estimate separation performances of new MOF-based MMMs for which experimental gas permeability data are not available. In this thesis, the same computational approach is used to predict CO_2 and N_2 permeabilities and CO_2/N_2 selectivities of 700 different MOF-based MMMs which have not been fabricated to date. Calculated gas permeability and selectivity data for all MOF-based MMMs are reported in Tables C2-C5.

Figure 5.3 shows predicted CO_2/N_2 selectivity and CO_2 permeability of 560 different MMMs composed of Ultem, Matrimid, polyimide, MEEP, modified PDMS, PIM-1, PIM-7, and 6FDA-DAM polymers. The volume fraction of the MOF fillers in MMMs was set to 0.3. Predicted gas permeabilities of different MOF-based MMMs composed of 6FDA-DAM,

Ultem, PIM-7, polyimide, Matrimid and MEEP are almost the same therefore a single symbol was used to represent different MOF-based MMMs of these polymers. In other words, the identity of the MOF used as filler particle does not affect the performance of MMMs composed of these six polymers. Ultem, Matrimid, polyimide and 6FDA-DAM are below the upper bound due to their low CO_2 permeabilities compared to other polymers. Results showed that adding MOFs as filler particles into these polymers increases the CO_2 permeability of polymers since all the studied MOFs have higher CO_2 permeability than these polymers. For example, CO_2 permeability increases from 1.4 to 3.2 Barrer for Ultem-based MMMs, 9 to 21 Barrer for Matrimid-based MMMs, 45 to 102.8 Barrer for polymide-based MMMs, 842.4 to 1908.7 Barrer for 6FDA-DAM-based MMMs. On the other hand, there is almost no change in CO_2/N_2 selectivity of these polymers.

With a CO_2/N_2 selectivity of 26.2 and CO_2 permeability of 1100 Barrer, PIM-7 is just below the upper bound. When MOFs are used as filler particles in this polymer, the MMM's permeability increases from 1100 to 2485.9 Barrer and as a result, PIM-7 can exceed the upper bound. This is an important result showing that highly permeable MOFs can significantly improve the CO_2 permeability of polymers and carry them above the upper bound. MEEP polymer is on the Robeson's upper bound and it easily exceeds the upper bound due to the improvement in CO_2 permeability by addition of MOF fillers. The CO_2 permeability of MEEP polymer increases from 250 to 570 Barrer with the incorporation of MOFs. No increase in the selectivity of MEEP was expected since it has the highest selectivity among all MOFs and polymers that were considered in this thesis. The identity of the MOF used as filler affects the performance of MMMs composed of modified PDMS and PIM-1. These two polymers have significantly higher CO_2 permeabilities than the other polymers, 2000 and 2300 Barrers, respectively. There is a single MOF, FEVFUJ, which adversely affects the selectivity of these two polymers. FEVFUJ is a N_2 selective MOF as shown in Figure 5.1. It has the lowest CO_2 selectivity (0.5) and the lowest CO_2 permeability

(40500 Barrer) among all the MOFs considered. If FEVFUJ is used as filler in modified PDMS and PIM-1, the CO_2 permeabilities still increase but at the expense of decreasing CO_2 selectivities as shown in Figure 5.3. For example, the CO_2/N_2 selectivity of modified PDMS (PIM-1) decreases from 34.2 to 30.7 (25 to 22.2) while the CO_2 permeability increases from 2000 to 4103.1 (2300 to 4650.5) Barrer. Incorporation of other MOFs into modified PDMS and PIM-1 give similar results, permeabilities are enhanced while selectivities remain constant.

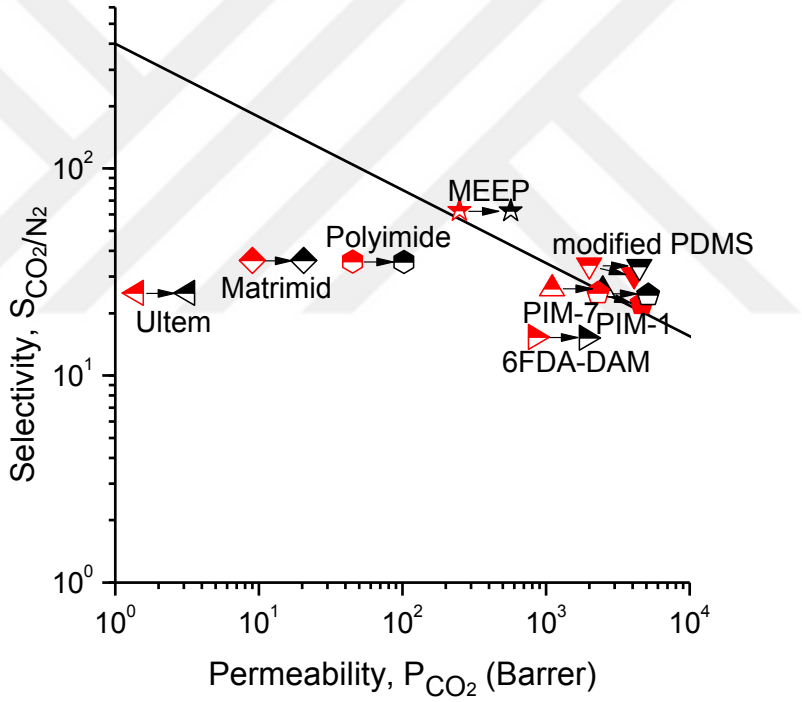

Figure 5.3. Predicted CO_2/N_2 selectivities and CO_2 permeabilities of 560 different MOF-based MMMs composed of Ultem, Matrimid and Polyimide, 6FDA-DAM, MEEP, PIM-7, PIM-1 and modified PDMS polymers. The line represents the Robeson's upper bound for the CO_2/N_2 separation. Half full red indicates pure polymers, half full black indicates the MOF/polymer MMMs and full red indicates FEVFUJ/polymer MMM.

PTMGP and PTMSP are the two polymers located at the lower right end of the Robeson's upper bound as shown in Figure 5.1. They have high CO_2 permeabilities (14000 and 29000 Barrer, respectively), but low CO_2/N_2 selectivities (14 and 10.7, respectively). The gas permeabilities of these two polymers are much closer to the gas permeabilities of MOFs compared to the other polymers. Because of this reason, MMMs composed of PTMGP and PTMSP exhibit significantly different separation performances based on the identity of the MOF used as fillers. Figure 5.4(a) shows predicted CO_2/N_2 selectivity and CO_2 permeability of 70 different MOF/PTMGP MMMs.

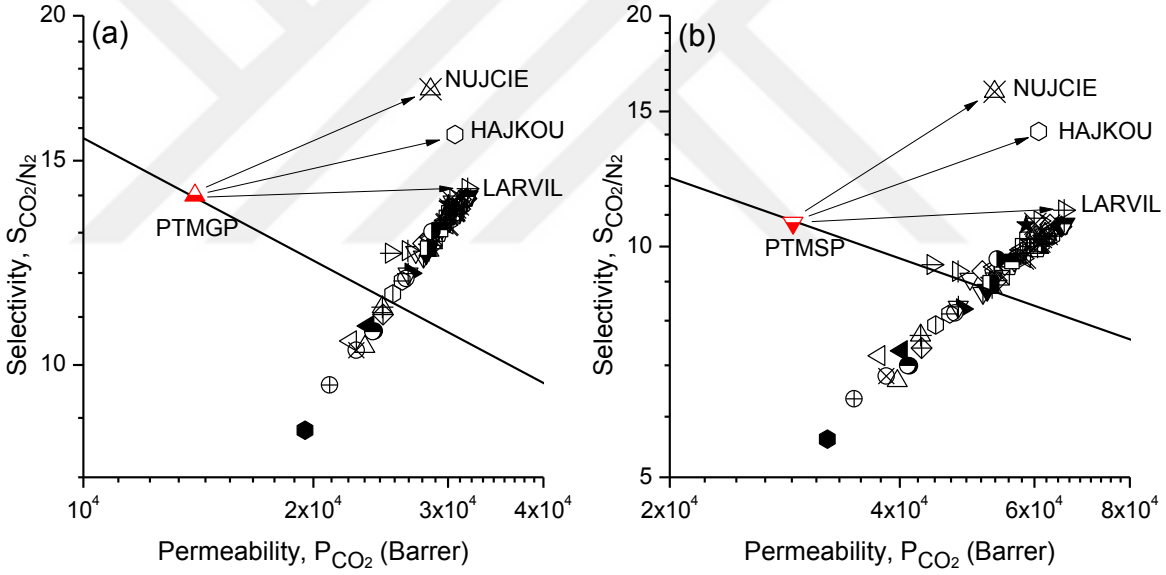

Figure 5.4. Predicted CO_2/N_2 selectivities and CO_2 permeabilities of 70 different MOF-based MMMs composed of (a)PTMGP (b)PTMSP polymers. Red symbols represent the pure polymer membranes, black symbols represent the MOF-based MMMs. Legend is same with Figure 5.1.

The effect of MOF fillers can be categorized into three: MOFs that increase both the CO_2 permeability and CO_2/N_2 selectivity, MOFs that increase the permeability without changing the selectivity, and MOFs that increase the permeability at the expense of decreasing selectivity. Each case is discussed in detail below:

(a) Only 3 MOFs, NUJCIE, HAJKOU and LARVIL can increase both the CO_2 permeability and CO_2/N_2 selectivity of PTMGP. The selectivity of PTMGP increases from 14 to 17.3 and its permeability increases from 14000 to 28500 Barrer when NUJCIE is used as a filler particle. If HAJKOU is used to make a MMM, then the selectivity increases to 16 and permeability increases to 30650 Barrer. LARVIL also slightly increases the CO_2 selectivity of PTMGP to 14.2 and significantly increases the CO_2 permeability to 31850 Barrer. All three MMMs, NUJCIE/PTMGP, HAJKOU/PTMGP and LARVIL/PTMGP can exceed the upper bound established for CO_2/N_2 separation.

(b) Several MOFs (19 among 70) improve the CO_2 permeability of PTMGP but they do not significantly affect its selectivity. All these MOFs carry PTMGP above the upper bound due to large increases in the CO_2 permeability. The highest permeability observed for PTMGP-based MMMs is 31900 Barrer with IDIWOH filler while selectivity is constant at 14.

(c) A significant number of MOFs (48 among 70) increases the CO_2 permeability of PTMGP but decreases its selectivity. The reason is that the CO_2 permeabilities of these MOFs are similar to the PTMGP while their CO_2/N_2 selectivities are significantly lower than the polymer. As a result, the improvement in the CO_2 permeability of polymers occurs at the expense of a reduction in the selectivity. For example, the CO_2 permeability of PTMGP increases from 14000 to 19500 Barrer while its selectivity decreases from 14 to 8.8 with the addition of FEVFUJ filler into the polymer.

Figure 5.4(b) shows predicted CO_2/N_2 selectivity and CO_2 permeability of 70 different MOF-based MMMs composed of PTMSP polymer. PTMSP-based MMMs show the same

trend with PTMGP-based MMMs. NUJCIE, HAJKOU and LARVIL are the MOFs that increase both permeability and selectivity of PTMSP. NUJCIE increases permeability (selectivity) from 29000 to 53200 Barrer (from 10.7 to 15.9), HAJKOU increases to 60800 Barrer (to 14.1) and LARVIL increases to 65650 Barrer (to 11.2). MMMs in which NUJCIE, HAJKOU and LARVIL are used as fillers exceed the upper bound established for CO_2/N_2 separation. There are 17 MOFs which improve the CO_2 permeability of PTMSP but do not significantly change the CO_2 selectivity. For example, IDIWOH increases the CO_2 permeability to 65800 Barrer but keeps the selectivity of MMM same with that of pure polymer. Permeability increases upon addition of MOF fillers carry the PTMSP-based MMMs above the upper bound. Most of the MOFs studied (50 among 70) increase the CO_2 permeability of PTMSP but decreased the CO_2 selectivity due to the same reason as discussed for PTMGP.

So far the widely studied polymers for CO_2/N_2 separation were examined. In fact, most of these polymers are located close to the upper bound and it is easy for these polymers to exceed the upper bound with the incorporation of highly permeable MOF fillers. The hypothetical polymers were created to understand which polymers can reap the largest advantages when used in combination with MOFs. Figure 5.5 shows 6 hypothetical polymers that lie along the Robeson's upper bound for CO_2/N_2 separation. By specifying the position of a polymer along the upper bound the information required to predict MMMs' performances was defined. The CO_2 permeabilities of selected hypothetical polymers are in the range of 90-3×10^6 Barrer and their CO_2/N_2 selectivities vary from 2 to 80. For each hypothetical polymer, 5 different MOFs were used as filler particles, NUJCIE, HAJKOU, LARVIL, IDIWOH and FEVFUJ. These MOFs are chosen to represent highly CO_2/N_2 selective and highly permeable fillers (NUJCIE, HAJKOU and LARVIL), a highly CO_2 permeable filler with low CO_2/N_2 selectivity (IDIWOH) and a N_2 selective filler with low CO_2 permeability (FEVFUJ). If the polymer membrane has a high selectivity for CO_2 but

low permeability such as the first two hypothetical polymers, adding a MOF can enhance the membrane's permeability with no change in the selectivity. In this limit, the identity of the MOF appears to be unimportant. The effect of MOF identity becomes important for the third polymer which has moderate selectivity and permeability. Highly permeable NUJCIE, HAJKOU, LARVIL, IDIWOH enhance permeability of the third polymer without changing its selectivity whereas FEVFUJ enhances its CO_2 permeability but decreases the CO_2/N_2 selectivity. Except FEVFUJ, selected MOF fillers improve both the CO_2 permeability and the CO_2/N_2 selectivity of the fourth and fifth polymers. This improvement depends on the identity of the MOF. MOFs like NUJCIE and HAJKOU significantly enhance the CO_2/N_2 selectivity whereas a MOF like LARVIL significantly enhances the CO_2 permeability. The most interesting results are observed for the sixth polymer which has very high permeability but very low selectivity. Highly permeable MOFs, LARVIL and IDIWOH enhance both the permeability and selectivity of that polymer but all the other MOFs cause a decrease in the CO_2 permeability although they increase the selectivity. These results support the idea that there is a wide range of polymers that have moderate selectivity and moderate permeability for which incorporation of an appropriate MOF can yield large separation performance enhancements. The polymers in this thesis generally have lower CO_2 permeabilities but relatively higher CO_2/N_2 selectivities compared to MOFs. For polymers that have high permeabilities and low selectivities, separation performances of the MMMs are strongly dependent on the type of MOF.

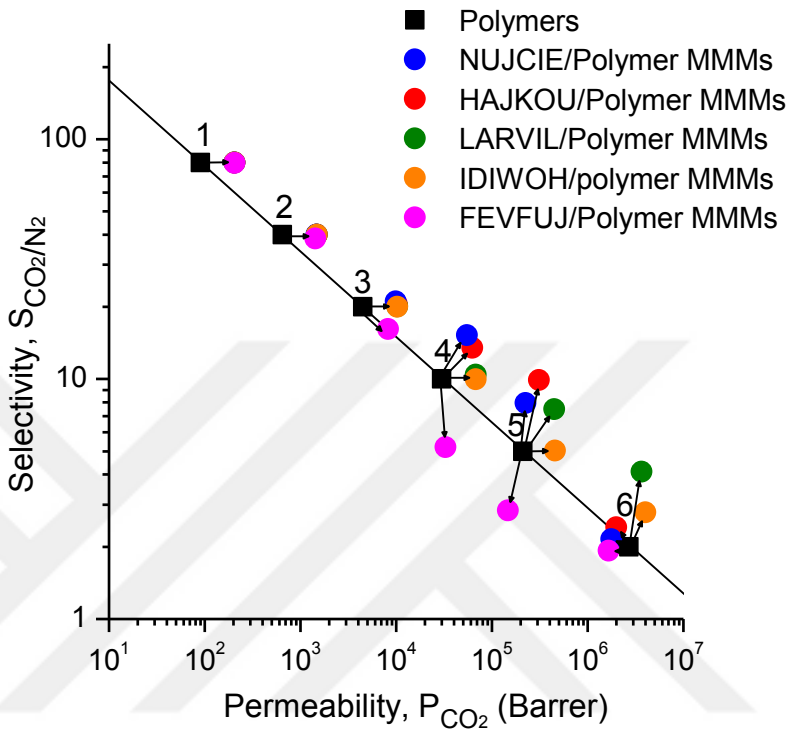

Figure 5.5. Predicted CO_2/N_2 selectivities and CO_2 permeabilities of 30 hypothetical MMMs. Black symbols represent pure hypothetical polymer membranes, color symbols represent the MOF-based MMMs.

Finally, it is important to discuss the assumptions of the computational approach that was used to screen MOF-based MMMs for CO_2/N_2 separation. Rigid MOF structures were used in our atomically-detailed simulations. This assumption has been widely used in almost all molecular simulation studies of MOFs in the literature since flexible simulations require significant amount of computational time and resources. Recently the effect of MOF's flexibility on the permeability and selectivity of MOF-based MMMs was investigated and it showed that flexibility of the MOFs can be neglected as a reasonable approximation if the MOF volume fraction is low and if the MOF is much more permeable than the polymer.[37]

The MOFs studied in this thesis were highly permeable compared to the polymers as shown in Figure 5.1 and the volume fraction of the MOF in the MMM was set to a low value, 0.3. Therefore, neglecting the flexibility of MOFs is a reasonable approximation especially for large-scale computational screening studies. Our atomically-detailed simulations do not provide any information about the stability of MOF/polymer MMMs. This issue is more likely to be investigated by experimentalists. The stability information for 3 MOFs were found, the MOFs were identified to improve both the selectivity and permeability of polymers, from their corresponding experimental synthesis papers. HAJKOU is reported to exhibit high thermal stability and permanent porosity,[82] LARVIL is reported to preserve its crystalline integrity at ambient conditions[83] and no information was found for the stability of NUJCIE.[84]

At that point one may think about why not to use MOFs as pure membranes rather than using them as filler particles in polymer membranes. MOFs exhibit high gas permeabilities and high gas selectivities as shown in Figure 5.1. However, fabrication of MOF membranes requires synthesis of MOFs in bulk amounts at low cost. MOFs are currently synthesized in small amounts at the lab scale and commercially available MOFs are expensive. Furthermore, it is experimentally challenging to fabricate defect-free thin film MOF membranes although recent studies described routes for processing MOF membranes in polymeric hollow fibers.[85, 86] On the other hand, fabrication of MOF-based MMMs on large scales can be done with relatively minor adaptation of existing commercial technology developed for fabrication of polymer membranes at a reasonable cost. Therefore, MOF-based MMMs are expected to be more widely used in gas separation applications compared to thin-film MOF membranes in near future. Hopefully, results of this thesis will motivate experiments to fabricate the most promising MOF-based MMMs for CO_2/N_2 separations.

Chapter 6

ADSORPTION AND MEMBRANE-BASED CH_4/N_2 SEPARATION PERFORMANCES OF MOFS*

In this chapter, molecular simulations were used to assess both adsorption-based and membrane-based CH_4/N_2 separation performances of 102 different MOFs. This is the largest number of MOF adsorbents and membranes studied to date for separation of CH_4/N_2 mixtures. Several adsorbent evaluation metrics such as adsorption selectivity, working capacity and regenerability were predicted and the top performing adsorbents were identified. Several MOFs were predicted to exhibit higher adsorption selectivities than the traditional adsorbents such as zeolites and activated carbons. Relation between adsorption-based separation performances of MOFs and their structural properties were also investigated. Results showed that MOFs having largest cavity diameters in the range of 4.6-5.4 Å, pore limiting diameters in the range of 2.4-3.7 Å, surface areas less than 2000 m^2/g and porosities less than 0.5 are promising adsorbents for CH_4/N_2 separations. Combination of adsorption and diffusion data obtained from molecular simulations were used to predict both membrane selectivities and gas permeabilities of MOFs for separation of CH_4/N_2 mixtures. A significant number of MOF membranes was identified to be CH_4 selective in contrast to the traditional membrane materials which are generally N_2 selective. Several MOFs exceeded the upper bound established for the polymeric membranes and many MOFs exhibited higher gas permeabilities than zeolites. The results of this study will be useful to guide the experiments to the most promising MOF adsorbents and membranes for efficient separation of CH_4/N_2 mixtures.

*The results given in this chapter were published in Industrial & Engineering Chemistry Research with following reference: Z. Sumer and S. Keskin, "Adsorption and Membrane-Based CH_4/N_2 Separation Performances of MOFs", Industrial & Engineering Chemistry Research (2017). The original manuscript has been rearranged to conform to the format requirements of the dissertation.

6.1. Separation Performances of MOF Adsorbents

In order to validate the accuracy of our molecular simulations, GCMC results with the available experimental data for gas uptake of various MOFs were compared. In a previous study of our research group,[44] the accuracy of our molecular simulations were validated for CH_4 uptake of different MOFs by comparing simulation results with 267 experimental data points and obtaining a high regression coefficient (R^2), 0.972. In this thesis, 79 experimental data points were collected for N_2 uptake of widely studied MOFs such as MOF-5 (also known as IRMOF-1), CuBTC, ZIF-8 in a pressure range of 0.1-15 bar at 298 K. Molecular simulations were performed exactly under the same temperature and pressure with the experiments for those MOFs. Figure 6.1(a) shows that our simulations predict the N_2 uptake of MOFs in a good agreement with the experiments, giving a high R^2 of 0.99. As discussed in the previous sections, a limited number of experimental and computational studies has focused on adsorption-based CH_4/N_2 separation using MOFs and only a few of them reported mixture selectivity of MOFs. Molecular simulations were performed for these MOFs under the same conditions and using the same CH_4/N_2 compositions. Figure 6.1(b) shows that there is a good agreement between our selectivity predictions and experimentally/computationally reported selectivities of MOFs. In fact, the limited number of data points in Figure 6.1(b) highlights the need for further studies on adsorption-based separation of CH_4/N_2 mixtures using MOFs. All the details of literature data used to compare our simulation results in Figure 6.1 such as name of the MOFs, operating conditions (pressure and temperature), and corresponding literature references are reported in Tables D1 and D2 of Appendix D. Overall, results of Figure 6.1 suggest that our molecular simulations are accurate to predict adsorption-based CH_4/N_2 separation performances of MOFs. Motivated from this result, adsorption-based CH_4/N_2 separation performances of 102 different MOF structures having different structural properties were predicted.

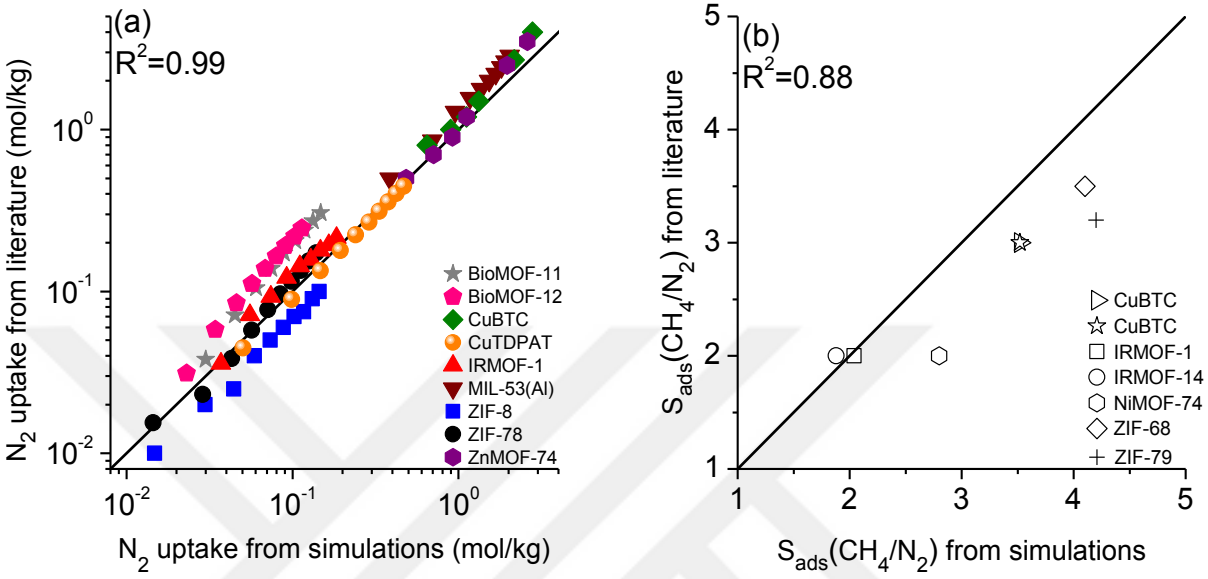

Figure 6.1. (a)Comparison of our molecular simulations with the experiments for N_2 uptake of MOFs at 298 K, 0.1-15 bar. (b)Comparison of our predicted adsorption selectivity with the experimentally/computationally reported selectivity for CH_4/N_2 separation at 298 K and 10 bar.

In order to quantitatively assess separation potential of MOF adsorbents, adsorption selectivities (S_{ads}), working capacities (ΔN), and percent regenerabilities (R%) of MOFs were computed. These parameters were calculated under two different conditions: Case 1 where adsorption pressure is 1 bar and desorption pressure is 0.1 bar, and Case 2 where adsorption pressure is 10 bar and desorption pressure is 1 bar. These two cases were chosen to investigate the effect of pressure on the performances of the MOF adsorbents. Molecular simulations showed that CH_4 is more strongly adsorbed compared to N_2 in both cases. This can be attributed to the stronger interaction of the CH_4 molecules with the MOF atoms compared to N_2. CH_4 molecule has a greater energy parameter (148 K) than N_2 (36.4 K) in molecular simulations. As a result, all MOFs are CH_4 selective in the adsorption process.

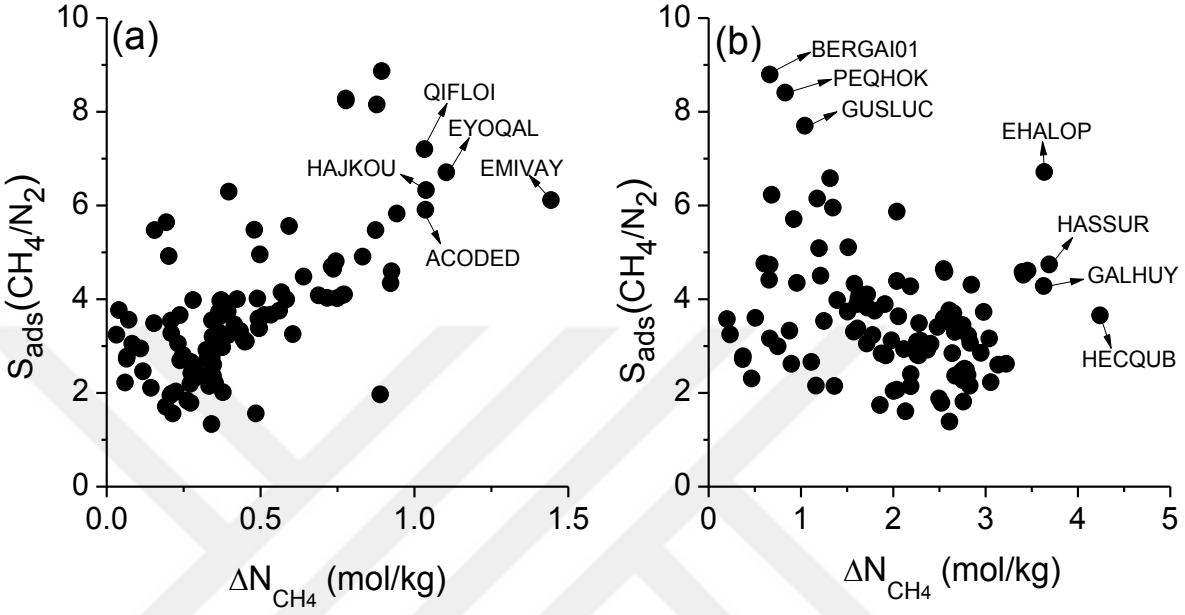

Figure 6.2. Adsorption selectivity and working capacity of MOFs for (a)Case 1 and (b)Case 2.

Figure 6.2(a) shows that CH_4 adsorption selectivities of MOFs range between 1.33-8.86, and CH_4 working capacities range between 0.03-1.44 mol/kg for Case 1. The low CH_4 working capacities can be explained by the similar CH_4 adsorption amounts of MOFs at 0.1 bar and at 1 bar. The highest working capacity in Figure 6.1(a) belongs to EMIVAY, 1.44 mol/kg, with a high CH_4/N_2 selectivity, 6.11. Four other MOFs, QIFLOI, EYOQAL, HAJKOU and ACODED also exhibit CH_4 working capacities greater than 1 mol/kg in addition to high CH_4 selectivities (7.20, 6.71, 6.33, and 5.91, respectively). Although selectivity range of Case 2 (1.39-8.79) is similar to that of Case 1, higher CH_4 working capacities (0.20-4.24 mol/kg) are observed in Case 2 as shown in Figure 6.2(b). This is due to the higher CH_4 uptake of MOFs at 10 bar compared to the one at 1 bar. In an adsorption-based separation process, both high selectivity and high working capacity are desired. In

other words, materials at the right upper corner of Figure 6.2 which offer both high selectivity and high working capacity are promising for CH_4/N_2 separation. One interesting outcome of Figure 6.2(b) is that CH_4/N_2 selectivity is generally inversely correlated with the CH_4 working capacity. MOFs with the highest CH_4 selectivities, such as BERGAI01 (8.79), PEQHOK (8.40), GUSLUC (7.70) tend to have low working capacities (0.66, 0.83 and 1.04 mol/kg, respectively). On the other hand, MOFs with the highest working capacities such as HECQUB (2.24 mol/kg), HASSUR (3.69 mol/kg), EHALOP (3.64 mol/kg) and GALHUY (3.63 mol/kg) have moderate CH_4/N_2 selectivities (3.66, 4.74, 6.71 and 4.28, respectively).

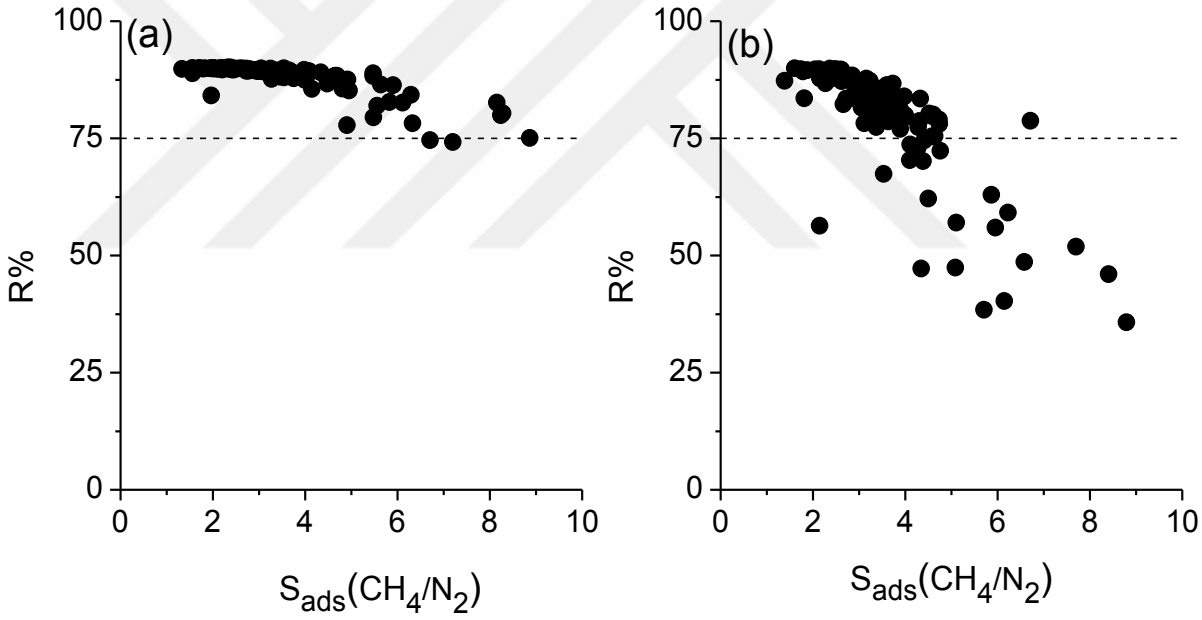

Figure 6.3. Regenerability and adsorption selectivity of MOFs for (a)Case 1 and (b)Case 2. Dashed line represents 75% regenerability, which was set as the minimum desired R%.

In Chapter 4 it was shown that per cent regenerability (R%) is a very important metric to identify the most promising adsorbents. For example, several MOFs with high CO_2 selectivity exhibit low regenerability, limiting their practical usage as adsorbents.[87] The

relation between R% and CH_4/N_2 selectivity of MOFs is shown in Figure 6.3. All MOFs show very high R%, ranging between 74.2-90.1% in Figure 6.3(a). As shown in Eq.(3), regenerability was calculated as the ratio of working capacity to the adsorbed amount of gas at the adsorption pressure. Since MOFs have lower working capacities and much smaller gas uptakes at the adsorption pressure of Case 1 compared to that of Case 2, regenerabilities obtained in Case 1 are higher than those in Case 2. OWITOE, OWITUK, OWITEU, OWIVAS and OWITAQ have the highest R% (~90%) but they have low CH_4/N_2 selectivities, between 2.31-2.40. MOFs with the highest selectivities such as BERGAI01, GUSLUC, PEQHOK and DEJROB have R% of 75.1%, 80.3%, 79.9% and 82.6%, respectively, suggesting that these MOFs can be used as efficient adsorbents. Figure 6.3(b) shows that R% of MOFs ranges between 35.8 to 89.9% in Case 2. Highly selective MOFs, BERGAI01 (8.79), PEQHOK (8.40), and GUSLUC (7.70) are likely to show low regenerabilities (35.8%, 46% and 51.8%, respectively) while 14 MOFs with high R% (89% and higher) have CH_4 selectivities less than 2.6. Therefore, our previous suggestion of using R% as a metric to screen the materials at the first step of the adsorbent search for CO_2 separation processes was found to be also valid for the CH_4/N_2 separation processes.[87]

Among the three metrics discussed, selectivity is generally considered as the most important one to evaluate a new adsorbent's performance. In order to compare CH_4/N_2 selectivity of the MOFs considered in this thesis with other materials reported in the literature, selectivity data of different adsorbents such as zeolites, activated carbons, molecular sieves were collected and presented in Table 6.1. The materials listed in Table 6.1 were previously identified as good adsorbents for CH_4/N_2 separations.[20] Selectivity of these adsorbents range from 1.75-3.4 at 1 bar and 1.9-3.2 at 10 bar whereas the selectivity of MOFs considered in this thesis ranges from 1.4 to 8.8 (1.3 to 8.9) at 1 bar (10 bar). In other words, MOFs considered in this thesis exhibit higher selectivity than the traditional adsorbents. Considering the fact that only 102 selected MOFs were studied in this thesis,

many other MOFs which may show higher CH_4/N_2 adsorption selectivity may exist in the database. Three MOFs that were identified with the highest CH_4/N_2 selectivities, BERGAI01, GUSLUC and PEQHOK were added into Table 6.1. It is important to note that although these MOFs show the highest CH_4/N_2 selectivities, they have low working capacities (0.66, 0.83 and 1.04 mol/kg, respectively) and low regenerabilities (35.8%, 46% and 51.8%, respectively) which may limit their practical usage.

Table 6.1. CH_4/N_2 selectivities of different adsorbents.

Adsorbents	**$S_{ads,\ CH_4/N_2}$**	**Condition**	**Method**	**Reference**
BERGAI01	8.80 (8.86)	298 K, 10 bar (1 bar)	a	This thesis
PEQHOK	8.40 (8.24)	298 K, 10 bar (1 bar)	a	This thesis
GUSLUC	7.70 (8.28)	298 K, 10 bar (1 bar)	a	This thesis
Linde 4A zeolite	3.40	302 K, 1 bar	b	[88]
F30-470 Degussa Activated Carbon	3.20	303 K, 10 bar	c	[89]
H^+ mordenite zeolite	3.20	302 K, 1 bar	b	[88]
SAPO-34 zeolite	3.00	298 K, 10 bar	d	[20]
BPL Calgon Carbon	2.80	298 K, 1 bar	b	[90]
Na-SAPO-34 zeolite	2.56	298 K, 1 bar	b	[91]
Linde 5A zeolite	2.20	298 K, 10 bar	d	[20]
Hβ zeolite	2.00	303 K, 1 bar	e	[75]
Bayer KEL2200 5A molecular sieve	1.90	303 K, 10 bar	c	[89]
Chabazite zeolite	1.90	302 K, 1 bar	b	[88]
Naβ zeolite	1.75	303 K, 1 bar	e	[75]

(a)Mixture simulations (CH_4/N_2:50/50), (b)Single-component adsorption experiments, (c)Single-component adsorption experiments and IAST calculations (CH_4/N_2:40/60), (d)Breakthrough experiments (CH_4/N_2:50/50), (e)Ratio of the Henry's coefficients obtained from the single-component adsorption experiments.

As discussed before, a good adsorbent should combine high selectivity with high working capacity and high regenerability to ensure an efficient and economic separation process. In order to identify the most promising MOF adsorbents that can satisfy all the

adsorbent evaluation metrics, some constraints were defined: minimum R% was set to 75% and minimum working capacity was set to 1 mol CH_4/kg of MOF. After these constraints, the top 5 MOFs with the highest CH_4/N_2 selectivities were focused on and their separation properties were listed in Table 6.2. For Case 1, there were only three MOFs which satisfy these constraints, therefore two other MOFs which have R% of 74% were included. There is no common MOF in the lists of Case 1 and Case 2, showing the importance of the operating conditions in selecting an efficient adsorbent material. Among the materials listed in Table 6.2, EHALOP is the best adsorbent candidate for Case 2 with a high selectivity of 6.71, high working capacity of 3.64 mol CH_4/kg MOF and high R% of 78.7%. EHALOP is one of the CCDC names of a widely-studied MOF, MIL-53(Al). Ren et al.[20] reported selectivity of MIL-53(Al) in the range of 3.8-4.8 and Hu et al.[22] reported its selectivity as 3.4 by performing breakthrough experiments with equimolar CH_4/N_2 mixtures. The reason of the difference between our predicted selectivity (6.71) and literature values (3.4-4.8) can be due the differences in the reported structures of synthesized MIL-53(Al), which may lead to different CH_4 and N_2 uptakes. Chung et al.[43] recently calculated CH_4 uptake of 13 different CCDC structures of MIL-53(Al), including EHALOP, and ended up with CH_4 uptake values varying between 180-267 vol_{STP} CH_4/vol (8-12.6 mol CH_4/kg) at 65 bar and 298 K depending on the structure. Our simulation result for CH_4 uptake in EHALOP at the same condition agrees with the literature (10.9 mol CH_4/kg). As a result, one of the experimentally reported MIL-53(Al) structures (EHALOP) was identified as a promising adsorbent for CH_4/N_2 separation.

Table 6.2. Top performing MOF adsorbents for CH_4/N_2 separation.

	Case 1				Case 2		
	$S_{ads,\ CH_4/N_2}$	ΔN (mol/kg)	R%		$S_{ads,\ CH_4/N_2}$	ΔN (mol/kg)	R%
QIFLOI	7.20	1.03	74.17	EHALOP	6.71	3.64	78.72
EYOQAL	6.71	1.10	74.63	HASSUR	4.74	3.69	78.08
HAJKOU	6.33	1.04	78.17	KARLAS	4.64	2.55	75.46
EMIVAY	6.11	1.44	82.59	DIDBID	4.61	3.46	80.06
ACODED	5.91	1.04	86.35	EBAMOL	4.58	2.56	75.39

Finally, the relation between adsorption selectivity and structural properties of MOFs were examined. Establishing relation between easily measurable/computable structural properties of MOFs and their separation performances would be very useful to save computational time and to guide the experimental efforts for the synthesis of materials with the desired topology. However, clear identification of this type of relations is challenging because separation performance of a material is determined by the interplay of various factors such as chemical topology, porosity, pore size, pore shape and it cannot be simply correlated to only a single or two structural properties.[92] Therefore, the relation between adsorption selectivity and easily computable structural properties of MOFs such as such as LCDs, PLDs, surface areas and porosities were examined. Figure 6.4 shows that MOFs having LCDs in the range of 4.6-5.4 Å, PLDs in the range of 2.4-3.7 Å, surface areas less than 2000 m^2/g and porosities less than 0.5 are promising adsorbents for both cases. MOFs with LCDs around 4.5-6 Å generally exhibit higher CH_4/N_2 selectivities (>4) than MOFs with larger pore sizes. As the LCD increases, selectivity generally decreases. MOFs that have large LCDs (>10 Å) show lower selectivities (<3) since both larger CH_4 and smaller N_2 molecules can easily adsorb into the pores. Figure 6.5 (a,c) shows that there is no strong correlation between working capacity and pore sizes/porosities/surface areas of MOFs for Case 1. MOFs with the LCD values between 4.4-6.7 Å have generally higher working capacities. On the other hand, as pore sizes, porosities and surface areas increase, working

capacities of MOFs are generally enhanced in Case 2 as shown in Figure 6.5(b,d). MOFs with the surface areas >1000 m^2/g and porosities >0.5 have higher working capacities. These results highlight the importance of the operation conditions and different material requirements of the VSA and PSA-based separation processes.

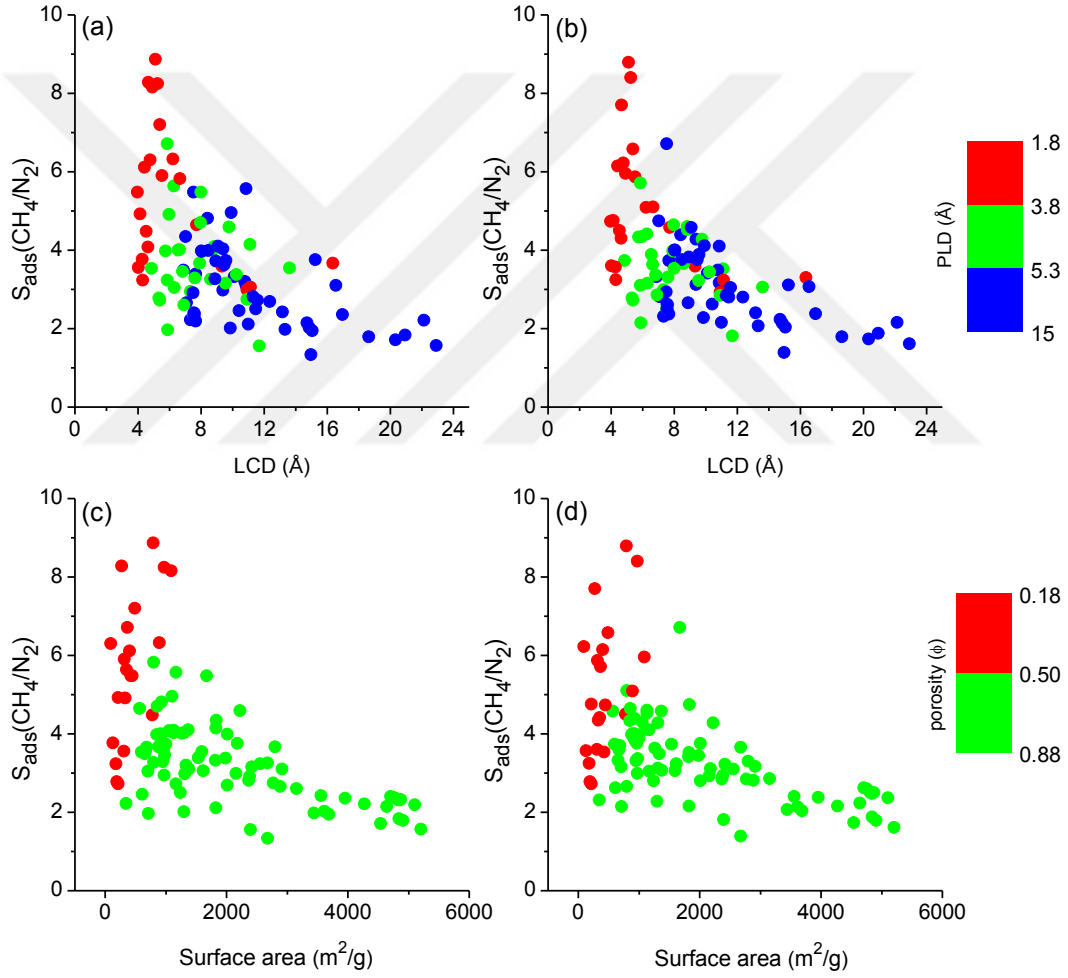

Figure 6.4. Adsorption selectivities of MOFs as a function of LCDs and PLDs for (a)Case 1 and (b)Case 2 and as a function of surface area and porosity for (c)Case 1 and (d)Case 2.

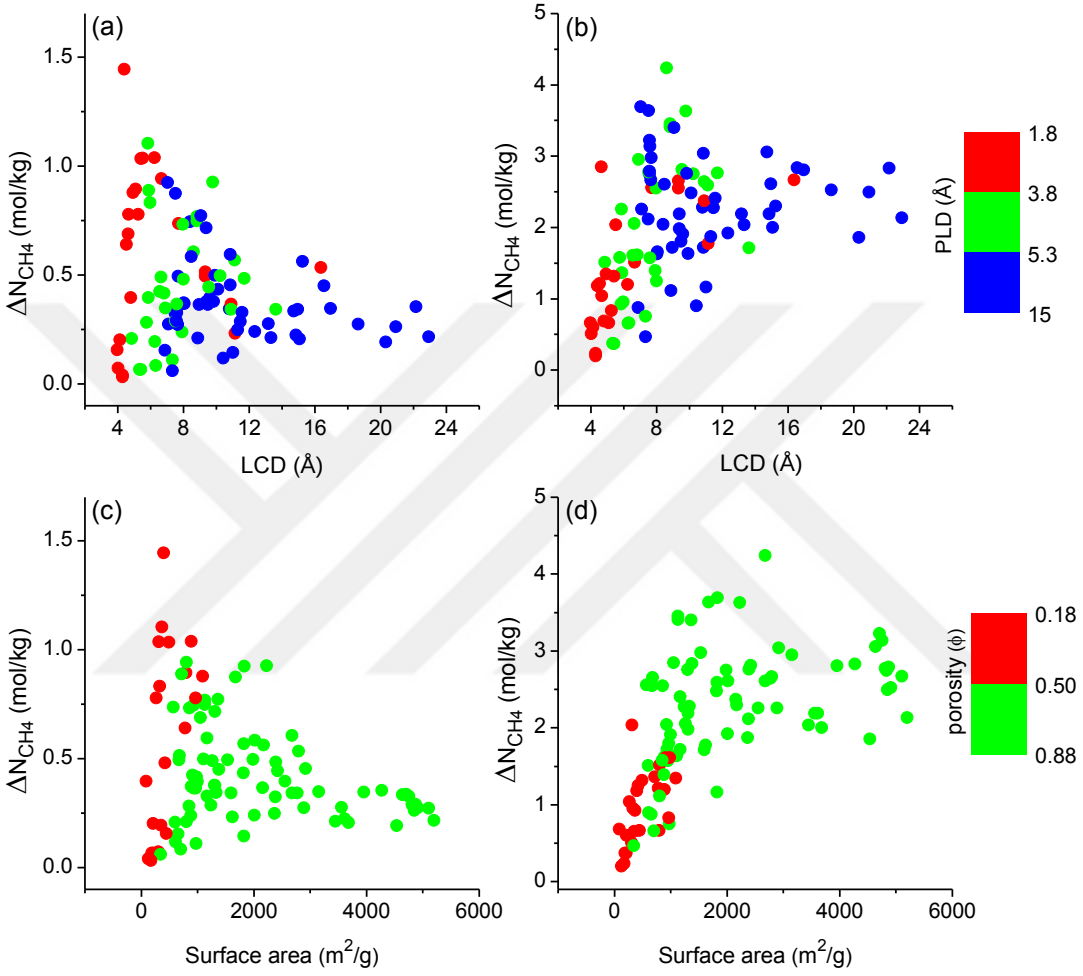

Figure 6.5. Working capacities of MOFs as a function of LCD and PLD for (a)Case 1 and (b)Case 2 and as a function of surface area and porosity for (c)Case 1 and (d)Case 2.

6.2. Separation Performances of MOF Membranes

Membrane-based CH_4/N_2 separation performances of MOFs were also investigated. In order to predict the membrane-based separation properties of MOFs, EMD simulations were performed to assess diffusivities of CH_4/N_2 mixtures in MOFs. Diffusion is not accessible at the nanosecond scale by EMD simulations if the computed self-diffusivities of gases are less than 10^{-8} cm^2/s. Therefore, 5 MOFs were eliminated in which diffusion was too slow and examined 97 MOFs as membranes. In Case 1, feed pressure of the membrane was set to 0.01 bar to represent dilute conditions and in Case 2 feed pressure was set to 10 bar to represent industrial operating conditions. Selectivity and gas permeability of the MOF membranes were examined for both cases. Figure 6.6 shows N_2/CH_4 selectivity of MOF membranes as a function of N_2 permeability. Different from the adsorption-based gas separation, N_2 selectivity was represented instead of CH_4 selectivity in order to compare MOF membranes' performances with the polymeric membranes which are known to be N_2 selective.[3] The Robeson's upper bound, which was prepared using the empirical permeability data of numerous polymeric membranes for the N_2/CH_4 separation, is also shown in Figure 6.[3] Polymers have N_2 selectivity ranging from 0.2 to 9, while their N_2 permeabilities vary between 0.01-10^4 Barrer. MOFs considered in this thesis have N_2 selectivities ranging between 0.08-26, and permeabilities ranging between 10^2-10^6 Barrer. MOF membranes generally exhibit lower N_2 selectivities than the polymeric membranes but many of them (38 out of 97 in Figure 6.6(a), 28 out of 97 in Figure 6(b)) exceed the upper bound due to their high N_2 permeabilities, $>10^4$ Barrer. The high gas permeability of MOFs can be attributed to the high surface area and high pore volume of MOFs compared to polymers.[93]

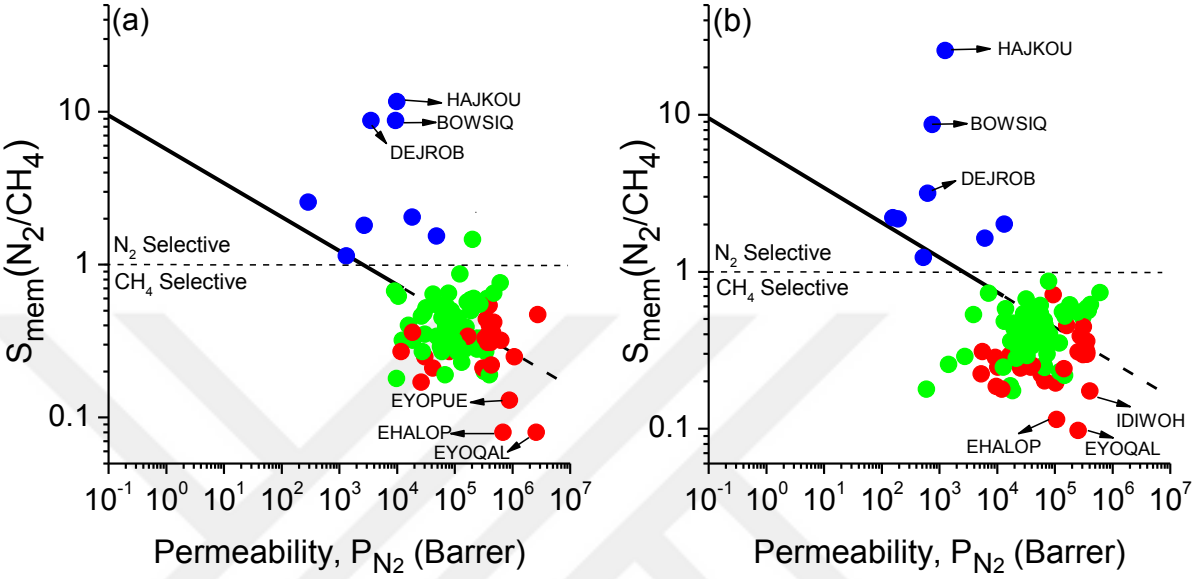

Figure 6.6. Membrane selectivity and permeability of MOFs for (a)Case 1 (b)Case 2. Solid lines represent the Robeson's upper bound for N_2/CH_4 separation.[3] Color coding is given in Figure 6.7.

The dashed line in Figure 6.6 represents the gas preference of the membranes. 9 (8) MOF membranes are N_2 selective whereas 88 (89) MOF membranes are CH_4 selective at 0.01 bar (10 bar) as shown in Figure 6.6a(b). In order to better understand the effects of adsorption and diffusion on the membrane selectivity of MOFs, the adsorption and diffusion selectivities were examined in detail and their relations were shown in Figure 6.7. All the MOFs considered in this thesis are CH_4 selective over N_2 in the adsorption process as discussed before. Therefore, N_2/CH_4 adsorption selectivities are always less than 1 in Figure 6.7. On the other hand, diffusion selectivity can favor either CH_4 or N_2. These two molecules have similar sizes and weights, therefore depending on the pore structure of the MOF, one can diffuse faster than another or the two molecules can have similar diffusion rates.

Diffusion selectivity of the MOFs in Figures 6.6 and 6.7 were color-coded. Red colors represent MOFs that are CH_4 selective in diffusion (N_2/CH_4 diffusion selectivity between 0.4-1 for Case 1 and 0.5-1 for Case 2), green colors represent MOFs that are N_2 selective in diffusion (N_2/CH_4 diffusion selectivity between 1-4) and blue colors represent MOFs that are strongly N_2 selective in diffusion (N_2/CH_4 diffusion selectivity between 4-80 for Case 1 and 4-131 for Case 2). As a result of these different diffusion selectivities, MOF membranes are categorized into three to discuss their separation performances: (i) MOFs in which both diffusion and membrane selectivity favor N_2, (ii) MOFs in which both diffusion and membrane selectivity favor CH_4, (iii) MOFs in which diffusion selectivity favors N_2 but membrane selectivity favors CH_4.

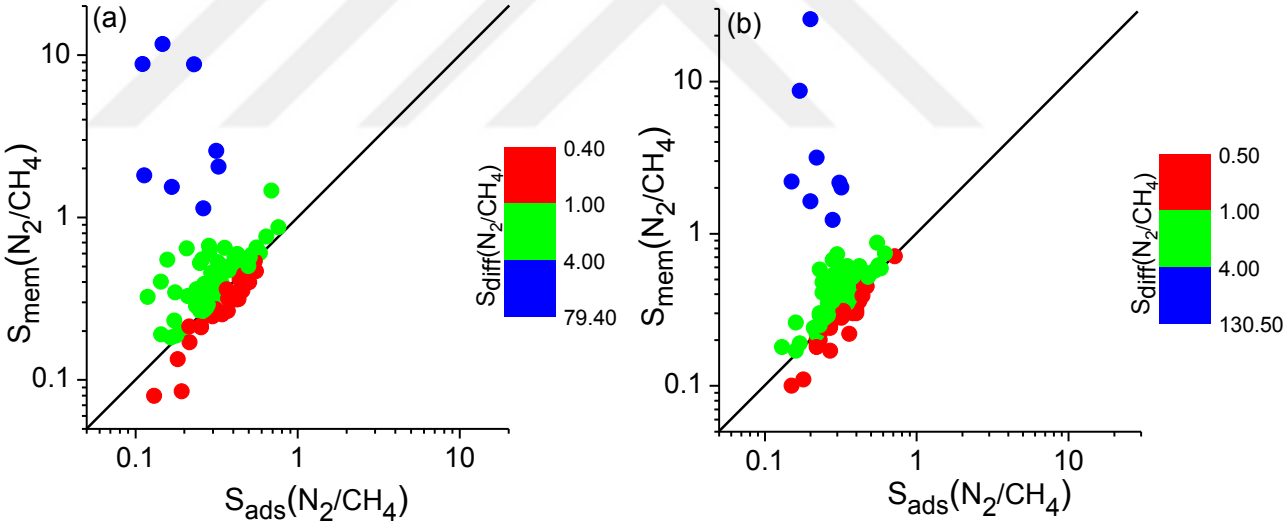

Figure 6.7. Adsorption, diffusion and membrane selectivity of MOFs for (a)Case 1 and (b)Case 2.

(i) For 8 MOFs, shown by blue in Figures 6.6 and 6.7, both diffusion and membrane selectivities favor N_2. Strong N_2 diffusion selectivity of these MOFs dominates the low

adsorption selectivity for N_2 (0.11-0.23) and makes the membrane selective for N_2. Three MOFs, HAJKOU, DEJROB and BOWSIQ are promising due to their high N_2 selectivity and high N_2 permeability and they exceed the upper bound as shown in Figure 6.6.

(ii) 26 (29) MOFs have CH_4 diffusion selectivities around 1-2 as shown in Figure 6.7a(b). Since both adsorption and diffusion favors CH_4 in these MOFs, these membranes are highly CH_4 selective. EHALOP and EYOQAL are promising membranes due to their high CH_4 selectivities, 11.78 (10.26) and 12.51 (8.72), respectively as shown in Figure 6.7a(b).

(iii) Majority of the MOFs (63 among 97 in Figure 6.7(a) and 60 among 97 in Figure 6.7(b)) weakly favor N_2 in diffusion but they are CH_4 selective in adsorption. N_2 diffusion selectivities ranges from 1.0 to 4.0 and CH_4 adsorption selectivities vary between 1.3 and 9. Adsorption selectivity dominates the weak N_2 diffusion selectivity and these MOFs become CH_4 selective membranes.

Overall analysis of these results can be summarized as follows: Adsorption selectivity always favor CH_4 in MOFs. The membrane selectivity is governed by the diffusion selectivity. If diffusion selectivity strongly (weakly) favors N_2, the MOF becomes highly N_2 (weakly CH_4) selective membrane. On the other hand, if diffusion selectivity favors CH_4 similar to adsorption selectivity, then the MOF becomes a highly CH_4 selective membrane. The most promising MOF membranes for selective separation of N_2 from CH_4 and selective separation of CH_4 from N_2 are listed in Tables 6.3 and 6.4, respectively. MOFs that have N_2/CH_4 membrane selectivities greater than 2 were considered and the first 5 MOFs with the highest N_2 permeabilities for each case were ranked in Table 6.3. The best performing MOF membranes are the same for the two cases. These MOFs are N_2 selective and N_2 permeable in a membrane-based separation process due to their high diffusion selectivities which dominates their low adsorption selectivities. Top 5 MOF membranes that are CH_4 selective over N_2 are listed in Table 6.4. MOFs with CH_4/N_2 selectivities greater than 5 were ranked

based on their CH_4 permeabilities in Table 6.4. It was previously shown that as long as a MOF does not possess high N_2 selectivity in diffusion, it becomes CH_4 selective in the membrane-based gas separation. MOFs in Table 6.4 show low diffusion selectivity for CH_4 and membrane selectivities of these MOFs are dominated by the high CH_4 adsorption selectivities.

Table 6.4. Top performing MOF membranes for selective separation of CH_4 from N_2. All selectivities are reported for CH_4 over N_2.

	Case 1				
	S_{ads}	**S_{diff}**	**S_{mem}**	**P, N_2 (Barrer)**	**P, CH_4 (Barrer)**
EYOQAL	7.67	1.63	12.51	2.58×10^{6}	3.22×10^{7}
EHALOP	5.18	2.27	11.78	6.88×10^{5}	8.10×10^{6}
EYOPUE	5.47	1.36	7.45	8.94×10^{5}	6.66×10^{6}
EMIVAY	5.58	0.96	5.33	4.02×10^{5}	2.15×10^{6}
AJIHOQ	5.25	0.96	5.05	3.25×10^{5}	1.65×10^{6}
	Case 2				
	S_{ads}	**S_{diff}**	**S_{mem}**	**P, N_2 (Barrer)**	**P, CH_4 (Barrer)**
EHALOP	6.71	1.53	10.26	2.55×10^{5}	2.61×10^{6}
EYOQAL	5.71	1.53	8.72	1.08×10^{5}	9.44×10^{5}
IDIWOH	3.73	1.55	5.76	4.05×10^{5}	2.33×10^{6}
EMIVAY	6.15	0.93	5.73	1.87×10^{4}	1.07×10^{5}
DIDBID	4.61	1.11	5.12	1.04×10^{5}	5.33×10^{5}

The membrane performances of the MOFs in this thesis for Case 1 (0.01 bar) were compared with the results of Qiao and coworkers,[25] who studied 17,257 hypothetical MOFs at dilute conditions. Before making a comparison, it is important to note that a small number of experimentally synthesized, real MOFs with PLDs in the range of 1.8-14.9 Å were considered whereas they studied a large number of hypothetical MOFs with PLDs ranging between 3-4 Å. They computed self-diffusivity of N_2 as 2×10^{-8}-5×10^{-5} cm^2/s and self-

diffusivity of CH_4 as 10^{-8}-5×10^{-5} cm^2/s in the pores of hypothetical MOFs at infinite dilution. Our computed diffusivities for real MOFs were 4.8×10^{-6}-1.7×10^{-3} cm^2/s for N_2 and 8×10^{-8}-2.8×10^{-3} cm^2/s CH_4 at 0.01 bar. Our higher gas diffusivities can be explained by the larger pore sizes of the studied MOFs. N_2 selectivities of hypothetical MOFs were reported to be 0.04-1000 while N_2 permeabilities were computed as 0.1-10^5 Barrer. Our predicted N_2 selectivities for real MOFs were between 0.08-11.66 and N_2 permeabilities were between 2.9×10^2-2.8×10^6 Barrer. This comparison shows that N_2 selectivities of real MOFs are lower than those of hypothetical MOFs, whereas N_2 permeabilities of real MOFs are higher than those of hypothetical MOFs. This result can be explained by the very narrow pore sizes of the hypothetical MOFs, which lead to higher selectivity but lower permeability of N_2. Similarities between membrane selectivities and permeabilities of real and hypothetical MOFs suggest that MOFs, real or computer-generated, have some common chemical and structural properties that lead to similar separation performances.

By studying the MOFs for both adsorption-based and membrane-based gas separations, it was also shown that a MOF with excellent properties as an adsorbent may have less exciting properties as a membrane. For example, QIFLOI has a high CH_4 adsorption selectivity (6.58) at 10 bar, but its membrane selectivity for CH_4 is too low, 0.45, to consider this material as a promising membrane. At that point, it is important to note that the materials that were identified as promising adsorbents and membranes must be tested under real industrial operating conditions and stability of the MOFs that will be used as adsorbents and/or membranes must be examined. The stability information for BERGAI01, EHALOP, HAJKIO and DEJROB were checked since they were identified as top adsorbents and membranes in this thesis. These MOFs were reported to be stable: BERGAI01 shows high thermo-stability,[94] EHALOP preserves its framework integrity at high temperature,[95] HAJKIO exhibits high thermal stability and permanent porosity,[82] and DEJROB has a thermally stable structure at ambient conditions.[96]

Chapter 7

CONCLUSION AND OUTLOOK

Design and development of efficient adsorbent and membrane materials is required for CO_2 separations. Due to the presence of very large number of distinct MOF structures, it is challenging to identify promising materials for a specific gas separation application. In this thesis, molecular simulations were performed to compute adsorption and permeability of gas mixtures such as CO_2/CH_4, CO_2/N_2 and CO_2/H_2 in MOFs to examine separation of CO_2 from natural gas, power plant flue gas and petroleum refineries. For the natural gas purification, N_2 removal is also highly important. Due to the similarity in physical and chemical properties of CH_4 and N_2 molecules, it is very difficult to find an efficient adsorbent and/or membrane material that can effectively separate CH_4/N_2 mixtures. Therefore, CH_4/N_2 separation was also studied throughout this thesis.

Firstly, 100 MOFs were ranked based on the widely used adsorbent evaluation metrics for CO_2/CH_4, CO_2/N_2 and CO_2/H_2 mixture separation processes. Results showed that although ranking of the adsorbents changes depending on the performance metrics used, the materials that appear in the top performing materials lists are generally similar except the ranking based on the regenerability. The top ten adsorbents identified based on R% values were completely different than the materials rankings based on other criteria. Therefore, it was suggested that large-scale material screening can be done to eliminate adsorbents with low R% (preferentially lower than 75%) and then to rank them based on their selectivities

and working capacities. In addition to ranking of MOF adsorbents, their separation performances with other well-known adsorbent materials such as zeolites were compared. Results showed that MOFs generally have similar CO_2 selectivities with the zeolites but significantly higher CO_2 working capacities for separation of CO_2/CH_4, CO_2/N_2 and CO_2/H_2 mixtures than traditional zeolites under similar operating conditions. Relationships between easily computable structural properties of MOFs and their CO_2 separation potentials were also examined. Supporting the previous findings for hypothetical MOFs, real MOFs with LCDs of 4-7 Å, surface areas of 200 to 800 m^2/g, and porosities less than 0.5 have the best potential to achieve high CO_2 selectivity. These findings will be helpful for the design of new MOF adsorbents with better CO_2 separation abilities. After identifying the top performing MOFs for adsorption-based CO_2/CH_4, CO_2/N_2 and CO_2/H_2 separations, kinetic separation performance of these MOFs was also examined. MOFs exhibit lower membrane selectivities than their adsorption selectivities. In other words, these MOFs are found to be more appropriate to be used as adsorbents rather than as membranes for CO_2 separations.

In the second part, atomically-detailed simulations were combined with the Maxwell model to make predictions for the performances of MOF-based MMMs in CO_2/N_2 separations. First of all, atomically-detailed simulations were performed to obtain adsorption and diffusion data of CO_2 and N_2 gases in MOFs. Adsorption, diffusion and permeation selectivities of MOFs were compared to understand the potential of MOFs in CO_2/N_2 separations. Results showed that adsorption selectivity favors CO_2 in all MOFs whereas diffusion selectivity can favor either CO_2 or N_2. As a result, permeation selectivities of MOFs are governed by the diffusion selectivity preference of the materials. Several promising MOFs with high CO_2/N_2 selectivities and high CO_2 permeabilities were identified. A large number of MOFs was found to be located above the upper bound established for polymers. Motivated from this result, the separation performances of 700 different MOF-based MMMs composed of 70 MOFs and 10 polymers were examined. This is the largest number of MOF-

based MMMs for which computational screening is done to date. Using MOFs as filler particles increased the CO_2 permeability of all 10 polymers but the change in selectivity varied with respect to position of the polymer on the upper bound. For polymers that have low CO_2 permeabilities but high CO_2 selectivities, the identity of the MOF used as filler is not important. All MOFs enhanced the CO_2 permeabilities of this type of polymers without changing their selectivities. On the other hand, for polymers that have high CO_2 permeabilities but low CO_2 selectivities, separation properties of the MMMs strongly depend on the identity of the filler particle. Highly selective MOFs were able to increase both CO_2 permeabilities and CO_2/N_2 selectivities of PTMGP and PTMSP.

Finally, adsorption and diffusion of CH_4/N_2 mixtures in 102 different MOFs were investigated to predict their adsorption-based and membrane-based separation performances. Several metrics such as adsorption selectivity, working capacity and regenerability which are required to evaluate the efficiency of an adsorption-based separation process were calculated and the top performing MOF adsorbents were identified based on these metrics. MOFs having LCDs in the range of 4.6-5.4 Å, PLDs in the range of 2.4-3.7 Å, surface areas less than 2000 m^2/g and porosities less than 0.5 were found to be promising adsorbents. In order to evaluate the membrane-based separation performances of MOFs, diffusivity of CH_4/N_2 mixtures through the MOFs' pores were computed and reported the diffusion selectivity of each material. Results showed that if the diffusion selectivity strongly (weakly) favors N_2, the MOF becomes highly N_2 (weakly CH_4) selective membrane whereas if the diffusion selectivity also favors CH_4 similar to the adsorption selectivity, then the MOF becomes a highly CH_4 selective membrane.

At that point, it is important to list and discuss the assumptions used in this thesis. 1) Only a fraction of the MOFs that are reported in CCDC were examined. There are thousands of MOFs in the database that might show better separation properties than the MOFs studied here. 2) In the calculations, stability of the material is not considered. During the simulations,

MOFs were assumed to preserve their uniform crystallinity, and pressure and/or temperature were assumed to not affect their functions. This issue is more likely handled by experimental studies. Once the potential value of a material has been demonstrated using molecular simulations, a more detailed experimental approach must be used to increase the precision of the assessment. 3) In the simulation boxes, solvent molecules that might be left inside the pores were not defined and crystal structures were assumed to be clear. Additionally, MOFs were assumed to be rigid and breathing effect was neglected. These assumptions are fastening the simulations, and it has been found out that the accuracy of results are usually not much affected by rigid framework assumption. Once a MOF is found to be promising, perhaps additional calculations can be performed by considering flexibility, in order to validate the results. 4) The materials that were identified as promising must be of course tested under real industrial operating conditions where other impurities exist in the gas mixtures. For example, a material cannot find place in practical adsorption processes if it is not stable in the presence of some impurities although it has a high selectivity.

The aim of this thesis was to initially perform a large-scale material screening in order to identify the most promising materials before extensive computational and/or experimental efforts. In Chapter 4, results showed that although ranking of the adsorbents changes depending on the performance metrics used, the materials that appear in the top performing materials lists are generally similar except the ranking based on the regenerability. In Chapter 5, it was concluded that for polymers that have low CO_2 permeabilities but high CO_2 selectivities, the identity of the MOF used as filler is not important. Finally, by studying the MOFs for both adsorption-based and membrane-based gas separations in Chapter 6, it was shown that a MOF with excellent properties as an adsorbent may have less exciting properties as a membrane. Hopefully, results of this thesis will be a guide for future computational studies to investigate more MOFs for different gas mixtures.

BIBLIOGRAPHY

[1] Simon, C.M., et al., The materials genome in action: identifying the performance limits for methane storage. *Energy & Environmental Science,* 2015. 8(4): p. 1190-1199.
[2] Bhadra, S. and S. Farooq, Separation of methane–nitrogen mixture by pressure swing adsorption for natural gas upgrading. *Industrial & Engineering Chemistry Research,* 2011. 50(24): p. 14030-14045.
[3] Robeson, L.M., The upper bound revisited. *Journal of Membrane Science,* 2008. 320(1): p. 390-400.
[4] Goh, P.S., et al., Recent advances of inorganic fillers in mixed matrix membrane for gas separation. *Separation and Purification Technology,* 2011. 81(3): p. 243-264.
[5] Keskin, S., *Recent Advances in Molecular Dynamics Simulations of Gas Diffusion in Metal Organic Frameworks,* in *Molecular Dynamics - Theoretical Developments and Applications in Nanotechnology and Energy*. 2012, InTech. p. 255-280.
[6] Ben-Mansour, R., et al., Carbon capture by physical adsorption: Materials, experimental investigations and numerical modeling and simulations–A review. *Applied Energy,* 2016. 161: p. 225-255.
[7] Basdogan, Y., K.B. Sezginel, and S. Keskin, Identifying highly selective metal organic frameworks for CH_4/H_2 separations using computational tools. *Industrial & Engineering Chemistry Research,* 2015. 54(34): p. 8479-8491.
[8] Keskin, S., T.M. van Heest, and D.S. Sholl, Can Metal–Organic Framework Materials Play a Useful Role in Large-Scale Carbon Dioxide Separations? *ChemSusChem,* 2010. 3(8): p. 879-891.
[9] Yazaydın, A.O.z.r., et al., Screening of metal− organic frameworks for carbon dioxide capture from flue gas using a combined experimental and modeling approach. *Journal of the American Chemical Society,* 2009. 131(51): p. 18198-18199.
[10] Yilmaz, G., A. Ozcan, and S. Keskin, Computational screening of ZIFs for CO_2 separations. *Molecular Simulation,* 2015. 41(9): p. 713-726.
[11] Wilmer, C.E., et al., Structure–property relationships of porous materials for carbon dioxide separation and capture. *Energy & Environmental Science,* 2012. 5(12): p. 9849-9856.
[12] Li, J.-R., R.J. Kuppler, and H.-C. Zhou, Selective gas adsorption and separation in metal–organic frameworks. *Chemical Society Reviews,* 2009. 38(5): p. 1477-1504.
[13] Qiao, Z., K. Zhang, and J. Jiang, In silico screening of 4764 computation-ready, experimental metal–organic frameworks for CO_2 separation. *Journal of Materials Chemistry A,* 2016. 4: p. 2105-2114.
[14] Sikora, B.J., et al., Thermodynamic analysis of Xe/Kr selectivity in over 137000 hypothetical metal-organic frameworks. *Chemical Science,* 2012. 3(7): p. 2217-2223.
[15] Liu, J., et al., Progress in adsorption-based CO_2 capture by metal–organic frameworks. *Chemical Society Reviews,* 2012. 41(6): p. 2308-2322.

[16] Yu, J., et al., CO_2 Capture and Separations Using MOFs: Computational and Experimental Studies. *Chemical Reviews*, 2017.
[17] Watanabe, T. and D.S. Sholl, Accelerating applications of metal–organic frameworks for gas adsorption and separation by computational screening of materials. *Langmuir*, 2012. 28(40): p. 14114-14128.
[18] Wu, D., et al., Revealing the structure–property relationships of metal–organic frameworks for CO_2 capture from flue gas. *Langmuir*, 2012. 28(33): p. 12094-12099.
[19] Möllmer, J., et al., Pure and mixed gas adsorption of CH_4 and N_2 on the metal–organic framework Basolite® A100 and a novel copper-based 1, 2, 4-triazolyl isophthalate MOF. *Journal of Materials Chemistry*, 2012. 22(20): p. 10274-10286.
[20] Ren, X., et al., Highly enhanced selectivity for the separation of CH_4 over N_2 on two ultra-microporous frameworks with multiple coordination modes. *Microporous and Mesoporous Materials*, 2014. 186: p. 137-145.
[21] Sun, T., et al., Experimental Evaluation of the Adsorption, Diffusion, and Separation of CH_4/N_2 and CH_4/CO_2 Mixtures on Al-BDC MOF. *Separation Science and Technology*, 2015. 50(6): p. 874-885.
[22] Hu, J., et al., Separation of CH_4/N_2 mixtures in metal–organic frameworks with 1D micro-channels. *RSC Advances*, 2016. 6(68): p. 64039-64046.
[23] Liu, B. and B. Smit, Comparative molecular simulation study of CO_2/N_2 and CH_4/N_2 separation in zeolites and metal−organic frameworks. *Langmuir*, 2009. 25(10): p. 5918-5926.
[24] Liu, B. and B. Smit, Molecular simulation studies of separation of CO_2/N_2, CO_2/CH_4, and CH_4/N_2 by ZIFs. *The Journal of Physical Chemistry C*, 2010. 114(18): p. 8515-8522.
[25] Qiao, Z., et al., High-throughput computational screening of 137953 metal–organic frameworks for membrane separation of a $CO_2/N_2/CH_4$ mixture. *Journal of Materials Chemistry A*, 2016. 4(41): p. 15904-15912.
[26] Car, A., C. Stropnik, and K.-V. Peinemann, Hybrid membrane materials with different metal–organic frameworks (MOFs) for gas separation. *Desalination*, 2006. 200(1): p. 424-426.
[27] Perez, E.V., et al., Mixed-matrix membranes containing MOF-5 for gas separations. *Journal of Membrane Science*, 2009. 328(1): p. 165-173.
[28] Basu, S., A. Cano-Odena, and I.F. Vankelecom, Asymmetric Matrimid®/[Cu 3 (BTC) 2] mixed-matrix membranes for gas separations. *Journal of Membrane Science*, 2010. 362(1): p. 478-487.
[29] Basu, S., A. Cano-Odena, and I.F. Vankelecom, MOF-containing mixed-matrix membranes for CO_2/CH_4 and CO_2/N_2 binary gas mixture separations. *Separation and Purification Technology*, 2011. 81(1): p. 31-40.
[30] Bae, T.-H. and J.R. Long, CO_2/N_2 separations with mixed-matrix membranes containing Mg 2 (dobdc) nanocrystals. *Energy & Environmental Science*, 2013. 6(12): p. 3565-3569.

[31] Duan, C., et al., Enhanced gas separation properties of metal organic frameworks/polyetherimide mixed matrix membranes. *Journal of Applied Polymer Science,* 2014. 131(17): p. 40719-40729.
[32] Kim, J., et al., Matrix effect of mixed-matrix membrane containing CO_2-selective MOFs. *Journal of Applied Polymer Science,* 2016. 133(1): p. 42853-42861.
[33] Keskin, S. and D.S. Sholl, Selecting metal organic frameworks as enabling materials in mixed matrix membranes for high efficiency natural gas purification. *Energy & Environmental Science,* 2010. 3(3): p. 343-351.
[34] Erucar, I. and S. Keskin, Computational screening of metal organic frameworks for mixed matrix membrane applications. *Journal of Membrane Science,* 2012. 407: p. 221-230.
[35] Erucar, I. and S. Keskin, Screening metal–organic framework-based mixed-matrix membranes for CO_2/CH_4 separations. *Industrial & Engineering Chemistry Research,* 2011. 50(22): p. 12606-12616.
[36] Yilmaz, G. and S. Keskin, Molecular modeling of MOF and ZIF-filled MMMs for CO_2/N_2 separations. *Journal of Membrane Science,* 2014. 454: p. 407-417.
[37] Altintas, C. and S. Keskin, Molecular simulations of porous coordination network-based mixed matrix membranes for CO_2/N_2 separations. *Molecular Simulation,* 2015. 41(16-17): p. 1396-1408.
[38] Rufford, T.E., et al., The removal of CO_2 and N_2 from natural gas: a review of conventional and emerging process technologies. *Journal of Petroleum Science and Engineering,* 2012. 94: p. 123-154.
[39] Van den Bergh, J., et al., Separation and permeation characteristics of a DD3R zeolite membrane. *Journal of Membrane Science,* 2008. 316(1): p. 35-45.
[40] Wu, T., et al., Influence of propane on CO_2/CH_4 and N_2/CH_4 separations in CHA zeolite membranes. *Journal of Membrane Science,* 2015. 473: p. 201-209.
[41] Keskin, S. and D.S. Sholl, Assessment of a metal−organic framework membrane for gas separations using atomically detailed calculations: CO_2, CH_4, N_2, H_2 mixtures in MOF-5. *Industrial & Engineering Chemistry Research,* 2008. 48(2): p. 914-922.
[42] Battisti, A., S. Taioli, and G. Garberoglio, Zeolitic imidazolate frameworks for separation of binary mixtures of CO_2, CH_4, N_2 and H_2: a computer simulation investigation. *Microporous and Mesoporous Materials,* 2011. 143(1): p. 46-53.
[43] Chung, Y.G., et al., Computation-Ready, Experimental Metal-Organic Frameworks: A Tool to Enable High-Throughput Screening of Nanoporous Crystals. *Chemistry of Materials,* 2014. 26(21): p. 6185-6192.
[44] Sezginel, K.B., A. Uzun, and S. Keskin, Multivariable linear models of structural parameters to predict methane uptake in metal–organic frameworks. *Chemical Engineering Science,* 2015. 124: p. 125-134.
[45] Allen, F.H., The Cambridge Structural Database: a quarter of a million crystal structures and rising. *Acta Crystallographica Section B: Structural Science,* 2002. 58(3): p. 380-388.

[46] Willems, T.F., et al., Algorithms and tools for high-throughput geometry-based analysis of crystalline porous materials. *Microporous and Mesoporous Materials*, 2012. 149(1): p. 134-141.
[47] Sarkisov, L. and A. Harrison, Computational structure characterisation tools in application to ordered and disordered porous materials. *Molecular Simulation*, 2011. 37(15): p. 1248-1257.
[48] Rappé, A.K., et al., UFF, a full periodic table force field for molecular mechanics and molecular dynamics simulations. *Journal of the American Chemical Society*, 1992. 114(25): p. 10024-10035.
[49] Ozturk, T.N. and S. Keskin, Predicting gas separation performances of porous coordination networks using atomistic simulations. *Industrial & Engineering Chemistry Research*, 2013. 52(49): p. 17627-17639.
[50] Ozturk, T.N. and S. Keskin, Computational screening of porous coordination networks for adsorption and membrane-based gas separations. *The Journal of Physical Chemistry C*, 2014. 118(25): p. 13988-13997.
[51] Mayo, S.L., B.D. Olafson, and W.A. Goddard, DREIDING: a generic force field for molecular simulations. *Journal of Physical Chemistry*, 1990. 94(26): p. 8897-8909.
[52] Potoff, J.J. and J.I. Siepmann, Vapor–liquid equilibria of mixtures containing alkanes, carbon dioxide, and nitrogen. *AIChE Journal*, 2001. 47(7): p. 1676-1682.
[53] Makrodimitris, K., G.K. Papadopoulos, and D.N. Theodorou, Prediction of permeation properties of CO_2 and N_2 through silicalite via molecular simulations. *The Journal of Physical Chemistry B*, 2001. 105(4): p. 777-788.
[54] Buch, V., Path integral simulations of mixed para-D_2 and ortho-D_2 clusters: The orientational effects. *The Journal of Chemical Physics*, 1994. 100(10): p. 7610-7629.
[55] Martin, M.G. and J.I. Siepmann, Transferable potentials for phase equilibria. 1. United-atom description of n-alkanes. *The Journal of Physical Chemistry B*, 1998. 102(14): p. 2569-2577.
[56] Wilmer, C.E., K.C. Kim, and R.Q. Snurr, An extended charge equilibration method. *The Journal of Physical Chemistry Letters*, 2012. 3(17): p. 2506-2511.
[57] Frenkel, D. and B. Smit, *Understanding Molecular Simulation: From Algorithms to Applications*. 2 ed. Computational Science Series. 2002, San Diego: Academic Press.
[58] Greathouse, J.A. and M.D. Allendorf, Force field validation for molecular dynamics simulations of IRMOF-1 and other isoreticular zinc carboxylate coordination polymers. *The Journal of Physical Chemistry C*, 2008. 112(15): p. 5795-5802.
[59] Haldoupis, E., et al., Quantifying Large Effects of Framework Flexibility on Diffusion in MOFs: CH_4 and CO_2 in ZIF-8. *ChemPhysChem*, 2012. 13(15): p. 3449-3452.
[60] Pérez-Pellitero, J., et al., Adsorption of CO_2, CH_4, and N_2 on zeolitic imidazolate frameworks: experiments and simulations. *Chemistry-A European Journal*, 2010. 16(5): p. 1560-1571.

[61] Bae, Y.S. and R.Q. Snurr, Development and evaluation of porous materials for carbon dioxide separation and capture. *Angewandte Chemie International Edition,* 2011. 50(49): p. 11586-11596.
[62] Notaro, F., et al., *Pressure swing absorption separation based on differences in polar characteristics of components of mixture*. 1998, Google Patents.
[63] Rege, S.U. and R.T. Yang, A simple parameter for selecting an adsorbent for gas separation by pressure swing adsorption. *Separation Science and Technology,* 2001. 36(15): p. 3355-3365.
[64] Keskin, S. and D.S. Sholl, Efficient methods for screening of metal organic framework membranes for gas separations using atomically detailed models. *Langmuir,* 2009. 25(19): p. 11786-11795.
[65] Krishna, R. and D. Paschek, Self-diffusivities in multicomponent mixtures in zeolites. *Physical Chemistry Chemical Physics,* 2002. 4(10): p. 1891-1898.
[66] Adatoz, E. and S. Keskin, Application of MD simulations to predict membrane properties of MOFs. *Journal of Nanomaterials,* 2015. 16(1): p. 193.
[67] Atci, E. and S. Keskin, Atomically detailed models for transport of gas mixtures in ZIF membranes and ZIF/polymer composite membranes. *Industrial & Engineering Chemistry Research,* 2012. 51(7): p. 3091-3100.
[68] Sholl, D.S., Understanding macroscopic diffusion of adsorbed molecules in crystalline nanoporous materials via atomistic simulations. *Accounts of Chemical Research,* 2006. 39(6): p. 403-411.
[69] Maxwell, J.C., *A Treatise on Electricity and Magnetism: By James Clerk Maxwell*. 1954: Dover.
[70] Myers, A. and J.M. Prausnitz, Thermodynamics of mixed-gas adsorption. *AIChE Journal,* 1965. 11(1): p. 121-127.
[71] Bae, Y.-S., et al., Enhancement of CO_2/N_2 selectivity in a metal-organic framework by cavity modification. *Journal of Materials Chemistry,* 2009. 19(15): p. 2131-2134.
[72] Kim, J., et al., Large-scale computational screening of zeolites for ethane/ethene separation. *Langmuir,* 2012. 28(32): p. 11914-11919.
[73] Cavenati, S., C.A. Grande, and A.E. Rodrigues, Adsorption equilibrium of methane, carbon dioxide, and nitrogen on zeolite 13X at high pressures. *Journal of Chemical & Engineering Data,* 2004. 49(4): p. 1095-1101.
[74] Merel, J., M. Clausse, and F. Meunier, Experimental investigation on CO_2 post-combustion capture by indirect thermal swing adsorption using 13X and 5A zeolites. *Industrial & Engineering Chemistry Research,* 2008. 47(1): p. 209-215.
[75] Xu, X., et al., Adsorption separation of carbon dioxide, methane, and nitrogen on Hβ and Na-exchanged β-zeolite. *Journal of Natural Gas Chemistry,* 2008. 17(4): p. 391-396.

[76] Krishna, R. and J.M. van Baten, In silico screening of metal–organic frameworks in separation applications. *Physical Chemistry Chemical Physics,* 2011. 13(22): p. 10593-10616.
[77] Tong, M., et al., Revealing the structure–property relationship of covalent organic frameworks for CO_2 capture from postcombustion gas: a multi-scale computational study. *Physical Chemistry Chemical Physics,* 2014. 16(29): p. 15189-15198.
[78] Zhu, C.-G., Synthesis, Structures, and Antimicrobial Activity of Solvated and Desolvated Polymeric Copper (II) Complexes Derived from {[1-(2-Hydroxyphenyl) methylidene] amino} acetic Acid. *Synthesis and Reactivity in Inorganic, Metal-Organic, and Nano-Metal Chemistry,* 2013. 43(7): p. 886-891.
[79] Wu, T., et al., Three-Dimensional Covalent Co-Assembly between Inorganic Supertetrahedral Clusters and Imidazolates. *Angewandte Chemie International Edition,* 2011. 50(11): p. 2536-2539.
[80] Gao, L., et al., Mixed solvothermal synthesis and X-ray characterization of a layered copper coordination polymer, $Cu(H_2O)(1,3\text{-}BDC)\cdot H_2O$ (BDC= benzenedicarboxylate). *Inorganic Chemistry Communications,* 2003. 6(9): p. 1249-1251.
[81] Krishna, R. and J.M. van Baten, In silico screening of zeolite membranes for CO_2 capture. *Journal of Membrane Science,* 2010. 360(1): p. 323-333.
[82] Pachfule, P., et al., Experimental and computational approach of understanding the gas adsorption in amino functionalized interpenetrated metal organic frameworks (MOFs). *Journal of Materials Chemistry,* 2011. 21(44): p. 17737-17745.
[83] Hou, Q., et al., Two new 3-D photoluminescence metal–organic frameworks based on cubane Cu 4 I 4 clusters as tetrahedral nodes. *Inorganica Chimica Acta,* 2012. 384: p. 287-292.
[84] Park, K., U. Lee, and T. Iwamoto, Three-Dimensional Metal Complex Host with Alternating Arrangement of the Occupied and Vacant Channels. The Crystal Structure of $Cd(NH_2CH(CH_3)CH_2NH_2)Ni(CN)_4\cdot$ 0.25G. *Bulletin of The Korean Chemical Society* 1996. 17(10): p. 919-924.
[85] Brown, A.J., et al., Interfacial microfluidic processing of metal-organic framework hollow fiber membranes. *Science,* 2014. 345(6192): p. 72-75.
[86] Cacho-Bailo, F., et al., ZIF-8 continuous membrane on porous polysulfone for hydrogen separation. *Journal of Membrane Science,* 2014. 464: p. 119-126.
[87] Sumer, Z. and S. Keskin, Ranking of MOF Adsorbents for CO_2 Separations: A Molecular Simulation Study. *Industrial & Engineering Chemistry Research,* 2016. 55(39): p. 10404-10419.
[88] Jensen, N.K., et al., Screening zeolites for gas separation applications involving methane, nitrogen, and carbon dioxide. *Journal of Chemical & Engineering Data,* 2011. 57(1): p. 106-113.

[89] Sievers, W. and A. Mersmann, Single and multicomponent adsorption equilibria of carbon dioxide, nitrogen, carbon monoxide and methane in hydrogen purification processes. *Chemical Engineering & Technology,* 1994. 17(5): p. 325-337.
[90] Baksh, M., R. Yang, and D. Chung, Composite sorbents by chemical vapor deposition on activated carbon. *Carbon,* 1989. 27(6): p. 931-934.
[91] Rivera-Ramos, M.E. and A.J. Hernández-Maldonado, Adsorption of N_2 and CH_4 by ion-exchanged silicoaluminophosphate nanoporous sorbents: Interaction with monovalent, divalent, and trivalent cations. *Industrial & Engineering Chemistry Research,* 2007. 46(14): p. 4991-5002.
[92] Ozturk, T.N. and S. Keskin, Computational screening of porous coordination networks for adsorption and membrane-based gas separations. *The Journal of Physical Chemistry C,* 2014. 118(25): p. 13988-13997.
[93] Sumer, Z. and S. Keskin, Computational Screening of MOF-Based Mixed Matrix Membranes for CO_2/N_2 Separations. *Journal of Nanomaterials,* 2016. 2016: p. 12.
[94] Luo, M.-B., et al., Framework isomers controlled by the speed of crystallization: different aggregation fashions of Zn (II) and 1, 2, 4-triazol-3-amine, distinct (3, 4)-connected self-penetrating nets, and various pore shapes. *Dalton Transactions,* 2013. 42(38): p. 13802-13805.
[95] Alaerts, L., et al., Selective adsorption and separation of ortho-substituted alkylaromatics with the microporous aluminum terephthalate MIL-53. *Journal of the American Chemical Society,* 2008. 130(43): p. 14170-14178.
[96] Wang, F., et al., Zeolitic Boron Imidazolate Frameworks with 4-Connected Octahedral Metal Centers. *Chemistry–A European Journal,* 2012. 18(38): p. 11876-11879.
[97] Chen, D.-L., et al., Transient breakthroughs of CO_2/CH_4 and C_3H_6/C_3H_8 mixtures in fixed beds packed with Ni-MOF-74. *Chemical Engineering Science,* 2014. 117: p. 407-415.
[98] Li, J., et al., Separation of CO_2/CH_4 and CH_4/N_2 mixtures using MOF-5 and $Cu_3(BTC)_2$. *Journal of Energy Chemistry,* 2014. 23(4): p. 453-460.
[99] Li, J.-R., et al., Carbon dioxide capture-related gas adsorption and separation in metal-organic frameworks. *Coordination Chemistry Reviews,* 2011. 255(15): p. 1791-1823.
[100] Remy, T., et al., Selective dynamic CO_2 separations on Mg-MOF-74 at low pressures: a detailed comparison with 13X. *The Journal of Physical Chemistry C,* 2013. 117(18): p. 9301-9310.
[101] Orefuwa, S., et al., Effects of nitro-functionalization on the gas adsorption properties of isoreticular metal-organic framework-eight (IRMOF-8). *Microporous and Mesoporous Materials,* 2013. 177: p. 82-90.
[102] Karra, J.R., et al., Adsorption study of CO_2, CH_4, N_2, and H_2O on an interwoven copper carboxylate metal-organic framework (MOF-14). *Journal of Colloid and Interface Science,* 2013. 392: p. 331-6.

[103] Debatin, F., et al., An Isoreticular Family of Microporous Metal–Organic Frameworks Based on Zinc and 2-Substituted Imidazolate-4-amide-5-imidate: Syntheses, Structures and Properties. *Chemistry–A European Journal*, 2012. 18(37): p. 11630-11640.
[104] Wang, B., et al., Tuning CO_2 Selective Adsorption over N_2 and CH_4 in UiO-67 Analogues through Ligand Functionalization. *Inorganic Chemistry*, 2014. 53(17): p. 9254-9259.
[105] Xian, S., et al., Highly enhanced and weakened adsorption properties of two MOFs by water vapor for separation of CO_2/CH_4 and CO_2/N_2 binary mixtures. *Chemical Engineering Journal*, 2015. 270: p. 385-392.
[106] Yang, Q., et al., Molecular simulation of separation of CO_2 from flue gases in CU-BTC metal-organic framework. *AIChE Journal*, 2007. 53(11): p. 2832-2840.
[107] García, E.J., et al., Role of Structure and Chemistry in Controlling Separations of CO_2/CH_4 and $CO_2/CH_4/CO$ Mixtures over Honeycomb MOFs with Coordinatively Unsaturated Metal Sites. *The Journal of Physical Chemistry C*, 2012. 116(50): p. 26636-26648.
[108] Chen, R., et al., A two-dimensional zeolitic imidazolate framework with a cushion-shaped cavity for CO_2 adsorption. *Chemical Communications*, 2013. 49(82): p. 9500-9502.
[109] Zhang, W., et al., Cooperative effect of temperature and linker functionality on CO_2 capture from industrial gas mixtures in metal-organic frameworks: a combined experimental and molecular simulation study. *Physical Chemistry Chemical Physics*, 2012. 14(7): p. 2317-25.
[110] Zhang, Z., et al., Enhancement of CO_2 Adsorption and CO_2/N_2 Selectivity on ZIF-8 via Postsynthetic Modification. *AIChE Journal*, 2013. 59(6): p. 2195-2206.
[111] Bloch, W.M., et al., Post-synthetic Structural Processing in a Metal–Organic Framework Material as a Mechanism for Exceptional CO_2/N_2 Selectivity. *Journal of the American Chemical Society*, 2013. 135(28): p. 10441-10448.
[112] Yang, Q. and C. Zhong, Molecular simulation of carbon dioxide/methane/hydrogen mixture adsorption in metal-organic frameworks. *The Journal of Physical Chemistry B*, 2006. 110(36): p. 17776-83.
[113] Wu, H., et al., Cu-TDPAT, an rht-type dual-functional metal-organic framework offering significant potential for use in H_2 and natural gas purification processes operating at high pressures. *The Journal of Physical Chemistry C*, 2012. 116(31): p. 16609-16618.
[114] Li, T., et al., Systematic modulation and enhancement of CO_2: N_2 selectivity and water stability in an isoreticular series of bio-MOF-11 analogues. *Chemical Science*, 2013. 4(4): p. 1746-1755.
[115] Karra, J.R. and K.S. Walton, Molecular simulations and experimental studies of CO_2, CO, and N_2 adsorption in metal−organic frameworks. *The Journal of Physical Chemistry C*, 2010. 114(37): p. 15735-15740.

[116] Li, B., et al., Enhanced Binding Affinity, Remarkable Selectivity, and High Capacity of CO_2 by Dual Functionalization of a rht-Type Metal–Organic Framework. *Angewandte Chemie International Edition*, 2012. 51(6): p. 1412-1415.
[117] Saha, D., et al., Adsorption of CO_2, CH_4, N_2O, and N_2 on MOF-5, MOF-177, and zeolite 5A. *Environmental Science & Technology*, 2010. 44(5): p. 1820-1826.
[118] Banerjee, R., et al., Control of pore size and functionality in isoreticular zeolitic imidazolate frameworks and their carbon dioxide selective capture properties. *Journal of the American Chemical Society*, 2009. 131(11): p. 3875-3877.

APPENDIX

Appendix A. Structural Properties of MOFs.

REFCODE	LCD (Å)	PLD (Å)	Surface Area (m^2/g)	Pore Volume (cm^3/g)	REFCODE	LCD (Å)	PLD (Å)	Surface Area (m^2/g)	Pore Volume (cm^3/g)
ACODED	5.52	3.38	314.49	0.43	KUGZIW	10.79	9.76	1331.61	0.65
ACUFEK	13.16	7.60	3558.03	1.31	LARVIL	7.32	7.08	347.97	0.24
AHORAR	6.63	4.31	1259.53	0.67	LASPOM	3.96	2.97	448.80	0.26
AJIHOQ	8.41	6.67	930.28	0.48	LECQEQ	11.46	10.71	1242.20	0.54
AVEROJ	6.88	6.49	654.75	0.34	LUKLIN	16.96	9.39	3955.12	1.61
BERGAI01	5.10	2.39	796.08	0.28	LUMDIG	7.91	4.95	880.17	0.42
BEYSEF	4.85	3.93	599.19	0.48	LUXDEO	5.05	2.36	1708.95	0.36
BOWSIQ	4.53	2.99	781.23	0.34	MOCKAR	10.86	6.77	2918.74	1.00
BUVWOF02	6.27	4.71	354.90	0.32	MOCKEV	10.91	3.75	2154.65	0.86
DEJROB	4.93	2.89	1090.32	0.39	NEFTOJ	4.65	3.63	1049.96	0.56
DIDBID	8.83	5.23	1133.64	0.59	NIBHOW	22.93	14.89	5202.76	3.03
DIDBOJ	8.82	5.29	1129.16	0.59	NIMPEG01	5.87	5.25	2557.83	0.88
EBAMOL	7.71	3.61	570.73	0.53	NUJCIE	4.30	3.45	176.25	0.28
EBEMOO	4.13	3.10	211.72	0.22	NUTQAV	10.91	4.12	2772.48	0.94
EDUSIF	15.06	7.93	3685.93	1.36	NUTQEZ	11.70	4.31	2392.98	0.81
EDUSUR	14.97	6.61	2675.83	1.06	OCIZIL	4.79	3.72	90.76	0.31
EDUVII	20.32	9.78	4540.87	2.03	OFERUN	11.14	2.79	1617.54	0.64
EDUVOO	20.94	10.64	4847.41	2.31	OHUKIM	14.71	8.30	4642.30	1.88
EHALOP	7.52	7.08	1671.71	0.69	OWITAQ	7.59	5.36	4752.93	1.18
EMIHAK	9.39	5.69	1313.24	0.45	OWITEU	7.56	5.32	4837.06	1.19
EMIHIS	9.39	5.69	1313.24	0.45	OWITIY	7.66	5.80	5105.51	1.30
EMIVAY	4.41	3.66	399.66	0.37	OWITOE	7.52	5.28	4809.83	1.17
EYOPOY	5.88	5.04	715.47	0.45	OWITUK	7.56	5.32	4875.38	1.19
EYOPUE	5.97	5.06	328.74	0.38	OWIVAS	7.56	5.34	4707.92	1.17
EYOQAL	5.85	5.17	369.39	0.37	OWIVEW	6.91	4.45	3152.82	0.86
EZILUV	9.32	3.50	683.87	0.63	PEQHOK	5.24	2.58	970.33	0.31
EZIMAC	9.34	3.50	671.44	0.63	PEVQEO	14.85	7.96	3614.62	1.33
FAYPUS	13.62	4.26	1598.02	0.78	PODKUQ	22.15	8.48	4273.23	1.78
FECXUI	10.11	5.68	1815.60	0.70	PURQOJ	11.31	6.85	2364.67	0.82
FEVFUJ	11.00	10.18	1826.46	0.83	QIFLOI	5.40	3.00	490.00	0.13
FIQCEN	11.12	5.24	1823.14	0.72	QOWQUO	16.36	2.71	2797.39	0.90
GALBUS	9.07	6.25	1368.15	0.62	RAYKEJ	9.59	7.36	1000.19	0.54

GALHUY	9.78	4.70	2225.98	0.79	RAYKIN	9.48	7.12	968.14	0.53
GITTUZ	10.86	8.04	1169.97	0.60	RAYKUZ	8.95	5.83	936.93	0.52
GITVEL	15.25	13.38	2177.20	0.94	RAYLAG	8.06	5.70	932.94	0.51
GIVDUL	6.31	4.76	704.16	0.32	RAYLEK	8.03	5.63	890.67	0.51
GIWNUV	4.28	1.79	126.70	0.14	RAYLIO	7.61	5.06	953.14	0.49
GUPCOK	7.33	4.70	973.12	0.56	RAYLOU	6.83	5.20	984.01	0.48
GUPDIF	4.02	3.18	308.58	0.36	RAYLUA	6.56	4.80	916.67	0.48
GUSLUC	4.66	3.70	270.70	0.35	SAHYIK	13.33	7.64	3445.98	1.31
HAJKIO	6.67	3.47	801.32	0.39	SOQSAU	9.55	4.98	2420.70	0.81
HAJKOU	6.23	3.27	892.17	0.39	SOQSEY	10.25	4.93	1987.79	0.76
HASSUR	7.03	5.33	1831.69	0.63	VEJYOZ	8.47	5.70	2016.54	0.78
HECQUB	8.60	5.10	2679.72	0.88	VEJZIU	12.35	7.49	2010.53	0.84
HIFVUO	7.50	5.98	2382.16	0.87	VOGTIV	9.85	8.26	1300.53	0.58
IDIWOH	7.68	7.19	1534.78	0.63	WOBHIF	11.58	10.81	1167.10	0.52
IMIXEI	7.09	5.53	2886.52	0.89	XALXUF01	16.56	6.67	2201.90	0.93
JENKIX	9.92	7.49	1105.15	0.56	YOZBIZ01	8.89	6.10	803.24	0.48
KARLAS	7.97	4.30	855.13	0.57	YOZBOF	8.00	4.95	426.36	0.43
KEYFIF	5.40	4.90	214.08	0.25	YUVSUE	5.76	4.59	851.70	0.44
KEYFIF01	5.33	4.84	191.96	0.24	ZELROZ	18.64	12.41	4912.93	2.67
KIPKIF	10.42	10.33	612.78	0.50					

Appendix B. Supplementary Information for Chapter 4

Table B1. Experimental data collected from the literature for single-component CO_2 adsorption in MOFs.

MOF	T (K)	P (bar)	Reference
Ni-MOF-74	298	1	[97]
IRMOF-1	298	0.1	[56]
IRMOF-1	298	1	[98]
CuBTC	298	0.1	[56]
CuBTC	298	10	[99]
Mg-MOF-74	298	0.1	[56]
Mg-MOF-74	298	1	[100]
IRMOF-3	298	0.1	[56]
IRMOF-8	298	30	[101]
ZIF-8	298	0.1	[56]
ZIF-8	298	30	[99]
MIL-47	298	0.1	[56]
MOF-14	298	5	[102]
Cd-ANIC-1	298	1	[82]
Co-ANIC-1	298	1	[82]
IFP-3	298	10	[103]
ZIF-68	298	1	[99]
ZIF-70	298	1	[99]
Zn-MOF-74	298	0.1	[56]
BUT-10	298	1	[104]
ZIF-79	298	1	[104]
MIL-53 (Al)	298	25	[101]

Table B2. Experimental data collected from the literature for CO_2 selectivity of MOFs.

MOF	T (K)	P (bar)	Adsorption measurement	Separation	Reference
IRMOF-1	303	1	Mixture	CO_2/CH_4	[105]
IRMOF-1	298	1	Single - IAST	CO_2/CH_4	[106]
CuBTC	298	1	Single- IAST	CO_2/CH_4	[106]
Ni-MOF-74	303	1	Mixture	CO_2/CH_4	[107]
ZIF-8	298	1	Single- IAST	CO_2/CH_4	[108]
UiO-66	273	1	Mixture	CO_2/CH_4	[109]
MIL-47	298	1	Single- IAST	CO_2/CH_4	[104]
Zn-MOF-74	303	1	Mixture	CO_2/CH_4	[107]
MOF-14	298	1	Mixture	CO_2/CH_4	[102]
BUT-10	298	vacuum	Single-IAST	CO_2/N_2	[104]
MOF-14	298	1	Mixture	CO_2/N_2	[102]
ZIF-8	298	5	Single- IAST	CO_2/N_2	[110]
Mg-MOF-74	296	1	Single- IAST	CO_2/N_2	[111]
CuBTC	298	1	Single- IAST	CO_2/N_2	[112]
ZIF-68	298	10	Single- IAST	CO_2/N_2	[24]
Mg-MOF-74	298	1	Single-IAST	CO_2/H_2	[113]
Mg-MOF-74	298	10	Single-IAST	CO_2/H_2	[113]
CuTDPAT	298	1	Single-IAST	CO_2/H_2	[113]
CuTDPAT	298	10	Single-IAST	CO_2/H_2	[113]

Table B3. Ranking of the top ten MOFs based on different metrics (Case 2).

CO_2/H_2

S_{sp}		S_{ads}		ΔN (mol/kg)		AFM (mol/kg)		S		R%	
AJIHOQ	243214.28	EYOQAL	999.57	NUTQEZ	7.71	AJIHOQ	5551.65	EMIHAK	176840.88	IDIWOH	91.60
EMIHAK	226414.68	EMIHAK	892.05	FIQCEN	6.65	EMIHIS	3943.16	AJIHOQ	128660.79	OWIVAS	91.49
EMIHIS	67774.19	EMIVAY	860.43	MOCKAR	6.33	EMIHAK	3814.32	EYOQAL	78144.63	OWITAQ	91.40
EYOPUE	42317.13	EYOPUE	742.72	LECQEQ	6.19	HASSUR	3455.53	EYOPUE	66671.93	OWITOE	91.40
HASSUR	42150.58	AJIHOQ	721.55	XALXUF01	6.07	GALBUS	3386.40	BOWSIQ	50938.00	OWITUK	91.35
EYOQAL	37543.56	QIFLOI	704.39	HASSUR	5.86	LECQEQ	3221.31	EMIVAY	42473.82	OWIVEW	91.31
LECQEQ	36726.27	OCIZIL	669.70	HECQUB	5.71	DIDBID	3022.33	KEYFIF01	41673.14	OWITEU	91.27
GALBUS	35880.93	BOWSIQ	636.23	GALBUS	5.53	NUTQEZ	2946.52	QIFLOI	41442.58	OWITIY	91.17
RAYLUA	34390.80	KEYFIF01	588.80	DIDBID	5.50	DIDBOJ	2686.29	RAYLIO	39304.65	HECQUB	91.11
BOWSIQ	33685.28	BERGAI01	547.27	DIDBOJ	5.40	FIQCEN	2364.78	OCIZIL	35625.01	GIVDUL	90.99

CO_2/N_2

S_{sp}		S_{ads}		ΔN (mol/kg)		AFM (mol/kg)		S		R %	
EMIHAK	15618.22	KEYFIF01	174.47	NUTQEZ	6.33	AJIHOQ	963.06	EMIHAK	7729.05	OWITAQ	91.52
AJIHOQ	9119.53	KEYFIF	170.46	FIQCEN	6.12	EMIHAK	700.10	EYOPUE	5960.03	OWIVAS	91.50
EYOPUE	8665.74	EYOQAL	131.37	MOCKAR	5.76	EMIHIS	515.52	KEYFIF01	4973.58	OWITUK	91.43
EYOQAL	4926.61	EYOPUE	120.26	LECQEQ	5.69	LECQEQ	448.65	KEYFIF	4657.05	OWITIY	91.30
KEYFIF01	4539.55	EMIHAK	107.81	XALXUF01	5.52	FIQCEN	398.06	EYOQAL	4387.67	OWITEU	91.29
KEYFIF	4130.54	EMIVAY	105.37	HASSUR	5.00	EYOPUE	281.39	AJIHOQ	3612.46	OWITOE	91.27
BOWSIQ	2138.22	AJIHOQ	88.60	HECQUB	4.69	HASSUR	280.97	BOWSIQ	1767.35	GIVDUL	90.48
HAJKOU	1764.03	BOWSIQ	86.12	GALBUS	4.61	GALBUS	264.00	EMIVAY	1282.75	OWIVEW	90.46
EMIHIS	1429.93	QIFLOI	78.42	EMIHIS	4.59	NUTQEZ	260.35	HAJKOU	1270.03	NIBHOW	90.43
QIFLOI	1147.79	RAYLIO	78.00	DIDBID	4.55	RAYLUA	239.79	QIFLOI	1128.40	PEVQEO	90.33

CO_2/CH_4

S_{sp}		S_{ads}		ΔN (mol/kg)		AFM (mol/kg)		S		R %	
EMIHIS	1400.28	KEYFIF	44.58	MOCKAR	6.66	EMIHIS	120.81	KEYFIF	1287.40	OWIVAS	85.73
EYOPOY	1253.76	KEYFIF01	44.28	NUTQEZ	6.61	NUTQEZ	115.27	KEYFIF01	1274.31	OWITAQ	85.39
KEYFIF	1013.92	EMIHAK	21.48	OWIVEW	6.41	WOBHIF	72.39	EYOPOY	876.42	OWITUK	85.00
KEYFIF01	1013.48	RAYLIO	19.91	HECQUB	5.98	LECQEQ	71.75	EMIHIS	779.97	OWITOE	84.66
EMIHAK	774.91	LARVIL	19.03	XALXUF01	5.89	AJIHOQ	67.85	EMIHAK	680.80	OWITEU	84.59
BOWSIQ	699.34	AJIHOQ	18.42	FIQCEN	5.19	FIQCEN	65.43	BOWSIQ	556.83	OWITIY	84.57
EYOPUE	441.18	EMIHIS	17.52	PODKUQ	5.03	OWIVEW	63.25	RAYLIO	408.41	NIBHOW	81.75
LUXDEO	432.14	LECQEQ	16.08	NUTQAV	5.11	KUGZIW	58.73	LARVIL	374.93	NUTQAV	81.69
RAYLIO	414.30	RAYLOU	15.45	IMIXEI	4.90	XALXUF01	52.41	EYOQAL	323.45	GIVDUL	81.19
EYOQAL	411.99	NUJCIE	14.67	SOQSAU	4.68	MOCKAR	45.56	LUXDEO	315.97	PEVQEO	81.14

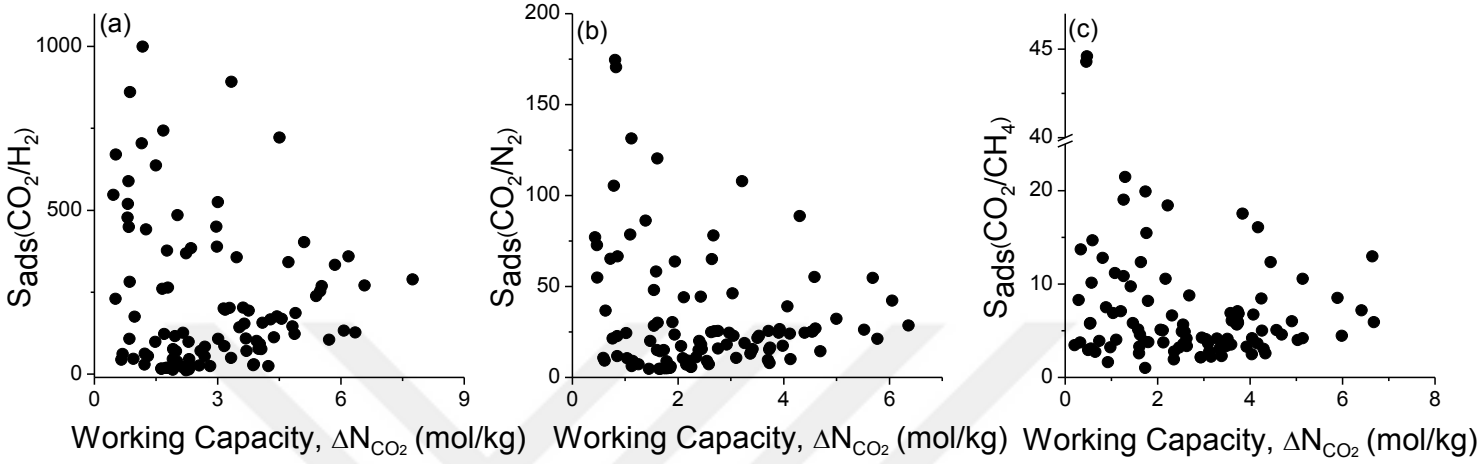

Figure B1. Adsorption selectivity (S_{ads}) vs. working capacity (ΔN_{CO_2}) of MOFs for separation of (a)CO_2/H_2 (b)CO_2/N_2 and (c)CO_2/CH_4 mixtures at adsorption pressure of 10 bar (a,b), 5 bar (c) and desorption pressure of 1 bar at 298 K.

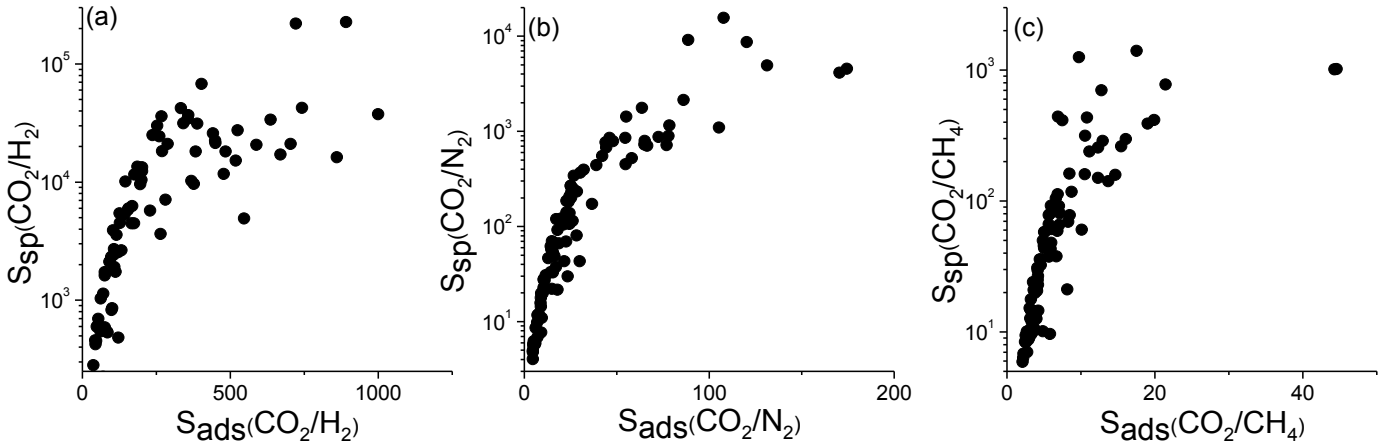

Figure B2. Sorbent selection parameter (S_{sp}) vs. adsorption selectivity (S_{ads}) of MOFs for separation of (a)CO_2/H_2 (b)CO_2/N_2 and (c)CO_2/CH_4 mixtures at adsorption pressure of 10 bar (a,b), 5 bar (c) and desorption pressure of 1 bar at 298 K.

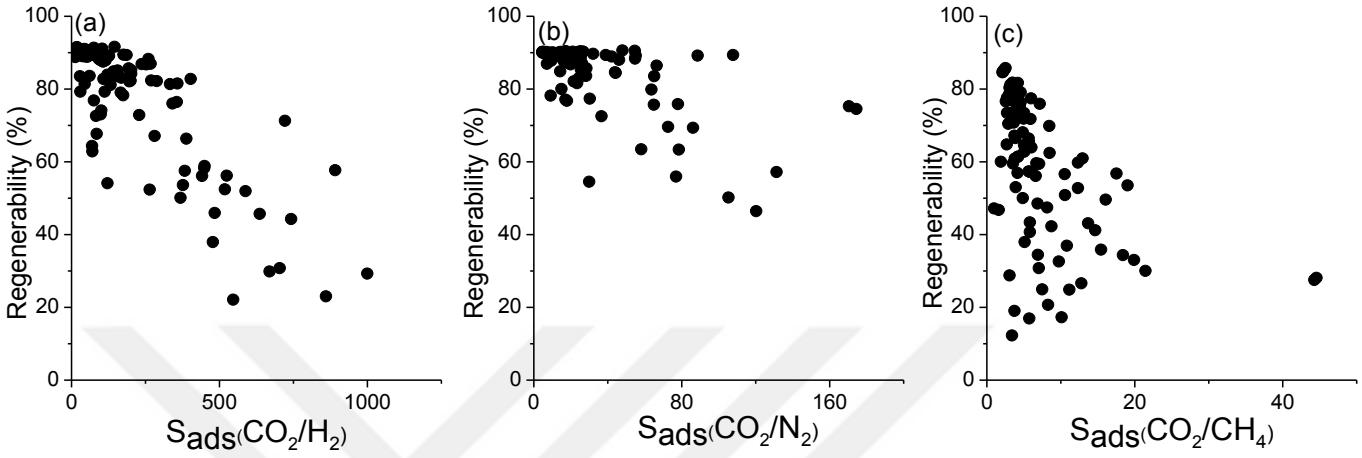

Figure B3. Regenerability (R%) vs. adsorption selectivity (S_{ads}) of MOFs for separation of (a)CO_2/H_2 (b)CO_2/N_2 and (c)CO_2/CH_4 mixtures at adsorption pressure of 10 bar (a,b), 5 bar (c) and desorption pressure of 1 bar at 298 K.

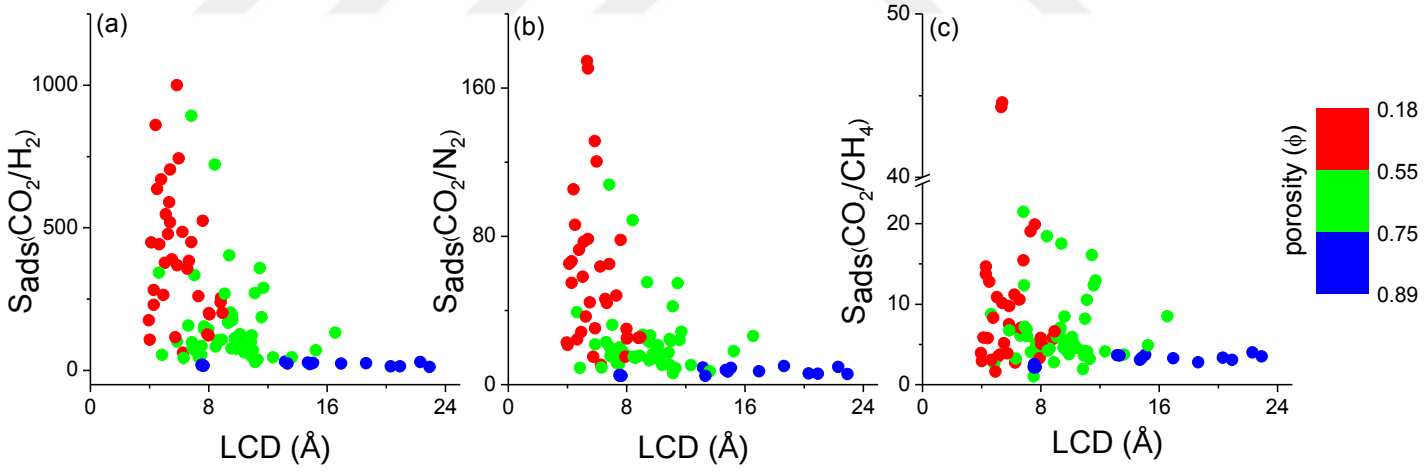

Figure B4. Adsorption selectivity (S_{ads}) of MOFs as a function of LCD and porosity for (a)CO_2/H_2 (b)CO_2/N_2 and (c)CO_2/CH_4 separations at adsorption pressure of 10 bar (a,b), 5 bar (c) and desorption pressure of 1 bar at 298 K.

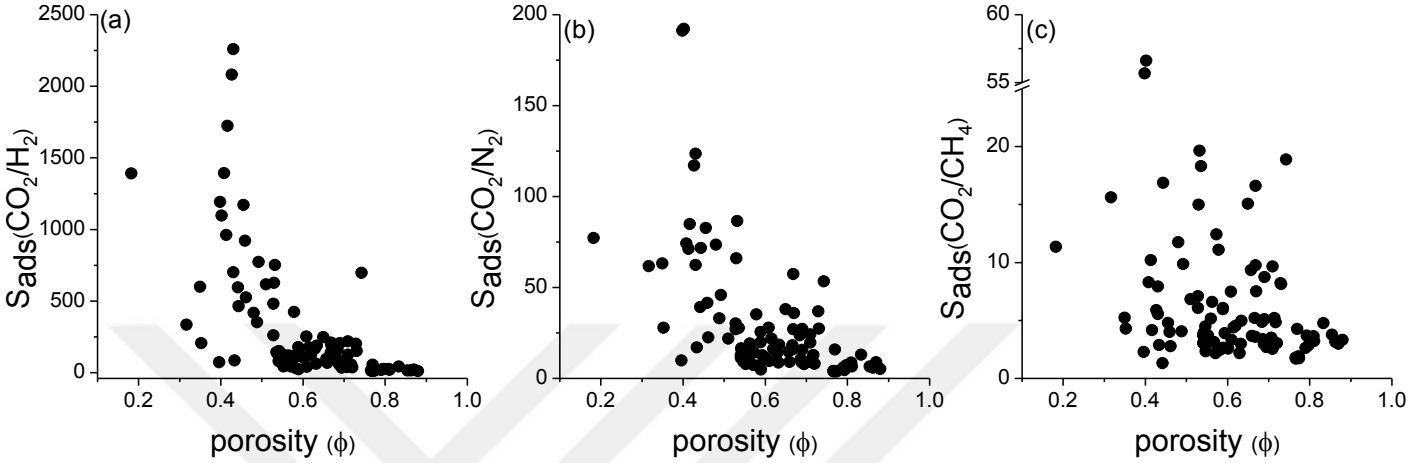

Figure B5. Adsorption selectivity (S_{ads}) vs porosities (ϕ) of MOFs for (a)CO_2/H_2 (b)CO_2/N_2 and (c)CO_2/CH_4 separations at an adsorption (desorption) pressure of 1 bar (0.1 bar) at 298 K.

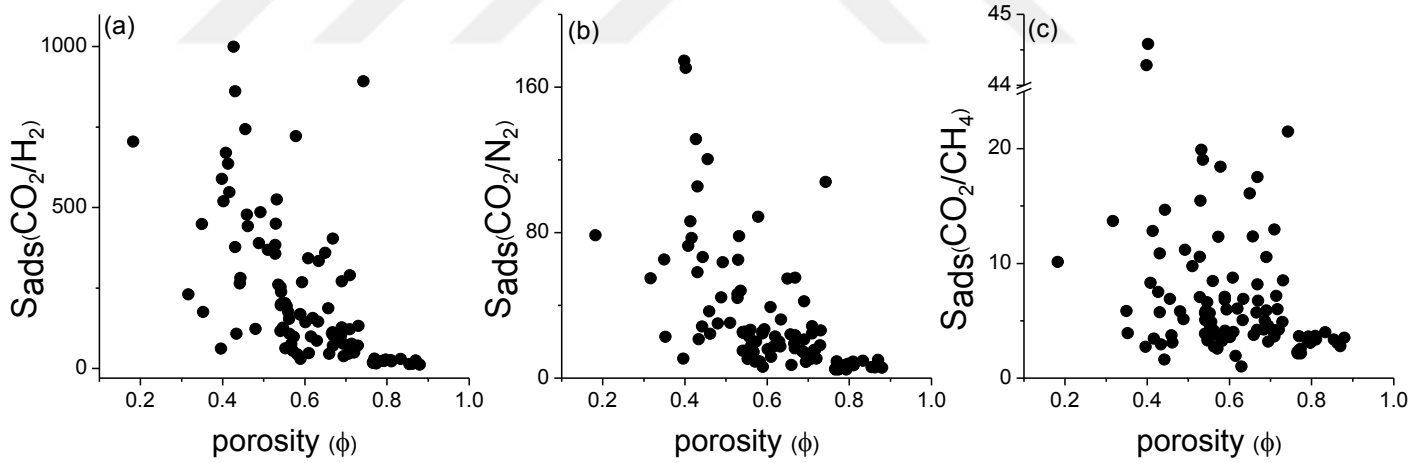

Figure B6. Adsorption selectivity (S_{ads}) vs porosities (ϕ) of MOFs for (a)CO_2/H_2 (b)CO_2/N_2 and (c)CO_2/CH_4 separations at an adsorption pressure of 10 bar (a,b), 5 bar (c) and desorption pressure of 1 bar at 298 K.

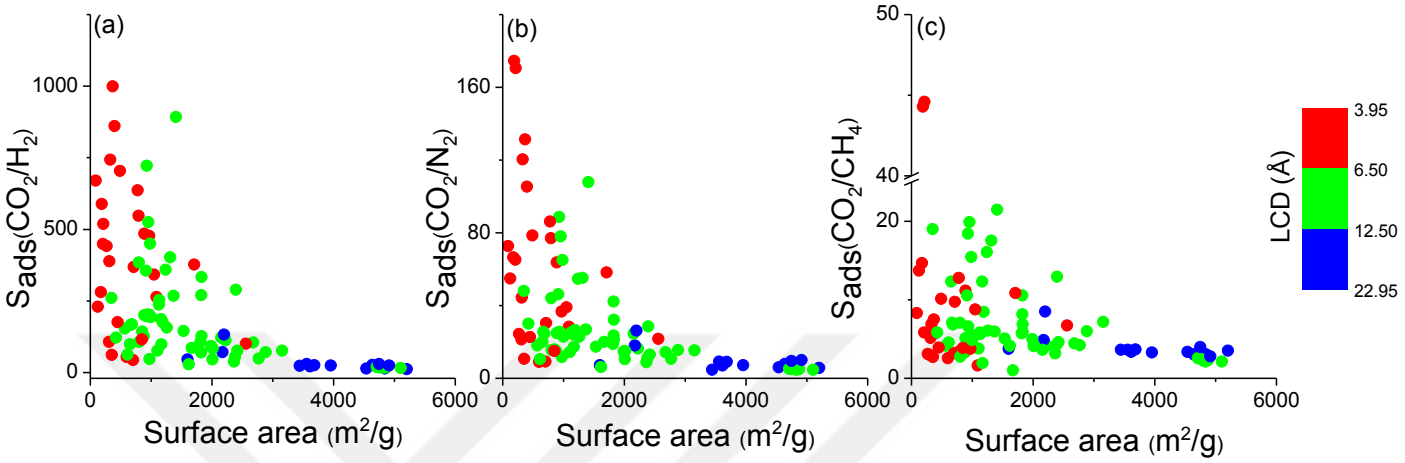

Figure B7. Adsorption selectivity (S_{ads}) of MOFs as a function of surface areas for (a)CO_2/H_2 (b)CO_2/N_2 and (c)CO_2/CH_4 separations at adsorption pressure of 10 bar (a,b), 5 bar (c) and desorption pressure of 1 bar at 298 K.

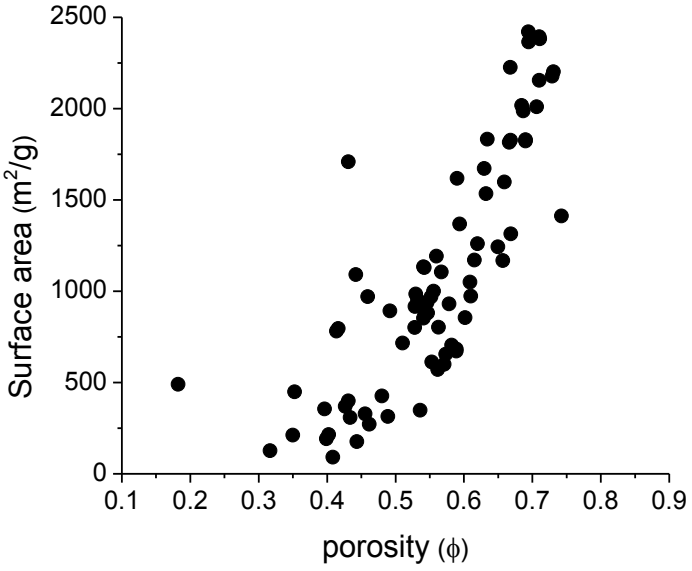

Figure B8. Surface area as a function of porosity of MOFs.

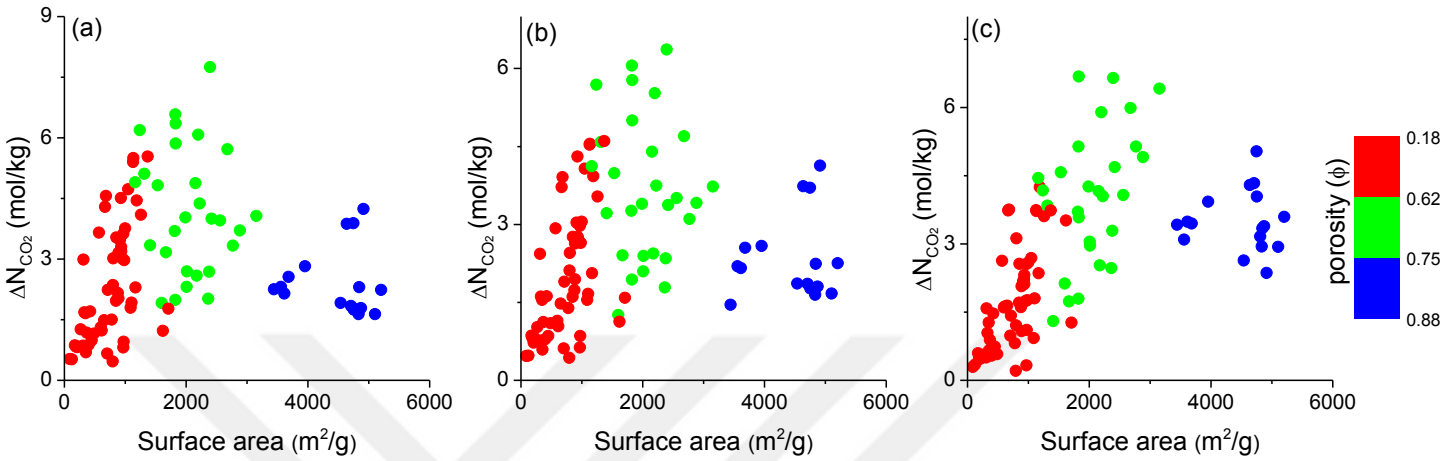

Figure S9. Working capacity (ΔN) of MOFs as a function of surface areas for (a)CO_2/H_2 (b)CO_2/N_2 and (c)CO_2/CH_4 separations at adsorption pressure of 10 bar (a,b), 5 bar (c) and desorption pressure of 1 bar at 298 K.

Appendix C. Supplementary Information for Chapter 5

Table C1. Calculated permeability and selectivity data of MOFs.

REFCODE	P_{CO2} (Barrer)	P_{N2} (Barrer)	$S_{CO2/N2}$	REFCODE	P_{CO2} (Barrer)	P_{N2} (Barrer)	$S_{CO2/N2}$
EDUSIF	248055.53	161812.06	1.53	NUJCIE	259189.19	5334.40	48.59
EDUSUR	89469.47	136662.96	0.65	NUTQAV	662910.22	64086.03	10.34
EDUVII	750391.61	564449.61	1.33	NUTQEZ	1283476.20	134367.94	9.55
EDUVOO	230761.17	159060.87	1.45	OCIZIL	484788.70	264877.93	1.83
EHALOP	3810483.09	1039911.52	3.66	OHUKIM	459543.21	234305.84	1.96
FAYPUS	82557.61	51088.99	1.62	OWITAQ	832012.08	412003.57	2.02
FEVFUJ	40491.81	83187.03	0.49	OWITEU	878701.57	245984.05	3.57
FECXUI	161663.36	104989.79	1.54	OWITIY	752611.95	290925.28	2.59
FIQCEN	501532.33	49799.88	10.07	OWITOE	1182658.40	393241.04	3.01
GALBUS	3860998.62	1023218.82	3.77	OWITUK	1102481.92	346693.15	3.18
GALHUY	641991.61	216976.51	2.96	OWIVAS	1113358.91	321974.81	3.46
GITTUZ	147793.18	89705.89	1.65	OWIVEW	979637.89	181115.59	5.41
GITVEL	79142.49	172541.87	0.46	PEVQEO	377507.01	131648.75	2.87
GIVDUL	179983.26	46667.15	3.86	PODKUQ	268948.10	162768.67	1.65
GUPCOK	213936.39	53129.80	4.03	PURQOJ	439299.73	105709.36	4.16
GUSLUC	66334.26	33338.20	1.99	QIFLOI	114200.69	17804.83	6.41
HAJKIO	780097.39	68281.24	11.42	QOWQUO	138909.54	74769.13	1.86
HAJKOU	752592.37	12664.41	59.43	RAYKEJ	859205.02	219801.96	3.91
HASSUR	1368332.43	368288.66	3.72	RAYKIN	338385.50	145463.26	2.33
HECQUB	1197848.42	315763.87	3.79	RAYKUZ	477762.42	202529.83	2.36
HIFVUO	343152.22	152947.03	2.24	RAYLAG	461506.18	95586.96	4.83
IDIWOH	9943242.60	1699898.18	5.85	RAYLEK	402353.80	132405.33	3.04
IMIXEI	516967.44	86429.25	5.98	RAYLIO	249259.55	202424.79	1.23
JENKIX	52211.95	51896.57	1.01	RAYLOU	215724.82	145120.21	1.49
KARLAS	100470.28	57673.00	1.74	RAYLUA	677139.27	113474.19	5.97
KEYFIF	154407.00	80382.66	1.92	SOQSAU	260057.29	69680.84	3.73
KEYFIF01	101347.16	98653.01	1.03	SOQSEY	153687.16	29982.45	5.13
KIPKIF	431823.75	126146.10	3.42	VEJYOZ	117902.45	66499.40	1.77
LARVIL	7052184.71	131439.91	53.65	VEJZIU	240292.89	102703.76	2.34
LECQEQ	1425808.39	969275.16	1.47	VOGTIV	719273.50	588304.69	1.22
LUMDIG	559027.00	118938.48	4.70	WOBHIF	6893062.80	1263801.28	5.45
MOCKEV	256998.63	87201.89	2.95	XALXUF01	360548.75	124427.10	2.90
NEFTOJ	505878.3	59361.54	8.52	YOZBIZ01	241602.71	119716.26	2.02
NIBHOW	297429.61	207749.42	1.43	YOZBOF	87832.18	120703.68	0.73
NIMPEG01	71010.81	71005.17	1.00	YUVSUE	272120.77	58360.15	4.66

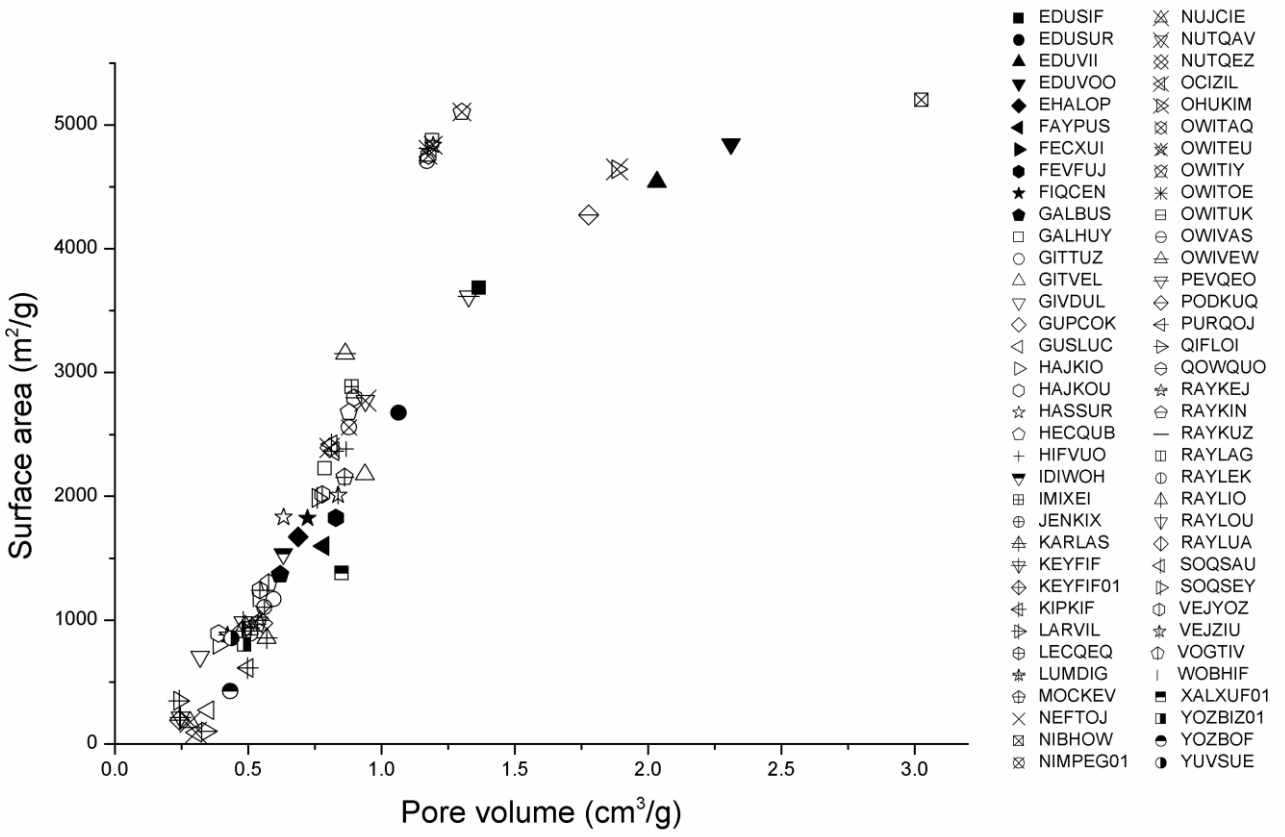

Figure C1. Calculated accessible surface area vs. pore volume of the MOFs.

Table C2. Calculated permeability and selectivity data for Ultem, Matrimid, Polyimide, MEEP, 6FDA-DAM, PIM-7 and modified PDMS based MMMs.

ϕ = 0.3	**P_{CO2} (Barrer)**	**$S_{CO2/N2}$**
Ultem based	3.2	25
Matrimid based	20.6	36
Polyimide based	102.8	35.4
MEEP based	570	62
6FDA-DAM based	1860-1920	15
PIM-7 based	2300-2500	24-26
PDMS based	4300-4600	30-34

Table C3. Calculated permeability and selectivity data for PIM-1-based MMMs.

ϕ = 0.3	P_{CO2} (Barrer)	$S_{CO2/N2}$	ϕ = 0.3	P_{CO2} (Barrer)	$S_{CO2/N2}$
EDUSIF	5143.11	24.49	NUJCIE	5147.87	25.48
EDUSUR	4956.72	23.61	NUTQAV	5213.67	24.88
EDUVII	5218.69	24.83	NUTQEZ	5234.56	24.93
EDUVOO	5134.83	24.45	OCIZIL	5197.94	24.74
EHALOP	5249.51	24.97	OHUKIM	5194.74	24.73
FAYPUS	4933.68	23.56	OWITAQ	5222.42	24.85
FEVFUJ	4650.49	22.17	OWITEU	5224.25	24.87
FECXUI	5084.89	24.23	OWITIY	5218.80	24.84
FIQCEN	5199.89	24.84	OWITOE	5232.65	24.90
GALBUS	5249.61	24.97	OWITUK	5230.88	24.89
GALHUY	5212.27	24.81	OWIVAS	5231.14	24.89
GITTUZ	5069.51	24.17	OWIVEW	5227.62	24.89
GITVEL	4920.94	23.43	PEVQEO	5181.44	24.68
GIVDUL	5101.72	24.38	PODKUQ	5151.72	24.53
GUPCOK	5125.54	24.48	PURQOJ	5191.91	24.74
GUSLUC	4862.66	23.28	QIFLOI	5017.74	24.16
HAJKIO	5220.14	24.90	QOWQUO	5058.13	24.12
HAJKOU	5218.80	25.25	RAYKEJ	5223.51	24.87
HASSUR	5235.96	24.91	RAYKIN	5172.88	24.64
HECQUB	5232.96	24.90	RAYKUZ	5197.08	24.74
HIFVUO	5174.03	24.64	RAYLAG	5195.00	24.76
IDIWOH	5254.21	24.99	RAYLEK	5186.03	24.70
IMIXEI	5201.57	24.80	RAYLIO	5143.64	24.49
JENKIX	4769.45	22.78	RAYLOU	5126.60	24.42
KARLAS	4987.31	23.81	RAYLUA	5214.57	24.85
KEYFIF	5077.17	24.21	SOQSAU	5148.22	24.56
KEYFIF01	4989.49	23.78	SOQSEY	5076.37	24.32
KIPKIF	5190.80	24.73	VEJYOZ	5024.81	23.97
LARVIL	5253.01	25.02	VEJZIU	5139.54	24.49
LECQEQ	5236.81	24.91	VOGTIV	5217.04	24.82
LUMDIG	5205.70	24.80	WOBHIF	5252.92	24.98
MOCKEV	5146.96	24.54	XALXUF01	5177.96	24.67
NEFTOJ	5200.37	24.82	YOZBIZ01	5140.15	24.49
NIBHOW	5161.57	24.57	YOZBOF	4951.56	23.59
NIMPEG01	4886.14	23.31	YUVSUE	5152.92	24.60

Table C4. Calculated permeability and selectivity data for PTMGP-based MMMs.

ϕ = 0.3	**P_{CO2} (Barrer)**	**$S_{CO2/N2}$**	**ϕ = 0.3**	**P_{CO2} (Barrer)**	**$S_{CO2/N2}$**
EDUSIF	28327.22	12.58	NUJCIE	28461.21	17.29
EDUSUR	24027.72	10.70	NUTQAV	30476.53	13.83
EDUVII	30643.88	13.46	NUTQEZ	31187.65	13.89
EDUVOO	28097.72	12.48	OCIZIL	29965.29	13.23
EHALOP	31719.95	13.91	OHUKIM	29863.68	13.20
FAYPUS	23599.10	10.80	OWITAQ	30769.95	13.54
FEVFUJ	19513.27	8.78	OWITEU	30832.06	13.62
FECXUI	26799.28	11.99	OWITIY	30647.65	13.52
FIQCEN	30027.51	13.76	OWITOE	31120.99	13.70
GALBUS	31723.57	13.91	OWITUK	31059.63	13.68
GALHUY	30430.21	13.46	OWIVAS	31068.45	13.69
GITTUZ	26427.05	11.87	OWIVEW	30947.00	13.72
GITVEL	23369.84	10.37	PEVQEO	29449.87	13.12
GIVDUL	27220.88	12.51	PODKUQ	28570.86	12.68
GUPCOK	27845.14	12.73	PURQOJ	29774.57	13.32
GUSLUC	22385.84	10.48	QIFLOI	25258.46	12.48
HAJKIO	30692.65	13.90	QOWQUO	26159.31	11.81
HAJKOU	30647.62	15.80	RAYKEJ	30806.90	13.63
HASSUR	31236.39	13.76	RAYKIN	29190.32	12.98
HECQUB	31131.73	13.72	RAYKUZ	29938.00	13.25
HIFVUO	29224.74	12.99	RAYLAG	29871.95	13.40
IDIWOH	31891.88	13.97	RAYLEK	29591.19	13.18
IMIXEI	30081.59	13.52	RAYLIO	28342.20	12.55
JENKIX	21003.37	9.61	RAYLOU	27873.53	12.40
KARLAS	24626.49	11.22	RAYLUA	30506.51	13.63
KEYFIF	26610.97	11.99	SOQSAU	28471.25	12.88
KEYFIF01	24670.37	11.05	SOQSEY	26591.54	12.54
KIPKIF	29739.75	13.26	VEJYOZ	25410.71	11.51
LARVIL	31847.85	14.19	VEJZIU	28227.64	12.64
LECQEQ	31266.21	13.71	VOGTIV	30588.74	13.44
LUMDIG	30214.96	13.49	WOBHIF	31844.36	13.96
MOCKEV	28435.63	12.78	XALXUF01	29343.49	13.08
NEFTOJ	30043.05	13.67	YOZBIZ01	28244.82	12.60
NIBHOW	28855.25	12.77	YOZBOF	23930.19	10.68
NIMPEG01	22770.08	10.30	YUVSUE	28605.06	13.02

Table C5. Calculated permeability and selectivity data for PTMSP-based MMMs.

ϕ = 0.3	P_{CO2} (Barrer)	$S_{CO2/N2}$	ϕ = 0.3	P_{CO2} (Barrer)	$S_{CO2/N2}$
EDUSIF	52788.70	8.89	NUJCIE	53212.63	15.91
EDUSUR	41203.43	6.99	NUTQAV	60173.73	10.71
EDUVII	60805.99	9.97	NUTQEZ	62924.67	10.68
EDUVOO	52072.78	8.78	OCIZIL	58296.94	9.68
EHALOP	65099.24	10.61	OHUKIM	57933.44	9.65
FAYPUS	40228.61	7.31	OWITAQ	61288.31	10.09
FEVFUJ	32155.75	5.61	OWITEU	61527.87	10.23
FECXUI	48250.69	8.29	OWITIY	60820.34	10.07
FIQCEN	58521.07	10.67	OWITOE	62659.51	10.32
GALBUS	65114.39	10.62	OWITUK	62416.78	10.30
GALHUY	60000.32	10.01	OWIVAS	62451.60	10.32
GITTUZ	47221.61	8.19	OWIVEW	61974.63	10.40
GITVEL	39718.44	6.68	PEVQEO	56484.21	9.60
GIVDUL	49450.97	9.08	PODKUQ	53562.89	9.02
GUPCOK	51299.46	9.29	PURQOJ	57617.16	9.90
GUSLUC	37613.01	7.21	QIFLOI	44164.56	9.47
HAJKIO	60991.94	10.79	QOWQUO	46498.46	8.17
HAJKOU	60820.21	14.12	RAYKEJ	61430.68	10.25
HASSUR	63119.53	10.41	RAYKIN	55600.01	9.41
HECQUB	62702.11	10.37	RAYKUZ	58198.99	9.73
HIFVUO	55716.19	9.41	RAYLAG	57962.89	10.02
IDIWOH	65824.08	10.71	RAYLEK	56973.59	9.68
IMIXEI	58716.82	10.21	RAYLIO	52835.87	8.83
JENKIX	34867.71	6.33	RAYLOU	51385.63	8.69
KARLAS	42612.97	7.65	RAYLUA	60286.32	10.32
KEYFIF	47726.58	8.34	SOQSAU	53244.56	9.41
KEYFIF01	42718.54	7.37	SOQSEY	47672.92	9.28
KIPKIF	57494.22	9.79	VEJYOZ	44548.66	7.90
LARVIL	65637.36	11.15	VEJZIU	52476.49	9.03
LECQEQ	63239.17	10.32	VOGTIV	60596.65	9.93
LUMDIG	59203.35	10.11	WOBHIF	65622.60	10.69
MOCKEV	53131.34	9.23	XALXUF01	56119.56	9.56
NEFTOJ	58577.20	10.49	YOZBIZ01	52530.18	8.97
NIBHOW	54485.61	9.10	YOZBOF	40979.17	6.99
NIMPEG01	38419.34	6.78	YUVSUE	53672.76	9.63

Appendix D. Supplementary Information for Chapter 6

Table D1. Corresponding references for comparison of our molecular simulations with the experiments for N_2 uptake of MOFs at 298 K.

MOFs	Pressure	References
BioMOF-11	0.1-1 bar	[114]
BioMOF-12	0.1-1 bar	[114]
CuBTC	1-15 bar	[115]
CuTDPAT	0.1-1 bar	[116]
IRMOF-1	0.1-1 bar	[117]
MIL-53(Al)	1-10 bar	[19]
ZIF-78	0.1-1 bar	[118]
ZnMOF-74	1-15 bar	[115]

Table D2. Corresponding references for comparison of our predicted adsorption selectivity with the experimentally/computationally reported selectivity for CH_4/N_2 separation at 298 K and 10 bar.

MOFs	References
CuBTC	[23]
CuBTC	[20]
IRMOF-1	[23]
IRMOF-14	[23]
NiMOF-74	[22]
ZIF-68	[24]
ZIF-69	[24]

VITA

Zeynep Sümer was born in İzmir, Turkey on September 9, 1991. In 2009, she graduated from Chemical Engineering Department of Middle East Technical University. She successfully got her M.Sc. degree from Chemical and Biological Engineering Department at Koç University. Her research interests include molecular thermodynamics, adsorption and diffusion phenomena in chemical systems and molecular simulations of chemistry related problems. She will continue her Ph.D. work at Chemical Engineering Department in University College London.

Publications:

1) Z. Sumer and S. Keskin, "Adsorption and Membrane-Based CH_4/N_2 Separation Performances of MOFs", accepted for publication in *Industrial & Engineering Chemistry Research*.
2) Z. Sumer and S. Keskin, "Molecular Simulations of MOF Adsorbents and Membranes for Noble Gas Separations", *Chemical Engineering Science*, 164, 108-121 (2017).
3) Z. Sumer and S. Keskin, "Ranking of MOF Adsorbents for CO_2 Separations: A Molecular Simulation Study", *Industrial & Engineering Chemistry Research* 55(39), 10404-10419 (2016).
4) Z. Sumer and S. Keskin, "Computational Screening of MOF-based Mixed Matrix Membranes for CO_2/N_2 Separations", *Journal of Nanomaterials*, 2016, 6482628, 1-12 (2016).